PhD
3rd CYCLE
FCUP
UA
UM
2024

U.PORTO

Constraining Cosmological Paradigms through Fine-Structure Constant Variations

João Diogo de Freitas Dias

FC

U.PORTO
FACULDADE DE CIÊNCIAS
UNIVERSIDADE DO PORTO

universidade de aveiro

Universidade do Minho

Constraining Cosmological Paradigms through Fine-Structure Constant Variations

João Diogo de Freitas Dias
Doctoral Program in Physics
Faculty of Sciences of the University of Porto, University of Aveiro and University of Minho
2024

U.PORTO
FACULDADE DE CIÊNCIAS
UNIVERSIDADE DO PORTO

universidade de aveiro

Universidade do Minho

PhD

PhD

Constraining Cosmological Paradigms through Fine-Structure Constant Variations

João Diogo de Freitas Dias
Thesis carried out as part of the Doctoral program in Physics
Faculty of Sciences, University of Porto
Department of Physics and Astronomy
2024

Supervisor
Dr Carlos Martins, CAUP

All the corrections determined by the jury, and only those, were made.

The Supervisor,

Assinado por: **CARLOS JOSÉ AMARO PARENTE MARTINS**
Num. de Identificação: 09497013
Data: 2025.06.25 11:08:48+01'00'

Porto, ______/______/__________

CARTÃO DE CIDADÃO

Acknowledgements

I wish to thank my supervisor, Carlos Martins, for his support and guidance throughout my PhD.

To the Phi in the Sky team, a big thanks for all the useful and interesting discussions. In particular, I thank Catarina for all the support, companionship and extreme patience in proofreading this thesis.

I want to thank Nils Schöneberg for all the help implementing the changes in the `CLASS` code.

To Léo, my friend, I want to thank you for all the enthusiastic brainstorming sessions, encouragement and good times discussing physics.

A big thank you to my friends, Rui, Tomás, Pedro, Ricardo and Tópê for supporting me and allowing me to share my enthusiasm about the cosmos by always asking me to share fascinating facts about the Universe.

A special thanks to my girlfriend, Maria, for the unrelenting support and always being there for me. Thank you for lending an ear when I expressed my frustrations about coding and writing this thesis; I truly couldn't have done it without you. I am also grateful for the invaluable help proofreading this thesis, even though what you really like is like enzymes and proteins.

I owe an enormous debt of gratitude to my parents, who always supported and believed in me, enabling me to achieve my dreams. And, of course, a big thanks to my brothers.

Abstract

The search for variations in nature's fundamental constants is essential for advancing our understanding of fundamental physics. This thesis explores various models that predict variations of the fine-structure constant α, focusing on extensions of the Bekenstein model, the runaway dilaton, rolling tachyon fields, and Swampland conjectures. These frameworks introduce scalar fields that, when coupled to the electromagnetic sector, lead to α variations, thus violating the Einstein equivalence principle and offering new insights into dark energy and the evolution of the universe. By exploring synergies between local, astrophysical, and cosmological datasets, and integrating the use of a Boltzmann code (Cosmic Linear Anisotropy Solving System) with Markov chain Monte Carlo simulations, we were able to establish stringent constraints on the above mentioned extensions of the ΛCDM model. We provide, for the first time, as far as our knowledge, constraints for the full parameters space on the phenomenological extended Bekenstein model and the string inspired runaway dilaton model. We found that couplings of the order of parts per million are excluded for the former, and of order unity for the latter. The rolling tachyon model was constrained, revealing that it is effectively indistinguishable from a cosmological constant, with any significant variations in α being highly suppressed. Finally, the Swampland conjectures, which offer a framework for understanding the compatibility of string theory with cosmology, are examined in light of recent cosmological data. The updated data confirms the existence of a tension with these criteria. This work provides tight bounds on models with varying fine-structure constant, contributing to our understanding the cosmological implications of these variations. The results of this thesis highlight the need for future experiments and observations to continue testing the limits of these models, ultimately advancing our understanding of fundamental physics.

Resumo

A busca por variações nas constantes fundamentais da natureza é essencial para aprofundarmos o nosso conhecimento da física fundamental. Esta tese explora vários modelos que preveem variações da constante de estrutura fina α, com foco nas extensões do modelo de Bekenstein, no *runaway dialton*, no *rolling tachyon* e em conjeturas do princípio de *Swampland*. Estes modelos teóricos introduzem campos escalares que, ao acoplarem-se ao setor eletromagnético, levam a variações de α, violando o princípio da equivalência de Einstein e oferecendo novas perspetivas sobre a energia escura e a evolução do universo. Explorando as sinergias entre conjuntos de dados locais, astrofísicos e cosmológicos, e integrando o uso de um código de Boltzmann (Cosmic Linear Anisotropy Solving System) com simulações de método de Cadeia de Markov Monte Carlo, conseguimos estabelecer restrições rigorosas para as extensões do modelo ΛCDM acima mencionadas. Fornecemos, pela primeira vez, tanto quanto sabemos, restrições para todo o espaço de parâmetros no modelo fenomenológico de Bekenstein e no modelo do *runaway dilaton* inspirado pela teoria das cordas. Reportamos que acoplamentos da ordem de partes por milhão são excluídos para o primeiro, e da ordem da unidade para o segundo. O estudo do *rolling tachyon* revelou que é efetivamente indistinguível de uma constante cosmológica, com quaisquer variações significativas em α altamente suprimidas. Finalmente, as conjecturas do princípio de *Swampland*, que servem de ponte entre a teoria de cordas e a cosmologia, são examinadas à luz dos dados cosmológicos recentes. Os dados mais recentes confirmam a existência de uma tensão com estes critérios. Este trabalho fornece limites estritos para modelos com variações da constante de estrutura fina, contribuindo para a nossa compreensão das implicações cosmológicas de tais variações. Os resultados destacam a necessidade de experiências e observações futuras para continuar a testar os limites desses modelos, avançando, assim, a nossa compreensão da física fundamental.

List of Publications

1. Dias et al. (2024). A speed limit on tachyon fields from cosmological and fine-structure data. JCAP 2024(11):030. Available at https://doi.org/10.1088/1475-7516/2024/11/030.

2. Schöneberg et al. (2023). News from the Swampland — constraining string theory with astrophysics and cosmology. JCAP 2023(10):039. Available at https://doi.org/10.1088/1475-7516/2023/10/039.

3. Vacher et al. (2023). Runaway dilaton models: Improved constraints from the full cosmological evolution. Phys.Rev. D 107.104002. Available at https://doi.org/10.1103/PhysRevD.107.104002.

4. Vacher et al. (2022). Constraints on extended Bekenstein models from cosmological, astrophysical, and local data. Phys.Rev. D 106.083522. Available at https://doi.org/10.1103/PhysRevD.106.083522.

Contents

List of Figures

List of Tables

Glossary

BAO	Baryon Acoustic Oscillations
BBN	Big Bang Nucleosynthesis
CDM	Cold Dark Matter
CMB	Cosmic Microwave Background
DE	Dark Energy
DM	Dark Matter
EEP	Einstein Equivalence Principle
EFE	Einstein Field Equations
EM	Electromagnetic
FLRW	Friedmann-Lemaître-Robertson-Walker
GR	General Relativity
LLI	Local Lorentz Invariance
LPI	Local Position Invariance
MCMC	Markov Chain Monte Carlo
QSO	Quasi-Stellar Objects
SNIA	Type Ia supernova
UFF	Universality of Free Fall

1

Introduction

Since ancient times, our attention has been drawn to the skies, captivated by the patterns formed by the bright spots scattered across the dark fabric of the cosmos. This fascination with the celestial sphere inspired the creation of myth, science and philosophy, playing a part in our development both as a species and as a society. Myth shaped cultures, the heavens' movements, influenced agriculture, navigation, and the passage of time. This sense of awe has accompanied us throughout history, and is still present today with every piece of knowledge we uncover about the Universe we live in.

1.1 Historical digression

Cosmology today is a branch of physics that studies the Universe and its constituents as a whole, with the primary aim of explaining the dynamics of its evolution – from the Universe's "birth" to the present – using models to make scientific predictions. Widely accepted by the scientific community, the Λ Cold Dark Matter model (ΛCDM) is a highly successful model in fitting the data. Its development was slow and gradual, with several major scientific discoveries contributing to our current understanding.

The fact that the Universe is expanding is a pivotal discovery from the 20th century. While it is usually attributed to Hubble (1929), this idea predates his work and was first predicted by Alexander Friedmann, who derived his famous equations in a 1922 paper, demonstrating that an expanding or contracting Universe was a natural solution to Einstein's field equations (Friedman, 1922). A few years later, Lemaitre (1927) showed a linear relation between the distance of a galaxy and the velocity at which it is moving away from us. He was able to compute the proportionality constant using data collected from measuring the redshift of about thirty galaxies (Slipher, 1917; Hubble, 1926).[1] Today, we know this as *Hubble-Lemaître law*, which states that the further away a galaxy is from us, the faster it is receding. This relationship is crucial because it provides insight into the Universe's rate of expansion and suggests that the Universe is not static but dynamic. The law is encapsulated in the equation $v = H_0\, r$, where r is the distance to the galaxy and H_0 is the proportionality constant, known as the *Hubble constant*. The value of this constant is currently debated, with its reasons explored in subsequent chapters.

For a long time, until the mid-1960s, the majority of our knowledge about the Universe was derived from observations of galaxy redshifts and distances. This paradigm shifted with the discovery of a nearly isotropic background of microwave radiation, the *cosmic microwave background* (CMB). This faint and very cold thermal radiation constitutes the oldest sky we can observe, with a temperature of around $2.7\,\mathrm{K}$ in every direction (see D. J. Fixsen, 2009). This relic radiation is a remnant of the hot, dense phase in the early Universe, and it was first predicted by Gamow (1946) when contemplating the formation of heavier elements. By then, it had already been understood that many elements could not be synthesized under the conditions found in stellar interiors (see Chandrasekhar and Henrich, 1942). During the early stages of its expansion, the Universe provides conditions of high temperature and density required to create heavier nuclei, the *primordial nucleosynthesis*, see Gamow (1948) and Alpher, Bethe & Gamow (1948). It was almost two decades after Gamow's proposal that, by accident, this relic radiation was first observed by Penzias & Wilson (1965). Working at the Bell Telephone Laboratories in New Jersey, they detected an unexplained background noise in their radio antenna that seemed to come from all directions in the sky. Despite their efforts to eliminate various sources of interference, they could not remove this signal. At the same time, in Princeton, an active search for the CMB was being conducted by Dicke et al. (1965), based on the theoretical predictions. The detection of the CMB not only confirmed a key prediction but also transformed cosmological theories, marking the dawn of precision cosmology, and reshaping our understanding of the Universe's origins and evolution. Precise measurements of the CMB have been instrumental in the development of current cosmological models, and continue to drive research into fundamental questions about the Universe.

Another significant and just as remarkable advancement is the discovery that our Universe today is not only expanding, but it is doing so at an increasing rate. To measure distances, astronomers rely on special objects referred to as "standard candles". These objects are invaluable, as their known absolute luminosities enable precise distance calculations. By comparing their intrinsic and apparent luminosities, astronomers can determine distances with remarkable accuracy. Together, these standard candles form a critical part of the cosmic distance ladder, allowing distances to be established on progressively larger

[1] Redshift is observed in light from objects moving away from the observer, where the relative motion causes the wavelengths of light to stretch, shifting them to longer (redder) wavelengths.

scales. This knowledge is essential for mapping the Universe's structure, determining its scale, and ultimately understanding its expansion. For a long time, the brightest galaxies in clusters were used to measure cosmological distances.[2] The use of type Ia supernovae (SNIa) as standard candles (see Branch and Miller, 1993) was instrumental in discovering the accelerated expansion of the Universe. As detailed in the works of Riess et al. (1998) and Perlmutter et al. (1999), this realization laid the groundwork for a new era in cosmology, which has been corroborated by independent observations.[3] This discovery puzzled cosmologists as gravity, which attracts matter, would be expected to decelerate the expansion of the Universe. What, then, could be driving this observed acceleration? One proposed explanation is the presence of a new form of energy, known as dark energy (see Huterer and Turner, 1999). The simplest and most successful candidate for dark energy (DE) is a cosmological constant Λ, where its energy density is constant in space and time. This proposition set in motion a great discussion about the nature of dark energy that carries on to this day. Throughout this thesis, the reader will encounter an exploration of possible alternative descriptions to the well-known cosmological constant Λ.

Our Universe is composed, in its majority, of dark energy. The second most common component is not matter (contrary to what we might be inclined to think) but some form of matter that is "invisible" to light, hence called *dark matter*. Since this form of matter does not interact with light – does not emit, absorb, or reflect light – we can only observe it indirectly, by its gravitational effects. One of the first pieces of evidence for dark matter was when Zwicky (1933) applied the virial theorem to the Coma cluster.[4] By measuring the radial velocities of galaxies in this cluster he concluded that their speeds could not be accounted for by the visible matter alone. Such high speed could only be explained by the existence of some form of matter that was invisible to our telescopes. Galaxy rotation curves also hint at the existence of dark matter. Observations of stars in galaxies showed that the ones far from the galactic center orbit at a speed that is close to the ones at the center, pointed out by Sofue et al. (1999) and Sofue & Rubin (2001) (ideas originally from Babcock, 1939; Rubin and Ford, 1970). According to Newtonian mechanics, this should not be possible, as the ones farther from the center should orbit more slowly. The existence of dark matter in the galaxies can help explain these high orbital velocities. There are other phenomena that provide evidence for the existence of this strange form of matter, such as gravitational lensing and the acoustic peaks in the CMB.[5]

Several other relevant discoveries can be mentioned, such as the first observation of gravitational waves by Abbott et al. (2016). Gravitational waves, first detected by the Laser

[2] For an extended discussion of cosmological distance measurements see Weinberg (2008).

[3] In Jimenez & Loeb (2002), Eisenstein et al. (2005), Betoule et al. (2014), Haridasu et al. (2017), and Planck Collaboration et al. (2020a).

[4] The virial theorem states that, for a stable, bound system in equilibrium, the time-averaged total kinetic energy of the particles is related to the time-averaged total potential energy of the system.

[5] See Clowe et al. (2006) and Hu & Dodelson (2002) for more information on evidence for dark matter using gravitational lensing and the CMB, respectively.

Interferometer Gravitational-Wave Observatory (LIGO), are ripples in spacetime caused by the acceleration of massive objects, such as colliding black holes or neutron stars. This discovery was significant because it opened a new avenue for observing the Universe, allowing scientists to gather information about cosmic events that were previously hidden from sight. Gravitational waves provide insight into the dynamics of the Universe, further enhancing our comprehension of its evolution. These advancements have been central to the development of our current knowledge of the Universe. Now, over a century after Friedmann's proposal of a homogeneous and expanding Universe, cosmologists have developed a model that has been tested countless times and is consistent with data. In the following section, the ΛCDM model will be explored in more depth. However, this discussion is preceded by a short section on General Relativity.

1.2 General Relativity

The discovery of General Relativity (GR) is considered as one of the greatest discoveries in the history of humanity. It drastically changed not only our knowledge about gravity and the Universe but very basic concepts, such as space and time. The principle of special relativity tells us that the laws of physics are invariant in all inertial frames of reference and that the speed of light c, in vacuum, is a constant and the same for any observer, putting space and time at an equal footing. General Relativity goes a step further by extending this principle to non-inertial frames. Gravity becomes a consequence of the geometry of spacetime, which curves in the presence of matter and energy. Einstein was the main motor behind these discoveries, and in 1915 he published a set of papers describing his theory of General Relativity in Einstein (1915a).[6]. The Einstein field equations (EFE) are

$$G_{\mu\nu} + \Lambda g_{\mu\nu} = 8\pi G T_{\mu\nu} \ , \tag{1.1}$$

expressed in natural units (with $c = \hbar = 1$). This set of nonlinear partial differential equations relates the spacetime geometry, given by the Einstein tensor $G_{\mu\nu}$ with its content, quantified by $T_{\mu\nu}$, and Λ is the cosmological constant. The Einstein tensor is defined as

$$G_{\mu\nu} = R_{\mu\nu} - \frac{1}{2} g_{\mu\nu} R \, , \tag{1.2}$$

and here we have $g_{\mu\nu}$ as the metric tensor, $R_{\mu\nu}$ and R as the Ricci tensor and scalar, respectively.

This equation can be derived from the Einstein-Hilbert action

$$S = \frac{M_{pl}^2}{2} \int d^4x \sqrt{-g} \, (R - 2\Lambda) \, , \tag{1.3}$$

[6] The other papers in Einstein (1915b), Einstein (1915c), and Einstein (1915d).

with $M_{pl}^2 = (8\pi G)^{-1}$.

This set of equations describes the evolution of the Universe and predicts phenomena such as the bending of light around massive objects (gravitational lensing), the slowing of time near strong gravitational fields (gravitational time dilation), and the existence of black holes and gravitational waves. GR has been tested countless times and it serves as the foundation for modern cosmology. The reader can find a review on the status of experimental tests of GR in Will (2014).

1.3 The ΛCDM model

After having been introduced to the basics of GR, we now need a set of equations that are more tractable and easily solved. From the EFE one can derive simpler equations describing the evolution of the Universe by relying on a simple assumption. The cosmological principle is the idea that the Universe is *homogeneous* and *isotropic* – uniform under translations and rotations, respectively. This means that, on a sufficiently large scale, the Universe looks the same for any observer, there is no "special" set of coordinates in the Universe. This cosmological principle is encapsulated in the Friedmann–Lemaître–Robertson–Walker metric (FLRW):

$$ds^2 = -c^2 dt^2 + a\left(t\right)^2 \left(\frac{dr^2}{1-kr^2} + r^2 d\Omega^2\right) , \tag{1.4}$$

where $d\Omega^2$ represents the angular part of the metric $d\theta^2 + \sin^2\theta d\phi^2$ and k is the curvature parameter ($k = 0$ for a flat Universe, $k = 1$ for a closed Universe, and $k = -1$ for an open Universe). The scale factor, denoted as $a\left(t\right)$, is a dimensionless factor used to measure the relative expansion (or contraction) of the Universe. By convention, the scale factor is often normalized to $a\left(t_0\right) = 1$ at the present time t_0, and $a\left(t\right) < 1$ at earlier times. This factor has a relation to redshift which is given by

$$a = \frac{1}{1+z} . \tag{1.5}$$

Using this metric in the EFE, combined with the further assumption that the Universe is completely filled with a perfect fluid with $T^{\mu}{}_{\nu} = \mathrm{diag}\left(-\rho, p, p, p\right)$, in the fluid's rest frame.[7] This fluid must obey the following equation of state

$$p = w\rho , \tag{1.6}$$

where p is the pressure, ρ the density, and w is the equation of state parameters. From the covariant conservation of the energy-momentum tensor, it follows that every constituent of

[7] Throughout this thesis, the mostly positive metric signature (-+++) will be used.

the Universe must obey this equation of state and the following continuity equation

$$\frac{\partial \rho}{\partial t} + 3H\left(1+w\right)\rho = 0\ , \tag{1.7}$$

which can be integrated to give

$$\rho\left(a\right) = \rho_0 a^{-3(1+w)}\ . \tag{1.8}$$

The equation of state parameter will assume a different value, depending on whether we are considering matter, radiation, or any other component.

Using the cosmological principle to write the FLRW metric, together with the stress-energy tensor for a perfect fluid one can write the EFE in Eq. (1.1) as the known Friedmann equations. Solving for the time component of the tensors one is able to derive the first of this set of equations

$$H^2 = \left(\frac{\dot{a}}{a}\right)^2 = \frac{8\pi G}{3}\rho - \frac{k}{a^2} + \frac{\Lambda}{3}\ . \tag{1.9}$$

This first equation gives the overall rate of expansion in terms of the energy density ρ of the Universe components, curvature, and cosmological constant. Hence, for a Universe composed of matter and radiation we have $\rho = \rho_m + \rho_r$. The second Friedmann equation, also known as Raychaudhuri equation, describes the acceleration of the Universe's expansion, influenced by the density, pressure, and cosmological constant

$$H^2 + \dot{H} = \frac{\ddot{a}}{a} = -\frac{4\pi G}{3}\left(\rho + 3p\right) + \frac{\Lambda}{3}\ . \tag{1.10}$$

These two equations are the foundation of the ΛCDM model, describing the evolution of the Universe's scale factor, which in turn determines the age, size, and future of the cosmos based on its contents. They can be written in a more compact form by defining the density parameter, using the critical density $\rho_c = 3H_0^2\left(8\pi G\right)^{-1}$. The Friedmann equations become

$$H^2 = H_0^2 \sum_i \Omega_i a^{-3(1+w_i)}\ , \tag{1.11}$$

and

$$H^2 + \dot{H} = -\frac{1}{2}\sum_i \Omega_i\left(1+3w_i\right)\ , \tag{1.12}$$

where the subscript i refers to each component of the Universe.

Having understood the fundamental equations governing the evolution of this homogeneous and isotropic Universe, we need describe its content. As far as we know, the Universe is composed of dark energy, matter (baryons and cold dark matter), and radiation.

Dark energy

As was corroborated in Planck Collaboration et al. (2020a), dark energy is the dominant component of our Universe (at $z = 0$), comprising approximately 70% of its total content. This fact shows us dark energy's profound role in this model, as it is responsible for driving the accelerated expansion of the Universe. We can understand dark energy as the term Λ present in the EFE, often called cosmological constant or vacuum energy. In terms of the Friedmann equations, a cosmological constant is a term with constant energy density, exerting a negative pressure, such that $w_\Lambda = (p/\rho)_\Lambda = -1$. In future sections of this thesis, I will discuss models where DE is dynamical. In these cases, we always require that $w_{DE} < -1/3$ in order to have an accelerated expansion. This can be seen from Eq. (1.10), since the requisite for an accelerated expansion is $\ddot{a} > 0$, and for this to be true we must have $p + 3\rho > 0$.

Matter

As established in the ΛCDM model, matter constitutes about 30% of the Universe's total content as can be seen in (Planck Collaboration et al., 2020a). This matter is split between baryonic matter – the ordinary matter composed of protons, neutrons, and electrons that form stars, planets, and galaxies – and cold dark matter (CDM), a non-luminous component that interacts only through gravity. Baryonic matter accounts for about 5% of the Universe's total energy density, while dark matter constitutes roughly 25%. Together, these matter components govern the gravitational structure formation in the Universe, influencing galaxy clustering, rotation curves, and the behavior of massive structures. In the Friedmann equations, matter is treated as a component with an equation of state parameter $w_m = 0$, meaning that it behaves as pressureless dust. From here it is easy to show that the energy density of matter decreases cubically with the Universe's expansion, $\rho_m \propto a^{-3}$.

Radiation

Contributing less than 1% of the Universe's content, radiation and neutrinos are less significant than dark energy or matter in the current epoch. They have however played a much more prominent role in the early Universe when higher temperatures and densities dominated (Planck Collaboration et al., 2020a). Radiation, including photons from the CMB, is characterized by an equation of state parameter $w_r = 1/3$, indicating that its pressure is one-third of its energy density. This relation affects the evolution of the scale factor, causing radiation energy density to scale as $\rho_r \propto a^{-4}$. The rapid dilution of radiation density with expansion led to a radiation-dominated Universe early on, giving way to the matter-dominated era as expansion continued. Neutrinos are another relativistic component that also behave as radiation in the early Universe due to their high velocities. While neutrinos currently make up only a small fraction of the Universe's energy density, they play a critical role in shaping the early Universe's thermal history and structure formation.

Curvature

Curvature is a parameter that captures the overall geometric shape of the Universe. It contributes to the total energy density in the Friedmann equations as a term scaling with $\rho_k \propto a^{-2}$. In the current cosmological model, the curvature is constrained to be nearly zero, suggesting a flat Universe (Planck Collaboration et al., 2020a). In this thesis it will always be assumed a vanishing curvature throughout.

This completes the general description of the standard model of cosmology, and it will serve as a baseline for future discussions. The following sections will highlight some problems with this model, possible solutions and alternative models.

1.4 Open problems in Cosmology

The standard model of cosmology, like any scientific model, is subject to criticism. Serving as the key observational and theoretical pillar of modern cosmology, it nonetheless faces limitations in explaining certain phenomena, leading to several open questions in research, which will now be discussed.

The cosmological constant problem – what is dark energy?

Arguably, the most enthralling of these questions is the so-called "cosmological constant problem". The cosmological constant has been a source of controversy since its first appearance in Einstein (1917), and it remains a hot topic to this day. Several authors have written exhaustive and detailed descriptions of the unraveling of these events, however a summarized version will be presented in this thesis.[8]

In Einstein (1915d), Einstein presents a formulation of his equations that possess general covariance:

$$R_{\mu\nu} - \frac{1}{2}g_{\mu\nu}R = 8\pi G T_{\mu\nu} \ . \tag{1.13}$$

A static solution to these equations could not be found. This fact troubled Einstein so much that in 1917 he published a paper introducing a "universal constant". This constant allowed for a static Universe with spherical geometry and constant matter density. This was the first appearance of the cosmological constant, and according to Einstein, its only purpose was to make the Universe static. As he stated in the paper: "That term is necessary only for the purpose of making possible a quasi-static distribution of matter, as required by the fact of

[8] For more information on the history of the cosmological constant see Weinberg (1989), Abbott (1988), Straumann (1999), and Amendola & Tsujikawa (2010).

the small velocities of the stars". However, the story does not end here. After the discovery of the expansion of the Universe in 1929, it became clear that the Universe was expanding after all. Even though a cosmological constant is needed for a static Universe, it is not required for an expanding one. At this point, Einstein rejected his idea of a cosmological constant, as one can see in this quote from a letter he wrote to Weyl: "If there is no quasi-static world, then away with the cosmological term!", as recounted in Weinberg (1989). However, it is not so simple to "remove" this constant from the EFE. The reason for this is that the vacuum energy density acts like a cosmological constant (Zel'dovich, Krasinski, and Zeldovich, 1968). Invariance arguments imply that the vacuum expectation value of the energy-momentum tensor for the vacuum energy be

$$\langle T_{\mu\nu}\rangle_{vac} = -\langle \rho\rangle_{vac}\, g_{\mu\nu} \ . \tag{1.14}$$

From a careful analysis of Eq. (1.1) it is straightforward to see that the above term is mathematically equivalent to a cosmological constant. This is identical to adding $8\pi G\rho_{vac}$ to an effective cosmological constant

$$\Lambda_{eff} = \Lambda_0 + 8\pi G\rho_{vac} \ , \tag{1.15}$$

where Λ_0 is the bare cosmological constant. It is now clear that even if we have $\Lambda_0 = 0$ there is still an effective cosmological constant that comes from the vacuum energy density.

This set in motion a program to measure the value of the cosmological constant. In terms of energy densities, this constant corresponds to

$$\rho_\Lambda \approx 10^{-47}\text{GeV}^4 \ , \tag{1.16}$$

from Lemaitre (1934). If one tries to compute the energy density of empty space

$$\rho_{vac} \approx 10^{74}\text{GeV}^4 \ , \tag{1.17}$$

which is 10^{121} orders of magnitudes larger the observed value in Eq. (1.16). This huge discrepancy is problematic because it implies that in Eq. (1.15) the two terms on the right-hand side have to cancel almost exactly. For this to happen, the value of Λ_0 would have to be extremely fine-tuned. Before the discovery of the accelerated expansion of the Universe in 1998, it was believed that the cosmological constant was exactly equal to zero. There were some ideas on how to go about canceling those two terms, which are nicely described in Weinberg (1989). However, none of those ideas were satisfactory, may it be by the conjuration of a special symmetry that explains this vanishing Λ (supersymmetry) or by an anthropic principle that does little more than sweep the problem under the rug.

We do know, however, that the Universe is undergoing an accelerated expansion, which means that there must be something driving this expansion. For this reason, even if the cosmological problem is resolved in such a way that Λ vanishes, we still need to find an alternative explanation for dark energy.

The H_0 and σ_8 tension

One of the fundamental quantities in cosmology is the current expansion rate of the Universe, represented by the Hubble constant H_0. The precise measurement of this quantity is essential for our cosmological models. However, this constant is plagued by a tension between measurements from the Planck satellite, using the CMB anisotropies, and local distance ladder measurements (Planck Collaboration et al., 2020b; Riess et al., 2022), which has now reached a significance of 5σ. A review of this topic can be found in Bernal, Verde & Riess (2016).[9] There are a number of possible solutions being exploited trying solve, or at least, alleviate this tension. Most of these are reviewed in Di Valentino et al. (2021).

Very similarly, we have the σ_8 tension. In Douspis, Salvati & Aghanim (2019), one can find a short review on the subject. This consists of a discrepancy between the calculated value of S_8, a parameterization of σ_8 and Ω_m (an amplitude of matter perturbations and the matter density parameter respectively). To put it simply, measurements of this quantity at low-redshift differ from those obtained from high-redshift probes at a significance of $\sim 2 - 3\sigma$. However, in Ghirardini et al. (2024) the authors manage to push the tension below 3σ, to a region they define as "consistent".

Throughout this thesis, several extensions to ΛCDM will be discussed, where some of them may be able to alleviate these tensions (although only the H_0 one will be mentioned).

Cosmological lithium problem

The cosmological lithium problem is a long-standing discrepancy in astrophysics concerning the predicted and observed abundances of lithium isotopes, particularly ^{7}Li, in the Universe. This issue arises from Big Bang nucleosynthesis (BBN) predictions. BBN describes the production of the lightest atoms, including the formation of ^{7}Li. It successfully predicts the primordial abundances of hydrogen, deuterium, and helium, matching observations with remarkable precision. However, it overestimates the primordial abundance of lithium, by a factor of three compared to measurements in the atmospheres of old, metal-poor stars, which are believed to retain the primordial chemical composition of the Universe. This translates into a tension of $2 - 3\sigma$.

Several proposed explanations have been explored, including astrophysical, nuclear physics, and others beyond the standard model type solutions, which are described in Fields (2011). However, this problem remains a critical open question in cosmology, challenging

[9] For reviews on this topic see Kamionkowski & Riess (2022) and Verde, Schöneberg & Gil-Marín (2023).

our understanding of early-Universe physics and the interplay between stellar and primordial nucleosynthesis. Its resolution may unveil new insights into fundamental physics or confirm the robustness of existing theories.

The nature of dark matter

One of the greatest puzzles in modern physics is the nature of dark matter. It is a question that troubles both particle physicists and cosmologists. Two of the best physics models are put in check by this elusive form of matter, that only interacts via gravitational force. The nature of dark matter eludes both the Standard Model of particle physics and ΛCDM. For this reason, it is a hot topic in research, and it is not difficult to find reviews on this subject.

It is quite remarkable that the dark sector – dark energy and dark matter – makes up about 95% of the Universe, and dark matter alone constitutes 25% of the Universe. Profumo, Giani & Piattella (2019) offers a good review on dark matter from the particle physics perspective, and Arbey & Mahmoudi (2021) a cosmology one. In this thesis, dark matter is briefly mentioned in a model (the extended Bekenstein model), where a coupling of the field to dark matter is allowed.

In this section, some areas have been highlighted where ΛCDM may need to be extended, or revised, to provide a more complete picture of the cosmos. There is still a great amount of work needed to improve our understanding of the Universe, and many researchers have been focusing their attention on solving these fundamental problems. The aim of this thesis is to deepen our understanding of a particular class of models – extensions of ΛCDM – where we have variations of fundamental constants, in particular, variations of the fine-structure constant. This has profound consequences, such as the violation of the Einstein Equivalence Principle. Some of the models presented in this work provide an alternate description of dark energy. Naturally, the next topic to introduce is the variations of the fine-structure constant.

1.5 Dark energy and the cosmological constant

The search for the source of dark energy is ongoing, and it counts with the combined efforts of theory and observation. Dark energy is supported by a great number of different observations that rely on: the age of the Universe; supernovae; the CMB; and Baryon acoustic oscillations (BAO). An extensive review of the probes searching for dark energy can be found in Huterer & Shafer (2018).

The age of the Universe t_0 can be used as evidence for dark energy by comparing its value, which can be roughly estimated by the inverse of H_0, with the age of oldest stars. Using the relation between time and redshift $\mathrm{d}t = -\mathrm{d}z/\left[(1+z)\,H\left(z\right)\right]$ we get an integral for time. The evolution of the Hubble parameter with redshift is given by

$$E(z) = \Big[\Omega_{k,0}(1+z)^2 + \Omega_{m,0}(1+z)^3 + \Omega_{DE,0}(1+z)^{3(1+w_{DE})} \\ + \Omega_{r,0}(1+z)^4\Big]^{1/2} , \tag{1.18}$$

where $E\left(z\right) = H\left(z\right)/H_0$. The age of the Universe is then expressed as

$$t_0 = H_0^{-1} \int_0^{\infty} \frac{\mathrm{d}z}{E\left(z\right)\left(1+z\right)} . \tag{1.19}$$

We can simplify this integral by noticing that it is dominated by the terms at low redshift. In this regime, the radiation term can be neglected, as it only becomes relevant for higher redshifts of about $z \sim 10^3$. For a flat Universe with a cosmological constant ($\Omega_{k,0} = 0$ and $w_{DE} = -1$) the integral becomes

$$t_0 = H_0^{-1} \int_0^{\infty} \frac{\mathrm{d}z}{\left(1+z\right)\left[\Omega_{m,0}\left(1+z\right)^3 + \Omega_{DE,0}\right]^{1/2}} . \tag{1.20}$$

This integral has an exact solution

$$t_0 = \frac{H_0^{-1}}{3\sqrt{1-\Omega_{m,0}}} \ln\left(\frac{1+\sqrt{1-\Omega_{m,0}}}{1-\sqrt{1-\Omega_{m,0}}}\right) , \tag{1.21}$$

using the following relation $1 = \Omega_{m,0} + \Omega_{DE,0}$. In the absence of the cosmological constant, the age of the Universe is

$$t_0 = \frac{2}{3} H_0^{-1} . \tag{1.22}$$

Using $H_0 = 73.04 \pm 1.04$ Km/s/Mpc from Riess et al. (2022) and the estimation from Eq. (1.22) one finds that the age of the Universe must be inside the range 8.8 Gyr $< t_0 <$ 9.1 Gyr. However, Jimenez et al. (1996) estimated the age of globular clusters in the Milky Way to be 13.5 ± 2 Gyr. This is clearly incompatible, and can only be avoided by the addition of dark energy. In Fig. 1.1 we can see that for an open Universe without cosmological constant, the product $H_0\, t_0$ is always inferior to the constraint coming from the oldest stellar ages. For the open Universe we have,

$$t_0 = \frac{H_0^{-1}}{1-\Omega_{m,0}} \left[1 + \frac{\Omega_{m,0}}{2\sqrt{1-\Omega_{m,0}}} \ln\left(\frac{1-\sqrt{1-\Omega_{m,0}}}{1+\sqrt{1-\Omega_{m,0}}}\right)\right] . \tag{1.23}$$

For a flat Universe with a cosmological constant we see that there is a region where the Universe, for a certain value of $\Omega_{m,0}$ has an age that is superior to that of the oldest stars. We can therefore conclude that the age of the Universe, and of its oldest stars, is robust evidence for the existence of dark energy.

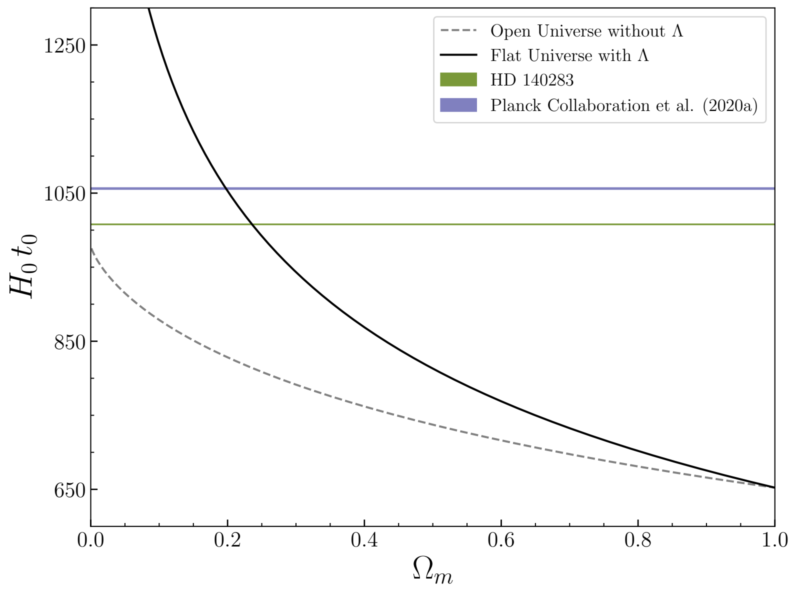

FIGURE 1.1: Plot of the cosmic age t_0 multiplied by the Hubble constant H_0. The solid dark curve corresponds to a flat Universe with a cosmological constant satisfying the relation $\Omega_{m,0} + \Omega_{DE,0} = 1$. The dashed gray line represents an open Universe without cosmological constant. The solid green line is the $H_0\,t_0$ constraint for the minimum age allowed for the Universe, coming from the age of the oldest stars. For this case, the star HD 140283 with $t_0 = 14.46 \pm 0.31$Gyr from Bond et al. (2013) was used. The solid blue line is the t_0 constraint coming from Planck Collaboration et al. (2020a). For all the above cases, the Hubble constant takes the value of $H_0 = 73.04$ Km/s/Mpc, from Riess et al. (2022).

The discovery of dark energy is usually attributed to the Supernova observations. Independently from one another, Riess et al. (1998) and Perlmutter et al. (1999) reported a late-time cosmic acceleration coming from the direct observation of redshift of distant supernovae of type Ia. As stated in previous sections, SNIA are very special objects that present an absolute magnitude M of about -19 at the peak of brightness. What is usually done, in very simplistic terms and ignoring many correction factors, is to observe the apparent magnitude m of these objects and compute their luminosity distance d_L from

$$m - m = 5\log_{10} d_L + 25\,. \tag{1.24}$$

To constrain the parameters of a model, one can use the relation to the luminosity distance to a source at a certain redshift z

$$d_L = (1+z)\,c\int_0^z \frac{dz'}{H(z')}\,, \tag{1.25}$$

where c is the speed of light and the Hubble parameter is given by $H(z) = H_0\,[\Omega_i f_i(z)]^{1/2}$. Note that the f_i are just functions of redshift relative to each component of the Universe, like $f_m(z) = (1+z)^3$ for the case of matter. In Fig. 1.2 we can see the constraint for the

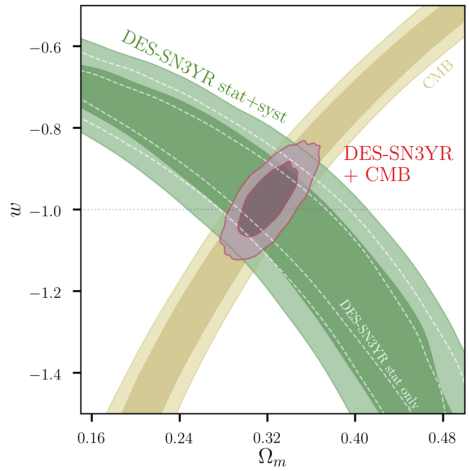

FIGURE 1.2: Constraints on $\Omega_{m,0}$ and w for the flat wCDM model. In this figure are represented the 68% and 95% confidence intervals. From Abbott et al. (2019)

dark energy equation of state parameter w_{DE} and the matter density parameter $\Omega_{m,0}$ for the wCDM model. The difference from ΛCDM, where dark energy comes from a cosmological constant and we have $w = -1$, is that in wCDM dark energy comes from an equation of state parameter w that can be different than -1. This is useful to study deviations from the accepted model. Pantheon+ is another important dataset using SNIA where a total of 1550 distinct Type Ia supernovae, ranging in redshift from $z = 0.001$ to 2.26, is used. The analysis can be found in Brout et al. (2022).

Another solid piece of evidence for dark energy is the cosmic microwave background. From the CMB one can constrain the so-called CMB shift parameter $\mathcal{R}$ that, for a flat Universe, is defined by

$$\mathcal{R} = H_0\sqrt{\Omega_{m,0}} \int_0^{z_{dec}} \frac{dz}{H(z)} , \tag{1.26}$$

where z_{dec} is the redshift at the decoupling epoch. In Fig. 1.3 one can find the constraints for

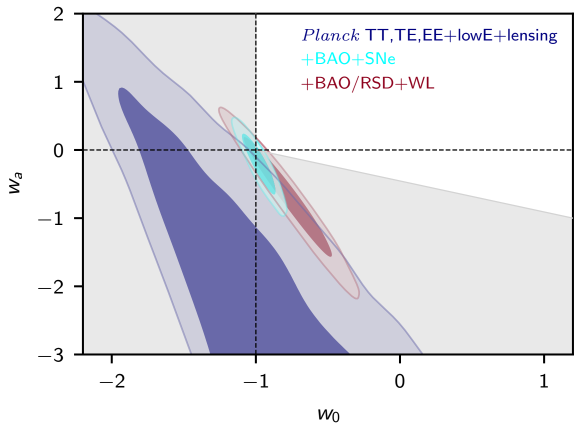

FIGURE 1.3: Posterior distributions of the w_0 and w_a parameters for several combinations of data. From Planck Collaboration et al. (2020a).

w_0 and w_a. In this case, a special parameterization was used for the dark energy equation of state parameter, known as Chevallier-Polarski-Linder parameterization (Chevallier and Polarski, 2001; Linder, 2003), CPL for short. This parameterization is given by

$$w(z) = w_0 + \frac{z}{1+z} w_a \, . \tag{1.27}$$

For ΛCDM we have $w_0 = -1$ and $w_a = 0$.

To conclude this discussion on the observational evidence for dark energy, it is necessary to point out that the baryon acoustic oscillations can provide a robust and independent method to measure the expansion history of the Universe. In the early Universe, before recombination, a hot plasma of baryons and photons coupled together permeated all of space. This plasma was subject to two clashing effects, on one hand a repulsive pressure, on the other gravity's attraction. These effects produced an interesting phenomenon, a series of sound waves that propagate through the baryon-photon plasma, leaving imprints in the baryon perturbations. At recombination, the Universe transitioned to a neutral state, forming the first neutral atoms. Shortly after, baryons and photons decouple; the wave freezes, and photons propagate freely, forming the CMB. The location of the peaks of the waves serves as standard rulers and can be used to constrain dark energy parameters. An interesting review on BAO's can be found in Bassett & Hlozek (2009). Very recently, the Dark Energy Spectroscopic Instrument (DESI) team has published new observations that shed new light on dark energy. They use BAO to constrain cosmological parameters, in particular the dark energy equation of state parameter, focusing on two models of interest: wCDM and w_0w_aCDM. This last model uses the parameterization in Eq. (1.27). They report, in Adame et al. (2024a), a preference in the data for w_0w_aCDM over wCDM. This conclusion is corroborated by an extended analysis in Adame et al. (2024b), which reports a preference for w_0w_aCDM over ΛCDM.

From the theoretical perspective, there are a great number of models described in the literature that attempt to explain dark energy. This thesis does not aim to extensively review all of these models. Instead, a few will be mentioned in this chapter and, in the following chapters, the focus will be on a specific set of models that can provide an alternative description of dark energy. There are two general categories that all of these models fall into. Starting from the Einstein equations, in Eq. (1.1), the first approach consists of modifying the energy-momentum tensor $T_{\mu\nu}$ on the right-hand side, consisting in the addition of new physical entities. In this category one can find wCDM, parameterizations of dark energy (such as CPL), and scalar fields (provided we specify a potential) such as in quintessence, Bekenstein model, runaway dilaton, rolling tachyon, and many others. In Motta et al. (2021) one can find a review of a great number of parameterizations of the dark energy equation of state parameter and constraints for each model, and in Tsujikawa

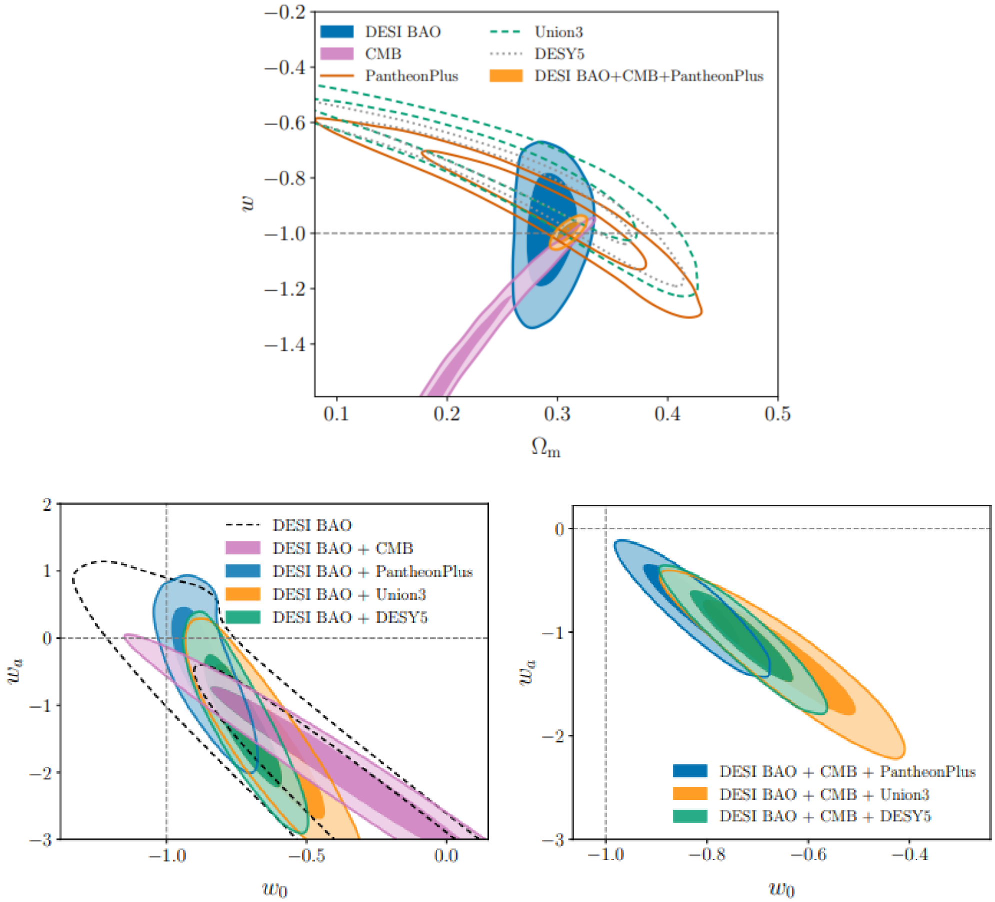

FIGURE 1.4: Constraints on $\Omega_{m,0}$ and w in the flat wCDM model on the top panel, showing the combined constraint from DESI, CMB and Pantheon+. On the bottom panel are represented the constraints for the flat $w_0 w_a$CDM model. From Adame et al. (2024a).

(2013) a review of the quintessence field. The second category consists in modifying the left-hand side of Einstein equations, which is the case for the modified gravity models, such as $f(R)$ gravity. See Tsujikawa (2010) for a review on modified gravity models. In summary, modifying the energy-momentum tensor in the Einstein equations equates to adding new entities to the theory. In modified gravity we change how curvature acts in the presence of matter, in contrast with the first category, where we are changing the form of the equations describing gravity.

Throughout this thesis, several models will be discussed, including the Bekenstein model, the runaway dilaton, single-field quintessence, and the rolling tachyon.

1.6 Fundamental constants and their stability

The previous sections described the current state of cosmology, starting from a historical perspective, presenting the current standard model of cosmology, and finally mentioning a few shortcomings that this model presents. Now, we get to the central point of this thesis, as it mostly concerns with the variation of fundamental constants, namely the fine-structure constant α. But what does it mean to have variable fundamental constants? What does it mean for cosmology? How can we incorporate it in our models? In this section, we find a brief historical context on the development of this idea and an explanation of some of the most fundamental consequences of the existence of these variations in the models presented in this thesis.

Fundamental constants are an important piece of any physical theory, setting the magnitude of the physical processes. By definition, the fundamental constants are not calculable within the framework of the physical theory. In fact, fundamental constants must be measured, thus endowing our theories with predictive power. One can make a list of constants needed for a given theory. The size of the list might change depending on the theory we are considering, and on our current knowledge. Increasing our understanding of a given theory can increase the number of fundamental constants. A good example of this is the case of the massive neutrinos in the standard model of particle physics. If the standard model is to be extended, considering massive neutrinos, it will have to include an extra seven new constants. One can also decrease the number of constants by implying an unification of interactions at some energy scale.

Table 1.1 summarizes the fundamental constants for the interactions of the standard model of particle physics and General Relativity, and it reveals the extent of parameters that our theories can't calculate. In this way, tests of the constancy of the fundamental parameters are, in a sense, a test of the validity of the theories themselves. If we were to measure any kind of variation (spatial or temporal) of any fundamental constant, we would have to change our theories. Thus, the study of the constancy of fundamental constants can reveal to us new physics. The idea of varying fundamental constants is not recent, and one can date it back to 1937. Dirac was among the first to question the constancy of fundamental physical constants, laying the foundation for an entirely new direction in theoretical physics, as described in Dirac (1937) and Dirac (1938). In particular, Dirac observed that certain dimensionless parameters constructed from ratios of fundamental constants were of similar order of magnitude, stating that it could not be a coincidence, and that it should be explained by an underlying physical principle. This idea set in motion a search for variations of fundamental constants. Following this pioneering work, it was proposed in Jordan (1937) that these constants could evolve dynamically over time, a concept now realized in various extensions of the standard model. This idea has since developed into a rich field of research focusing on variations of the fine-structure constant α, the proton-to-electron

Constant	**Symbol**	**Value**
Speed of light	c	$299\,792\,458\,\mathrm{m\,s^{-1}}$
Planck constant (reduced)	$\hbar$	$1.054571817\ldots \times 10^{-34}\,\mathrm{J\,s}$
Newton constant	G	$6.67430(15) \times 10^{-11}\,\mathrm{m^2\,kg^{-1}\,s^{-2}}$
Charge of the electron	e	$1.602\,176\,634 \times 10^{-19}\,\mathrm{C}$
Weak coupling constant (at m_Z)	$g_2(m_Z)$	0.6520 ± 0.0001
Strong coupling constant (at m_Z)	$g_3(m_Z)$	1.221 ± 0.022
Weinberg angle	$\sin^2\theta_W\,(91.2\,\mathrm{GeV})_{\overline{MS}}$	0.23121 ± 0.00004
Electron Yukawa coupling	h_e	2.94×10^{-6}
Muon Yukawa coupling	h_μ	0.000607
Tauon Yukawa coupling	h_τ	0.0102156
Up Yukawa coupling	h_u	0.000016 ± 0.000007
Down Yukawa coupling	h_d	0.00003 ± 0.00002
Charm Yukawa coupling	h_c	0.0072 ± 0.0006
Strange Yukawa coupling	h_s	0.0006 ± 0.0002
Top Yukawa coupling	h_t	1.002 ± 0.029
Bottom Yukawa coupling	h_b	0.026 ± 0.003
Quark CKM matrix angle	$\sin\theta_{12}$	0.22650 ± 0.00048
	$\sin\theta_{23}$	$0.04053^{0.00083}_{0.00061}$
	$\sin\theta_{13}$	$0.00361^{+0.00011}_{-0.00009}$
Quark CKM matrix phase	δ_{CKM}	$1.196^{+0.045}_{-0.043}$
Higgs potential quadratic coefficient	$\hat{\mu}$	$\simeq 88.4\,\mathrm{GeV}$
Higgs potential quartic coefficient	λ	$\simeq 0.13$
QCD vacuum phase	θ_{QCD}	$< 10^{-10}$

TABLE 1.1: List of fundamental constants of our standard model, from Uzan (2024).

mass ratio μ, and the gravitational constant G. As stated previously, this thesis will focus on variations of the fine-structure constant, for which we have extensive reviews summarizing the current state of the art, available in Uzan (2011), Martins (2017), and Uzan (2024). This dimensionless constant quantifies the strength of electromagnetic interactions, and it is defined by

$$\alpha = \frac{e^2}{4\pi\epsilon_0\hbar c}\,, \tag{1.28}$$

where ϵ_0 is the permittivity of free space, and the values of the electron charge e, the reduced Planck constant $\hbar$, and the speed of light c are presented in Table 1.1. The fine-structure constant, with the approximate value of $\alpha \simeq 1/137.03599917721 \pm 1.6 \times 10^{-10}$ from Mohr et al. (2024), was first introduced in Sommerfeld (1916) to explain the gap in the fine-structure of the spectral lines of the hydrogen atom. While this program started nearly a century ago and has attracted the attention of many researchers today, it was fairly neglected until a claim by Webb et al. (1999) stating that the fine-structure constant was smaller in the past. We have several experiments (local, astrophysical, and cosmological) inquiring about the constancy of α. Even though there are studies investigating spatial variations of α (see Webb et al., 2011) it is common to assume homogeneity and search for time variations. While astrophysical data measures α-variations directly as

$$\frac{\Delta\alpha}{\alpha} = \frac{\alpha\,(z) - \alpha_0}{\alpha_0}\;, \tag{1.29}$$

where α_0 is the value of the fine-structure constant today, local data measure the current *drift* of this constant, usually defined as

$$\frac{1}{H_0}\left(\frac{\dot{\alpha}}{\alpha}\right)_0\;. \tag{1.30}$$

How do we measure this constant? There is a wide range of different experiments one can conduct to determine the fine-structure constant: local – atomic clocks; astrophysical – quasar spectra; cosmological – CMB and BBN; geophysical – natural nuclear reactors.

Atomic clocks

Regarding local data, we have the atomic clocks, which consist of laboratory constraints of α based on frequency measurements. Most commonly using atoms of cesium, rubidium, hydrogen, strontium or aluminum, atomic clocks work by measuring the frequency of light emitted when an atom transitions between energy levels. These energies are know and can be very precisely calculated theoretically using fine and hyperfine corrections of the atomic spectra, that are directly proportional to α. By measuring these frequencies for long periods, we can calculate small changes in their value, corresponding to a drift in the fine-structure constant. In Uzan (2024) one can find an extended discussion on this subject, and a great number of measurements of this phenomena. In this thesis, it will be used the constrain

$$\frac{1}{H_0}\left(\frac{\dot{\alpha}}{\alpha}\right)_0 = (0.014 \pm 0.015)\ \text{ppm}\;, \tag{1.31}$$

from Lange et al. (2021) and the updated constraint

$$\frac{1}{H_0}\left(\frac{\dot{\alpha}}{\alpha}\right)_0 = (0.0024 \pm 0.0035)\ \text{ppm}\;, \tag{1.32}$$

from Filzinger et al. (2023), which is the latest constraint we have. We might see, in the future, an improvement on this constraints coming nuclear clocks, see Fadeev, Berengut & Flambaum (2020).

Natural nuclear reactor

Regarding geophysical data, we can constrain the fine-structure constant at a redshift of around $z \sim 0.14$, using the natural nuclear reactor in Oklo. This natural fission reactor in

Gabon was active about two billion years ago, and it provides a window to time variations of α, since a different value of this constant would alter the interaction cross-sections and decay rates of the nuclei (Damour and Dyson, 1996). One finds a constraint of

$$\frac{\Delta\alpha}{\alpha} = (0.005 \pm 0.61)\ \text{ppm}\ , \tag{1.33}$$

from Gould, Sharapov & Lamoreaux (2006) and Onegin (2012).

Quasar spectra

The measurement of redshift is of great relevance in astrophysics and it relies on the analysis of absorption and emission spectra. Quasi-stellar objects (QSO), usually referred to as quasars, are extremely luminous galactic cores. Dust and gas falling into the supermassive black hole emit radiation, placing quasars among the brightest objects in the Universe. Their absorption spectra provide a powerful tool for the investigation of variations of the fine-structure constant, which we can access through the presence of clouds in the line of sight. The value of the fine-structure constant has an impact on the relative position of the absorption lines. By analyzing the spectra we can compute the value of α in the redshift at which the absorption system is found. There is a large amount of spectroscopic data from QSO, however, not all of that data is dedicated to the study of fundamental constants. On one hand, we have a set of 293 measurements using the Keck-HIRES and VLT-UVES spectrographs from Webb et al. (2011). The analysis of the measurements taken from quasars at $0.22 \leq z \leq 4.18$ suggests a spatial variation of α with a 4.2σ significance, constraining its value at

$$\frac{\Delta\alpha}{\alpha} = (-2.16 \pm 0.86)\ \text{ppm}\ . \tag{1.34}$$

It is important to note that there are some concerns regarding systematics in the data, which are not yet fully resolved, Whitmore & Murphy (2015). On the other hand, there is a a dedicated set of measurements, specifically designed for the analysis of the fine-structure constant. Even though they are fewer (about 30), they carry more statistical significance, and extend the redshift to up to $z \sim 7.06$. These include measurements from VLT-UVES and Keck-HIRES instruments listed on Martins (2017), from the Subaru telescope reported in Murphy & Cooksey (2017), from HARPS and ESPRESSO spectrographs in Milaković et al. (2020) and Murphy et al. (2022), respectively. The combination of these measurements amounts to

$$\frac{\Delta\alpha}{\alpha} = (-0.23 \pm 0.56)\ \text{ppm}\ . \tag{1.35}$$

It is clear that these two sets of measurements are in disagreement. While the former prefers a negative variation of α, the latter is consistent with a non-variation.

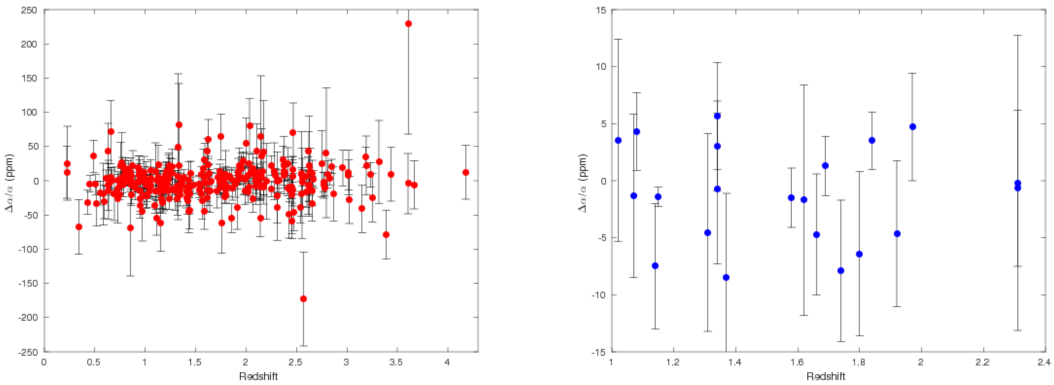

FIGURE 1.5: This figure, from Martins (2017), displays the astrophysical measurements of α. The figure on the left represents the dataset from Webb et al. (2011), and the figure on the right the data points from VLT-UVES and Keck-HIRES in Table 1 of Martins (2017). Noticing the ranges in the vertical axes of both plots, we can see the improvement in precision.

Cosmic microwave background

The CMB can also be used to constrain variations of the fine-structure constant by analyzing CMB temperature anisotropies and recombination, since both depend on α, see Galli et al. (2011) and Uzan (2024). Using data from Planck Collaboration et al. (2020a), one can find

$$\frac{\Delta\alpha}{\alpha} = (-700 \pm 2500) \text{ ppm} , \tag{1.36}$$

from the analysis in Hart & Chluba (2018). This allows for a constraint of the fine-structure constant at a very high redshift of $z \sim 10^3$.

Big Bang nucleosynthesis

The fine-structure constant α plays a crucial role in determining the rates of electromagnetic interactions, which are fundamental to nuclear reactions during BBN. Changes in α would alter the cross-sections of nuclear reactions, ultimately affecting the relative abundances of light elements. Thus, observational data on primordial element abundances can be used to place constraints on any variation in α during BBN. Deal, M. & Martins, C. J. A. P. (2021) report a variation of

$$\frac{\Delta\alpha}{\alpha} = 2.1^{+2.7}_{-0.9} \text{ ppm} , \tag{1.37}$$

constraining α at a redshift of $z \sim 10^8$. This way, models with variations of the fine-structure constant can be used to, at least, alleviate the cosmological lithium problem. In this analysis, the authors report a 2σ tension, in contrast to the 5σ mentioned above. This is a very promising area of study, however this analysis is highly model-dependent.

Using this wide range of local, astrophysical, cosmological, and even geophysical data we can constrain α with great precision. However, having explored the different types of α constraints available, how can we motivate such studies? Variation in the fine-structure constant α has been suggested as a potential solution to the H_0 tension. The idea is that early variation in fundamental constants, specifically α, can shift the redshift at which recombination occurs. This delay in recombination would consequently affect the expansion rate of the Universe during the epoch of the last scattering, potentially alleviating discrepancies in the value of the Hubble constant between local distance ladder measurements and those inferred from the Cosmic Microwave Background (CMB) measurements (Hart and Chluba, 2020). The addition of the electron-to-proton mass ratio to these models can further alleviate this tension, while being in agreement with other constraints on the variation of constants (Chluba and Hart, 2023).[10] While this approach holds promise, challenges remain in constructing α-variation models that are both physically plausible and consistent with local constraints on α. These constraints, particularly from atomic clocks, impose stringent limits on the variation of α, creating a fine-tuning issue for such models. Vacher & Schöneberg (2024) have shown that solving the H_0 tension by incorporating the α-variation into cosmological models leads to significant fine-tuning problems, since the necessary changes in α would conflict with the strict local constraints on its current value. This highlights the delicate balance necessary to solve the H_0 tension, while maintaining consistency with local measurements of fundamental constants.

In addition to potentially resolving the H_0 tension, varying α may provide insights into the nature of dark energy. Additionally, the accelerated expansion of the universe and potential variations in fundamental constants, such as α, may be related. Models with variations of fundamental constants can be categorized into two classes, depending on their relation with dark energy. Class I models are, by definition, models for which the same field is the source for dark energy and α-variation. Such models, like the rolling tachyon in Dias et al. (2024) and the runaway dilaton (with exponential potential) in Vacher et al. (2023), can provide a source for dark energy, thus removing the need for a cosmological constant. In contrast with Class I, we have Class II models where the degrees of freedom responsible for the varying fundamental constants do not account for dark energy. This is the case for the model explored in Vacher et al. (2022), where the field couples to the dark energy sector, but still requires a cosmological constant. Before starting the discussion of these models, there is an important consequence of having a varying α to discuss.

[10] For the reader interested in knowing more about the subject, I suggest having a look at these papers Lee et al. (2023), Sekiguchi & Takahashi (2021), and Schöneberg & Vacher (2024).

1.7 Fine-structure constant variations – connection with the EEP

The equivalence principle is one of the cornerstones of General Relativity. While it started as an empirical truth stating that, in the absence of other forces, all bodies in an external gravitational field will fall with the same acceleration, now it has been elevated to the status of principle. What is described above is the so-called universality of free fall. The EEP we know today is composed of three conditions:

Universality of free fall (UFF): in an external gravitational field, the trajectory of any free-falling test-body is independent of its internal structure (mass or chemical composition). This is an equivalent statement to saying that the inertial and gravitational masses are equal.

Local position invariance (LPI): any non-gravitational experiment will yield the same results independently of where and when in the Universe it is performed. The laws of physics are invariant under spacetime translations.

Local Lorentz invariance (LLI): any non-gravitational experiment performed in an inertial frame will yield the same results independently on the velocity of its rest frame. In order words, LLI states that all inertial frames are equivalent.

Schiff's conjecture states that for a complete and self-consistent theory of gravity that satisfies the UFF (ocasionally called the weak equivalence principle, or WEP) will necessarily fulfill the EEP (Will, 2014). Now, let us just imagine two identical laboratories performing (locally) identical experiments to determine α. One located here on Earth, and another in our neighbour, the Andromeda galaxy. According to the LPI they should measure exactly the same thing, in other words, α must indeed be constant. If this is not true, then we are breaking LPI, and thus, according to Schiff's conjecture, violating the broader EEP (Will, 2014). This way, testing the constancy of fundamental constants is a test of this principle. In subsequent chapters we will find tests of the WEP, namely the MICROSCOPE experiment (Touboul et al., 2022), can be used to constrain α-varying models. Even though this is the most accurate test for the WEP available to us at the time, there are still constraints using lunar ranging and torsion balance measurements, found in Wagner et al. (2012) and Müller, Hofmann & Biskupek (2012) respectively.

The violation of the EEP is an important consequence of any theory that encompasses a variation of the fine-structure constant, which will be discussed in more detail in Chapter 2.

1.8 String theory and the Swampland

In modern physics, one of the main motivations to search for new physics is the search for a unified description of all fundamental forces. One of the main contenders for providing a unification between particle physics and gravity is string theory. String theory proposes to replace the fundamental building blocks of nature with vibrating strings. It is the vibration of these strings that gives rise to the particles and forces observed in nature. String theory offers a potential path toward a consistent theory of quantum gravity, while adding certain complexity to the mathematics that describe the Universe, requiring the existence of additional spatial dimensions beyond the familiar four-dimensional spacetime. These extra dimensions, compactified at scales beyond current experimental reach, offer a vast array of possibilities for model building.[11] However, this complexity comes with significant challenges, including the problem of vacuum selection in the string Landscape. The string Landscape comprises the space of solutions to the equations governing string theory, each corresponding to a different vacuum state with its own physical properties. This leads to a question about the predictability of string theory. The Swampland is the space of low-energy effective field theories that do not complete in the ultraviolet, see Vafa (2005).

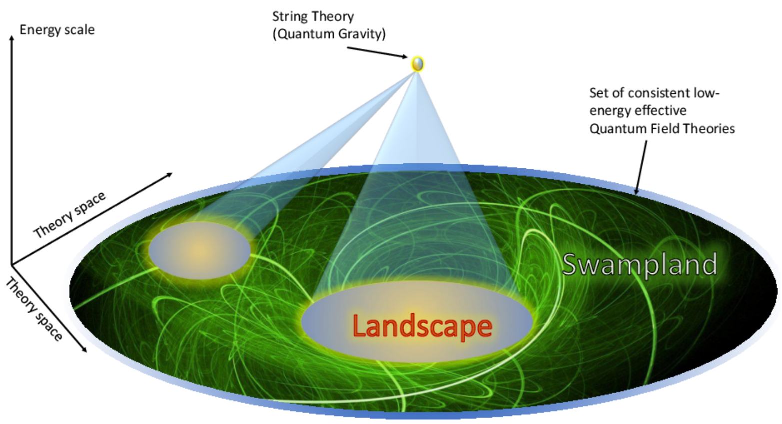

Figure 1.6: A schematic illustration of the space of the string Landscape and the string Swampland, from Palti (2019).

The problem with the Swampland, represented in Fig. 1.6, is that in order to search for a complete theory of quantum gravity, one must be able to find the precise boundary between the Landscape and the Swampland, distinguishing the different vacua. The Swampland program, proposed in recent years, consists of a set of conjectures serving as general guidelines to construct stable quantum field theories of gravity Palti (2019). This

[11] The different ways to compactificatify the extra spatial dimensions lead to a large number of possible solutions, bigger than 10^{755} (Halverson, Long, and Sung, 2017).

thesis does not focus on the theory behind string theory or on the validity of such conjectures. It will, however, make use of string theory motivated models and Swampland conjectures.

1.9 Outlook of the thesis

The fine-structure constant is one of the fundamental parameters in physics, governing the strength of electromagnetic interactions and playing a pivotal role in a wide range of physical phenomena, and studying its variation may lead to the discovery of new physics. A variation of α would directly imply a breakdown of the EEP, representing a profound shift in our understanding of nature, challenging the foundations of General Relativity and offering insights into a unified theory of quantum gravity. Variations of α can be modeled by coupling scalar fields to the electromagnetic sector, or occurring naturally as a consequence of certain string theories. The dynamics of these scalar fields over cosmological timescales leads to measurable changes in α. As stated previously, Class I models can provide with dark energy, removing the necessity of a cosmological constant. By studying these models, we can test the interplay between fundamental constants and the dynamics of the Universe's expansion, providing new light to dark energy and the cosmological constant problem. Cosmological and astrophysical phenomena also offer key motivations, as in the case of BBN and the lithium problem. Additionally, variations in α have effects on the cosmic microwave background and large-scale structure, allowing us to probe early-Universe physics and constrain cosmological parameters. It can also prove useful for the H_0 tension.

Empirical studies of α-variation span a wide range of methods, ranging from quasar absorption spectra, which probe the conditions in distant astrophysical environments, to highly precise atomic clock experiments conducted on Earth. These complementary techniques have yielded some of the stringent constraints on α. Exploring the behavior of the fine-structure constant not only allows us to test existing theories, but also opens the door to the potential discovery of new physical laws that govern the Universe. As such, the study of α-variations represents a relevant area of research with far-reaching implications for cosmology and particle physics.

This concludes the introduction chapter. Chapter 2 extends on some of the topics discussed in this chapter including fine-structure constant variations, their relation with the EEP and dark energy, descriptions of the Bekenstein model in Vacher et al. (2022), string theory motivated models including the runaway dilaton, and rolling tachyon models discussed in Vacher et al. (2023) and Dias et al. (2024), respectively. In addition, the compatibility of the Swampland criteria with the latest cosmological data (including fine-structure constant data) will be examined, applying these constraints to various quintessence models for dark energy, as explored in Schöneberg et al. (2023). Chapter 3 details the datasets used throughout this work and the methodologies and codes used to constrain the models. Finally, in Chapter 4 we can find the results of the studies conducted, and the respective discussion, followed by the conclusion in Chapter 5.

2

Theoretical Framework

Before describing the models studied in this thesis, it is important to discuss in more detail some of the theories behind the variations of the fine-structure constant and its connections to the EEP. It is useful to start with a simple phenomenological model, proposed by Jacob Bekenstein.

2.1 Variations of the fine-structure constant *à la* Bekenstein

In 1982, Bekenstein published a paper, whose title, "Fine-structure constant: Is it really a constant?", inspired many others to ask the same question. In Bekenstein (1982), he proceeds to describe a theory of a varying fine-structure constant, highlighting the fundamental ingredients necessary to do it consistently. This is done by slightly modifying the Lagrangian for the Electromagnetic (EM) field. In order to get a fine-structure constant that is spacetime dependent, we can impose a variation of the elementary charge, since $\alpha = e^2/\left(4\pi\epsilon_0\hbar c\right)$. It is easy to see that, in this scenario, we do not have charge conservation. So, the need arises to adopt certain postulates for the framework. First, for a constant α, one must recover Maxwellian EM. Secondly, variations of α must arise from dynamical equations, implying that the variations influence charged matter while charged matter influences α. We must also require that these dynamical equations are derived from an invariant action, which must be locally gauge invariant and respect causality. It must also be time reversal invariant. The author imposes that the theory must be valid up to a certain scale, the Planck's length. Finally, gravity is described by Einstein's equations, however the EEP must not be assumed, otherwise α variability is out of the question.

Now that the fundamental postulates of the theory have been established, one can start to think about how to write down the Lagrangian. As stated above, we vary α by requiring a variation in the elementary charge e. Considering neutral atoms, we must require that

e changes in the same way for all particles as $e = e_0\varepsilon\left(x^\mu\right)$, where e_0 is a constant and ε describes the variation of the charge, is a constant for all particles. The simplest action to consider is

$$S_{em} = -\frac{1}{16\pi}\int d^4x\,\sqrt{-g}\,F^{\mu\nu}F_{\mu\nu}\ , \tag{2.1}$$

where $F_{\mu\nu} = \varepsilon^{-1}\left[\partial_\mu\left(\varepsilon A_\nu\right) - \partial_\nu\left(\varepsilon A_\mu\right)\right]$, recovering the usual tensor for constant ε. It is important to note that $F_{\mu\nu}$ is gauge invariant, where the gauge transformation for the vector potential is $\varepsilon A_\mu \rightarrow \varepsilon A_\mu + \partial_\mu\chi$. Terms such as $m^2 A_\mu A^\mu$ violate gauge invariance, and higher order terms in $F_{\mu\nu}$ do not give Maxwellian electrodynamics for constant α.

When varying S_{em}, one does not get a dynamical equation for ε. One of the postulates is that the dynamics for the variation of α must be derived by an action principle. For this reason, one must have a separate action for ε. We want the action to be invariant under rescaling of ε, so the Lagrangian density must be constructed from the metric and $\varepsilon^{-1}\partial_\mu\varepsilon$. Given that ε is a dimensionless quantity, the Lagrangian density $\mathcal{L}_\varepsilon \propto \varepsilon^{-2}\,\partial_\mu\varepsilon\,\partial^\mu\varepsilon$ does not have the required dimensions, for any given combination of $\hbar$ and c. Any combination of the Lagrangian above with the Ricci scalar or Ricci tensor can give the correct dimensions, although such terms will introduce extra derivatives on $\partial_\mu\varepsilon\,\partial^\mu\varepsilon$, violating causality. This problem can be solved by introducing a length scale l

$$S_\varepsilon = -\frac{1}{2}\hbar c l^{-2}\int d^4x\,\sqrt{-g}\,\varepsilon^{-2}\,\partial_\mu\varepsilon\,\partial^\mu\varepsilon\ . \tag{2.2}$$

The introduction of l causes problems for scale invariance, but the theory is safe for 10^{-15} cm $> l \geq\ 10^{-33}$ cm. As long as l is between those values, the theory does not contradict the experimental tests of electromagnetic theory. An extended discussion on this model can be found in Bekenstein (2002).

This model is a good starting point if one wishes to build a cosmological model for varying α. This is exactly what is done in Sandvik, Barrow & Magueijo (2002). Starting from Bekenstein's idea of a varying α they build a more general model, where they include the effects of the gravitational dynamics of the expansion of the Universe. The Lagrangian densities for the scalar field ε and for the EM part of the theory are the same as the ones shown above. As in Magueijo, Sandvik & Kibble (2001), by introducing the transformation $\psi := \ln\varepsilon$ the Lagrangians becomes

$$\mathcal{L}_{em} = -\frac{1}{4}\varepsilon^{-2}F_{\mu\nu}F^{\mu\nu} = -\frac{1}{4}e^{-2\psi}F_{\mu\nu}F^{\mu\nu}\ , \tag{2.3}$$

and

$$\mathcal{L}_\psi = -\frac{\omega}{2}\partial_\mu\psi\partial^\mu\psi\ , \tag{2.4}$$

where $\omega = \hbar c/l^2$. The action for this model is

$$S = \int d^4x\,\sqrt{-g}\,\left(\mathcal{L}_g + \mathcal{L}_{mat} + \mathcal{L}_\psi + \mathcal{L}_{em}\,e^{-2\psi}\right)\ , \tag{2.5}$$

where $\mathcal{L}_g = (16\pi G)^{-1} R$ and $\mathcal{L}_{mat}$ is the Lagrangian for the matter content. An auxiliary gauge field $a_\mu := \varepsilon A_\mu$ can be introduced, so that $f_{\mu\nu} = \varepsilon F_{\mu\nu} = \partial_\mu a_\nu - \partial_\nu a_\mu$, recovering the usual form of the EM Lagrangian. At this point, one can vary the action in terms of the metric to derive the cosmological equations, or in terms of the scalar field ψ to obtain the dynamics describing the variations of α. It can be shown that varying the action in terms of the metric yields

$$G_{\mu\nu} = 8\pi G \left(T^{mat}_{\mu\nu} + T^{\psi}_{\mu\nu} + T^{em}_{\mu\nu}\, e^{-2\psi}\right) \ . \tag{2.6}$$

This equation describes how the contents of the Universe and spacetime curvature affect each other. For the dynamics of ψ one can find

$$\Box\, \psi = -\frac{2}{\omega}\, e^{-2\psi} \mathcal{L}_{em} \ . \tag{2.7}$$

For pure radiation $\mathcal{L}_{em} \propto (E^2 - B^2) = 0$, so the equation of motion for ψ becomes

$$\Box\psi = 0 \ . \tag{2.8}$$

Thus, in a radiation-dominated Universe, the contribution to the change in e is negligible. The α variation effect must come from the matter and dark energy dominated epochs.

One can now ask how does the Universe evolve with this field as one of its contents. The first step is to write the Friedmann equation

$$G_{00} = 8\pi G \left(T^{mat}_{00} + T^{\psi}_{00} + T^{em}_{00}\, e^{-2\psi}\right) \ . \tag{2.9}$$

Assuming a spatially-flat, homogeneous and isotropic FLRW metric with the scale factor $a(t)$ we find

$$\left(\frac{\dot{a}}{a}\right)^2 = \frac{8\pi G}{3}\left[\rho_m \left(1 + \zeta\, e^{-2\psi}\right) + \rho_r\, e^{-2\psi} + \frac{\omega}{2}\dot{\psi}^2 + \rho_\Lambda\right] \ , \tag{2.10}$$

where $\rho_\Lambda = \Lambda/\left(8\pi\right)$ is the cosmological vacuum energy and ζ a coupling constant. This equation describes the rate of expansion of the Universe dictated by its contents. From Eq. (2.7), using the FLRW metric, one can find the following equation dictating the dynamics of the field

$$\ddot{\psi} + 3H\dot{\psi} = \frac{\omega}{2} e^{-2\psi} \zeta\, \rho_m \ . \tag{2.11}$$

The conservation equations for the matter and radiation densities are

$$\dot{\rho}_m + 3H\rho_m = 0 \ , \tag{2.12}$$

$$\dot{\tilde{\rho}}_r + 4H\tilde{\rho}_r = 2\dot{\psi}\rho_r \ , \tag{2.13}$$

Eq. (2.10)-(2.13) describe the cosmological evolution for this model. To quantify the amount by which the fine-structure varies for this model is fairly simple. Recalling the relation $\psi = \ln \varepsilon$ one finds

$$\frac{\Delta\alpha}{\alpha} = \frac{\alpha}{\alpha_0} - 1 = \left(\frac{\varepsilon}{\varepsilon_0}\right) - 1 = e^{2\Delta\Psi} - 1 \,, \tag{2.14}$$

where the subscript 0 refers to the value of that quantity today.

Another interesting quantity to compute is the Eötvös parameter η, which quantifies weak equivalence principle violations. This parameter is defined by a ratio of accelerations of two different bodies

$$\eta := 2\frac{|a_1 - a_2|}{a_1 + a_2} \,, \tag{2.15}$$

which in this case is

$$\eta = \frac{\zeta_E \, |\zeta_1 - \zeta_2|}{\pi\omega} = \frac{\zeta_E \, |\zeta_1 - \zeta_2|}{\pi\zeta_p} \frac{\zeta_p}{\zeta_m} \frac{\zeta_m}{\omega} \,, \tag{2.16}$$

where E denotes Earth, and the numbers 1 and 2 refer to two different test bodies.

This analysis is useful to get an initial idea on how the variations of the fine-structure constant arise and how they lead to violations of the EEP. A more detailed analysis of this model is present in Barrow, Sandvik & Magueijo (2002), and in Barrow, Magueijo & Sandvik (2002) one can find variations of the model described above, where the authors consider inhomogeneous cosmological variations in the fine-structure "constant".

2.2 Dynamical coupling constants and EEP violation

In Kaluza (1921) it was first proposed to extend the spacetime metric to a 5-dimensional quantity, coming to the conclusion that the fine-structure constant depended on the size of the extra-dimension (compactified in a circle). In 1967, Weinberg (1967) used the Brout-Englert-Higgs mechanism to write the masses of leptons. What were once thought fixed structures of the physical world evolved into quantities determined by dynamical effects. In 1964, it was shown that in any theory in which the coupling constants are spacetime dependent, there will be some sort of violation of the weak equivalence principle (DeWitt and DeWitt, 1964). Since then, many authors have applied this idea to specific models. One example of this is the dilaton model, from a string theory background, where all the couplings are spacetime dependent and that dependence is monitored by a scalar field (see Damour and Polyakov, 1994). A general formula for the structure of Einstein's equivalence principle violations for the dilaton is derived from this last paper.

The EEP is a cornerstone of the theory of general relativity. It is a statement about the equivalence of the gravitational and inertial mass. In other words, the acceleration experienced by a falling body is equivalent to the presence of an external gravitational field. This idea was of the utmost importance when Einstein was building his theory of general relativity. Even though Einstein added the EP as a hypothesis, it arises as a direct consequence of the existence of a universal coupling between matter and gravity, the curved spacetime metric, see Damour (2012). There are several models that predict the violation of this principle. A dynamical scalar field leading to a varying α will necessarily violate the EEP. The relation between these observables is model-dependent, but calculable in a given model. Understanding these consistency conditions is therefore important, not only for comparing the results of different observational probes, but also as a discriminating test between alternative models. It is important to investigate if these kinds of models are compatible with all the extremely accurate tests of the EP, such as Touboul et al. (2022), Wagner et al. (2012), and Müller, Hofmann & Biskupek (2012). Most EEP tests done so far are local, performed on the ground or on orbiting satellites.

It is of the utmost importance to understand how the EEP is violated and how to quantify this violation, if one is to test it. To quantify violations of the EEP we define the so-called Eötvös parameter as

$$\eta = 2\frac{|a_A - a_B|}{a_A + a_B} , \tag{2.17}$$

where A and B are indices referring to two different particles. Usually, we would have $a_A - a_B = 0$ but, with variations of the fine-structure constant, two different objects (with different nuclear compositions) will accelerate at distinct rates when placed in a gravitational field. How does one compute the acceleration of an object placed in a gravitational field when the fundamental constants are spacetime dependent? In Damour (2012) we can get a good idea of how this can be done. Starting with the action of a point particle in a gravitational field

$$S = -\int m_i \left[\alpha\left(\phi\right)\right] \sqrt{-g_{\mu\nu} dx^{\mu} dx^{\nu}} , \tag{2.18}$$

where we are only considering the variation of the fine-structure constant. Note that now the mass of a particle is dependent on the value of the fine-structure constant, since among other things, it receives a contribution from EM interactions. The acceleration is then given by

$$a_i = g - \nabla \ln m_i \left[\alpha\left(\phi\right)\right] = g - m_i^{-1} \frac{\partial m_i \left[\alpha\left(\phi\right)\right]}{\partial \alpha} \nabla \alpha . \tag{2.19}$$

From this equation it is clear that a variation of α, corresponding to $\nabla\alpha \neq 0$, will result in a violation of the UFF ($a_i \neq g$). From Uzan (2003) we have that, for a model with coupling to F^2

$$m\left(A, Z, \phi\right) = Z m_p + \left(A - Z\right) m_n + E_s + E_{EM}\left(\phi\right) . \tag{2.20}$$

By specifying the degrees of freedom responsible for the variations of α, one can get a general expression for the Eötvös parameter, using the empirical mass formula above. The next logical step in this thesis is to look at such models.

2.3 Olive & Pospelov - the extended Bekenstein model

The so-called extended Bekenstein model is a generalization of the model described in Section 2.1. Now, instead of having a scalar field coupled to the EM sector, we can have a general function of the scalar field $B_F(\phi)$, responsible for the variations of the fine-structure constant. Dubbed as O&P model, this model assumes a coupling of the scalar field ϕ with all the fermion fields of the standard model ψ, the dark energy assumed to be a cosmological constant Λ, and a dark matter particle χ, as proposed in Olive & Pospelov (2002). Therefore the cosmological action becomes

$$\begin{aligned} S = \int d^4x\sqrt{-g}\,\Big\{&-\frac{1}{2}M_{\rm Pl}^2 R + \frac{1}{2}M_*^2\partial_\mu\phi\partial^\mu\phi - M_{\rm Pl}^2\Lambda_0 B_\Lambda(\phi) \\ &- \frac{1}{4}B_F(\phi)\,F_{\mu\nu}F^{\mu\nu} + \bar{\psi}\left[i\gamma^\mu D_\mu - m_\psi B_\psi(\phi)\right]\psi \\ &+ \bar{\chi}\left[i\gamma^\mu D_\mu - M_\chi B_\chi(\phi)\right]\chi - V(\phi)\Big\}\,. \end{aligned} \tag{2.21}$$

In this work it is considered that $V(\phi) = 0$ and that the field is homogeneous, with no spatial variations. It is important to notice that, the term $M_{Pl}^2\Lambda_0 B_\Lambda(\phi)$ is effectively acting as a potential for the scalar field. Assuming that the field value remains small on cosmological time scales, one can expand the couplings up to the first order obtaining the evolution of the fine-structure constant with the field

$$\frac{\Delta\alpha}{\alpha} = \frac{\alpha(\phi)}{\alpha_0} - 1 = B_F^{-1}(\phi) - 1 = -\zeta_F\Delta\phi\,, \tag{2.22}$$

by expanding the couplings up to first order $B_i(\phi) = 1 + \zeta_i(\phi - \phi_0)$. Expanding to first order in ϕ is enough, since $\Delta\alpha/\alpha$ is constrained to be very close to 0. From this expression, one can derive today's time derivative of α as

$$\frac{1}{H_0}\left(\frac{\dot{\alpha}}{\alpha}\right)_{z=0} = -\zeta_F\phi_0'\,. \tag{2.23}$$

As in Olive & Pospelov (2002), we also assume that the background cosmology evolution in the O&P model is given by the FLRW metric, where the field's density and pressure are given by $\rho_\phi = \frac{1}{2}M_*^2\dot{\phi}^2$, $P_\phi = \frac{1}{2}M_*^2\dot{\phi}^2$. Here, M_* is a mass scale associated to the ϕ sector. Throughout this work, it was assumed that the energy scale associated with the varying α is of the order of the Planck scale, $M_* = M_{Pl}$. Minimizing the action with respect to ϕ gives the coupled Klein-Gordon equation of motion

$$\ddot{\phi} + 3H\dot{\phi} = -\frac{1}{M_*^2}\sum_i \rho_i\zeta_i\,, \tag{2.24}$$

where $\zeta_i = (\zeta_\chi, \zeta_\Lambda, \zeta_b)$. Note that ζ_F does not appear in the equation of motion due to a null averaging of the photon fields $\langle F^2\rangle$.

One can also define the Eötvös parameter for this model. For a system of two masses of Aluminium and Platinum, the Eötvos parameter η, quantifying deviations from the WEP, can be expressed as in Olive & Pospelov (2002)

$$\eta \simeq 2.9 \cdot 10^{-2} \zeta_b \zeta_F \ , \tag{2.25}$$

where ζ_b is the coupling constant of the field to baryons. It is important to note that this expression is obtained assuming that the field ϕ does not distinguish between protons and neutrons, coupling the same way for both.

In Vacher et al. (2022), two scenarios of this model were explored. The first, where we assume that the field couples identically to baryons and dark matter ($\zeta_m = \zeta_b = \zeta_\chi$) and finally, a scenario where we allow for these coupling to be different ($\zeta_b \neq \zeta_\chi$). Due to the degeneracies of the parameter space appearing in the observables, one can only constrain their product. As such, we introduce the new product parameters η_i defined as $\eta_i = \zeta_F \, \zeta_i$.

2.4 Runaway dilaton

In opposition to the more phenomenological models presented above, we now present the runaway dilaton. In string theory, GR emerges as a low-energy limit of string theory, predicting the existence of a scalar partner of the graviton, known as the dilaton. For a massless dilaton, one finds that all the coupling constants in the theory become dependent on the dilaton ϕ, hence becoming spacetime dependent.

As in Damour & Polyakov (1994), the low-energy effective action for the massless modes of a string is given by

$$\begin{aligned} S = \int d^4x \, \sqrt{g} \Big\{ \frac{B_g(\phi)}{\mu'} R + 4 \frac{B_\phi(\phi)}{\mu'} \left[\Box\phi - (\nabla\phi)^2 \right] - B_F(\phi) \frac{1}{4} F^2 \\ - B_\psi(\phi) \overline{\psi} \not{D} \psi + \dots \Big\} \ , \end{aligned} \tag{2.26}$$

where μ' (usually defined as α' in the literature but redefined in this work to avoid confusion with the fine-structure constant) is a quantity related to the string scale, and the B_i are coupling functions to the different sectors of the theory. One can then introduce the following rescaling, for the metric, such that we recover the usual Lagrangian for gravity.

$$g_{\mu\nu} := C B_g(\phi) \, \tilde{g}_{\mu\nu} \ , \tag{2.27}$$

where we choose C such that, at the present time $CB_g(\phi_0) = 1$. With these rescalings, one finds that the total action in the Einstein frame is given by

$$S = \int d^4x \sqrt{g}\Big[\frac{R}{16\pi G} + \frac{1}{8\pi G}\left(g^{\mu\nu}\partial_\mu\phi\partial_\nu\phi - V(\phi)\right) \\ -\frac{1}{4}B_F(\phi)F^a_{\mu\nu}F^{a\mu\nu} - B_\psi(\phi)\bar{\psi}\not{D}\psi + \dots,\Big] . \tag{2.28}$$

One can now wonder what are the cosmological consequences of this model. The way to proceed is exactly like before: vary the action with respect to the metric to find the equations describing the evolution of the Universe, and vary with respect to the rescaled dilaton field to find its dynamical equation. The Friedmann equation and the runaway dilaton equation for this model are

$$H^2 = \frac{8\pi G}{3}\rho , \tag{2.29a}$$

$$\ddot{\phi} + 3H\dot{\phi} = 4\pi G\sigma , \tag{2.29b}$$

where the ρ is the total density of all components of the universe (including the dilaton). Furthermore, the σ parameter is given by

$$\sigma = \sigma_V + \sigma_m = -\frac{1}{8\pi G}\frac{\partial V(\phi)}{\partial\phi} + \sum_i \alpha_i(\phi)\left(3P_i - \rho_i\right) , \tag{2.30}$$

where $\alpha_i(\varphi)$ are the dilaton couplings to each field i, not to confuse with the fine-structure constant α. The total energy and density of the field ϕ are defined by

$$\rho_\phi = \rho_T + \rho_V = \frac{1}{8\pi G}\left[\dot{\phi}^2 + V(\phi)\right] , \tag{2.31}$$

$$P_\phi = P_T + P_V = \frac{1}{8\pi G}\left[\dot{\phi}^2 - V(\phi)\right] , \tag{2.32}$$

where T and V denote the kinetic and potential contributions respectively.

The coupling of ϕ to the hadronic matter is a relevant parameter, and its evolution is given by

$$\alpha_h(\phi) \sim 40\,\frac{\partial \ln B_F^{-1}(\phi)}{\partial\phi} = 40\, b_F\, c\, e^{-c\phi} , \tag{2.33}$$

where α_h is the coupling of the scalar field to hadronic matter and b_F is a constant. Setting $c = 1$ one can eliminate b_F by diving the coupling by the present day coupling of the field to hadronic matter ($\alpha_{h,0}$)

$$\frac{\alpha_h}{\alpha_{h,0}} = e^{-(\phi-\phi_0)} , \tag{2.34}$$

and ϕ_0 is a scalar field at present time.

There are two local constraints for the current value of the coupling, the Eddington's parameter γ that quantifies the amount of deflection of light and the Eötvös parameter. The

Cassini spacecraft constrains the Eddington parameter (Bertotti, Iess, and Tortora, 2003) as

$$\gamma - 1 = (2.1 \pm 2.3)\, 10^{-5} \,, \tag{2.35}$$

and we have that

$$\gamma - 1 = -2\alpha_{h,0}^2 \,. \tag{2.36}$$

As for the Eötvös parameter, for two different particles A and B, it is given by

$$\eta_{AB} \sim 5.2 \times 10^{-5} \alpha_{h,0}^2 \,, \tag{2.37}$$

We are interested in studying spacetime variations of the fine-structure constant for this class of models. Following the previous assumption that all gauge fields must couple to the same $B_F\,(\phi)$ we must have

$$\alpha_{EM} \propto B_F^{-1}\,(\phi) \propto \left(1 - b_F\, e^{-c\phi}\right) \,, \tag{2.38}$$

which implies that the fine-structure constant (α_{EM}) is related to the hadronic coupling. The dynamical equation describing the evolution of the fine-structure constant is given in Damour, Piazza & Veneziano (2002), where the authors perform a similar analysis starting from the same assumptions, finding

$$\frac{1}{H}\frac{\dot{\alpha}}{\alpha} = \frac{b_F\, e^{-c\phi}}{1 - b_F\, e^{-c\phi}}\phi' \sim b_F\, e^{-c\phi}\phi' \sim \frac{\alpha_h}{40}\phi' \,. \tag{2.39}$$

In order to figure out the evolution of the fine-structure constant, one can integrate Eq. (2.39) to get α in function of redshift

$$\frac{\Delta\alpha}{\alpha}\,(z) := \frac{\alpha\,(z) - \alpha_0}{\alpha_0} = B_F^{-1}\,(\phi\,(z)) - 1 = b_F\left(e^{-\phi_0} - e^{\phi(z)}\right) \,. \tag{2.40}$$

Making explicit the dependence on the hadronic coupling

$$\frac{\Delta\alpha}{\alpha}\,(z) = \frac{1}{40}\alpha_{h,0}\left[1 - e^{1-e^{-(\phi(z)-\phi_0)}}\right] \,. \tag{2.41}$$

In Vacher et al. (2023), different scenarios were explored: a runaway dilaton with a cosmological constant Λ; a runaway dilaton with a constant coupling to dark energy; and a runaway dilaton with an exponential potential. For the first two cases the potential is set to $V = 0$ and for the last case, with the exponential potential, the dilaton can provide dark energy.

2.5 Rolling tachyon

The rolling tachyon, similarly to the runaway dilaton, is a model that arises from string theory. In particular, when studying Dp-branes one finds that they incorporate both massless and massive scalar fields, gauge fields, and a tachyon, commonly referred to as the rolling tachyon (see Sen, 2002a). The Dp-branes are p-dimensional objects where the endpoints of open strings are constrained to move under Dirichlet boundary conditions. These branes are fundamental components of any string theory framework and can be regarded as distinct dynamical entities, carrying momentum, energy, and charges. The low-energy effective action governing the behavior of D-branes is known as the Dirac-Born-Infeld (DBI) action (in Leigh, 1989; Gibbons, 2002), being initially introduced as a generalization of electromagnetism (Dirac, 1962; Born and Infeld, 1934). The tachyon is characterized by an imaginary mass, which, in classical terms, might suggest superluminal motion. Nonetheless, they maintain causal commutation relations, ensuring that causality is preserved. The units of this field are unconventional. Because $\dot{\phi}$ is dimensionless, it follows that ϕ carries units of time, or equivalently inverse energy—unlike a canonical scalar field, which is either dimensionless or expressed in energy units via the Planck mass. Meanwhile, the potential retains the standard units of energy density. Consequently, the field's values must generally be interpreted relative to the coefficients appearing in the potential.

From a cosmological perspective, the tachyon field exhibits a notable property: its dynamics are described by a non-canonical Lagrangian. This leads to unconventional forms for the energy density and pressure associated with the field. The Lagrangian density for the tachyon field is

$$\mathcal{L}_T = -V(\phi)\sqrt{1-\partial_\mu\phi\partial^\mu\phi}\,, \tag{2.42}$$

and the energy density and pressure are given by

$$\rho_\phi = \frac{V(\phi)}{\sqrt{1-\partial_\mu\phi\,\partial^\mu\phi}}\,, \tag{2.43}$$

$$p_\phi = -V(\phi)\sqrt{1-\partial_\mu\phi\,\partial^\mu\phi}\,. \tag{2.44}$$

From this, one can express the equation of state as

$$w_\phi \equiv \frac{P_\phi}{\rho_\phi} = \dot{\phi}^2 - 1\,, \tag{2.45}$$

which is constrained between $-1 < w_\phi < 0$. To derive the equation of motion for the rolling tachyon we analyze the following action for the field ϕ

$$S = \int d^4x\sqrt{-g}\left[-\frac{R}{2k^2} - V(\phi)\sqrt{1-\partial_\alpha\phi\partial^\alpha\phi}\right]\,, \tag{2.46}$$

where $k = \sqrt{8\pi G}$. It is important to note that the variation of the fine-structure constant is derived from the following interaction term

$$\mathcal{L}_{int} = \frac{\left(2\pi\alpha_s'\right)^2}{4\beta^2} V\left(\phi\right) \mathrm{Tr}\left(g^{-1}Fg^{-1}\right) + ... \tag{2.47}$$

where α_s is a quantity related to the string mass scale and β is a warped factor. The first term is the usual term describing gravity, followed by the rolling tachyon term (with he field ϕ), the electromagnetic sector coupled to the rolling tachyon field $B_F\left(\phi\right)$ and finally the Lagrangian for the term containing the matter content of the Universe. In order to investigate the dynamics of the tachyon field one has to vary the action with respect to the scalar field as $\delta S/\delta\phi \equiv \delta S = 0$. By doing this, one finds

$$\delta S = -\int d^4x\sqrt{-g}\left[\delta\left(V\left(\phi\right)\sqrt{1-\partial_\alpha\phi\partial^\alpha\phi}\right) + \frac{1}{4}F_{\mu\nu}F^{\mu\nu}\delta B_F\left(\phi\right)\right] = 0\,. \tag{2.48}$$

Computing each term separately, for the first term one finds

$$\delta\left(V\left(\phi\right)\sqrt{1-\partial_\alpha\phi\partial^\alpha\phi}\right) = V'\left(\phi\right)\sqrt{1-\partial_\alpha\phi\partial^\alpha\phi}\,\delta\phi + V\left(\phi\right)\delta\sqrt{1-\partial_\beta\phi\partial^\beta\phi}\,, \tag{2.49}$$

where the primed quantities are derivatives with respect to the tachyon field. The variation of the square-root term can be a bit more complicated

$$\int d^4x\sqrt{-g}\,\delta\sqrt{1-\partial_\alpha\phi\partial^\alpha\phi} = \int d^4x\sqrt{-g}\,\left(1-\partial_\alpha\phi\partial^\alpha\phi\right)^{-1/2}\partial^\beta\phi\,\partial_\alpha\delta\phi\,. \tag{2.50}$$

By applying partial integration to the expression above, and neglecting the boundary terms as they do not contribute to the equation of motion, we are left with

$$V'\left(\phi\right)\sqrt{1-\partial_\alpha\phi\partial^\alpha\phi} + \nabla_\beta\left[\frac{V\left(\phi\right)\partial^\beta\phi}{\sqrt{1-\partial_\tau\phi\partial^\tau\phi}}\right] = 0\,. \tag{2.51}$$

We will consider an homogeneous, isotropic and flat Universe, and for that using the FLRW metric. We will also assume the field to be homogeneous ($\partial_\mu\phi = -\partial_t\phi$). It will be required to compute the d'Alembertian operator of the scalar field, which we can easily see that it is

$$\Box\phi = g^{\mu\nu}\nabla_\mu\partial_\nu\phi = g^{\mu\nu}\left(\partial_\mu\partial_\nu\phi - \Gamma^\alpha{}_{\mu\nu}\partial_\alpha\phi\right) = -\ddot{\phi} - 3H\dot{\phi}\,. \tag{2.52}$$

Finally, one can write the dynamical equation for the rolling tachyon as

$$\frac{\ddot{\phi}}{1-\dot{\phi}^2} + 3H\dot{\phi} + \frac{1}{V}\frac{dV}{d\phi} = 0\,. \tag{2.53}$$

It is interesting to note that, while the Lagrangian for the rolling tachyon is non-canonical, for $|\dot{\phi}| \ll 1$ the field behaves like a canonical scalar field (a short discussion on this can be found in Appendix A of Dias et al., 2024).[1] Furthermore, in the limit of $\dot{\phi} \to 0$, the field behaves like a cosmological constant. The tachyon field is a natural candidate to explain the late-time expansion history. Throughout this thesis, we will assume that the field alone is sufficient to play the role of dark energy.

Another interesting consequence of the DBI action is that the coupling of the tachyon field to the EM sector arises naturally, in opposition to the previous models where a coupling like B_F has to be postulated. This can be seen from the more general DBI action for a D-brane

$$S = -\int d^4x V(\phi) \sqrt{-\det\left(g_{\mu\nu} + \partial_\mu \phi \partial_\nu \phi + 2\pi\mu' \beta^{-1} F_{\mu\nu}\right)}\,, \tag{2.54}$$

where β is a warped factor, related to the compactification of the extra dimensions, and M_s is the string mass scale Sen (2002a), Sen (2002b), Garousi, Sami & Tsujikawa (2005), Copeland et al. (2005), and Martins & Moucherek (2016). One can show that the last term in the integral is equivalent to the usual term describing the EM sector, coupled to the tachyon field. By expanding the determinant one finds

$$\mathcal{L}_{EM} = -\frac{(2\pi\alpha')^2 V(\phi)}{4\beta^2} F^{\mu\nu} F_{\mu\nu}\,, \tag{2.55}$$

where we can compare the factors multiplying F^2 with the coupling function B_F. A detailed derivation can be found in Appendix A of Dias et al. (2024). Realizing that, for string theory, the fine-structure constant is defined as

$$\alpha(\phi) = \frac{\beta^2 M_s^2}{2\pi V(\phi)}\,. \tag{2.56}$$

We can express the variation of the fine-structure constant, independently of β and M_s, as

$$\frac{\Delta\alpha}{\alpha_0} = \frac{V(\phi_0)}{V(\phi)} - 1\,. \tag{2.57}$$

The fact that the variation arises naturally means that this model is restricted by cosmological and fine-structure constant constraints, preventing a fast evolution within the potential, as we will see in Chapter 4. In this limit, there is also a canonical field equivalent.

There are a number of different potentials well motivated from a high energy perspective. It was considered in this thesis a set of potentials proposed in Garousi, Sami & Tsujikawa (2005) and Copeland et al. (2005) due to their cosmological relevance. The most relevant of those will be discussed, however for a full description of all the potentials see Dias et al. (2024).

[1] In order to see this it is required to re-normalize it as $\widetilde{\phi} = \int \sqrt{V} \mathrm{d}\phi$.

Massive rolling scalar potential

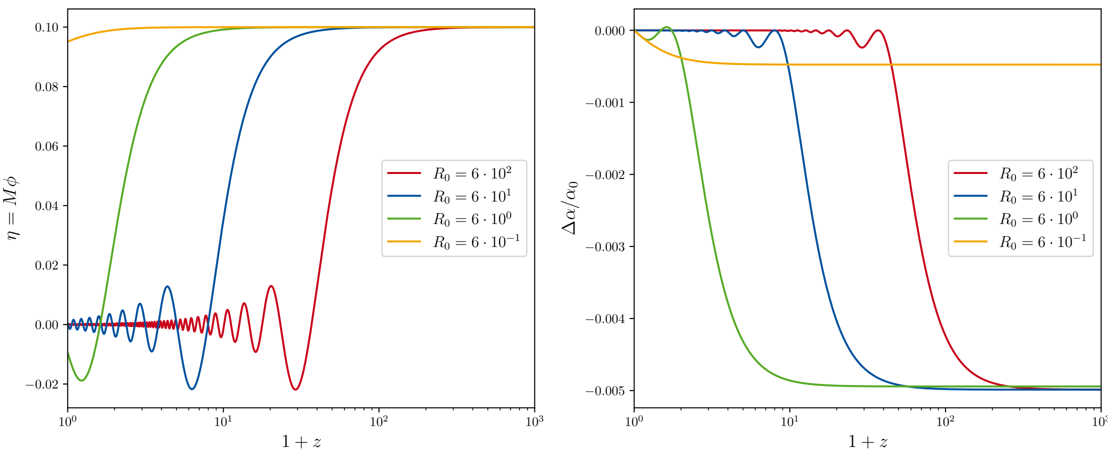

Figure 2.1: Plots for the evolution of the massive rolling scalar potential and variation of the fine-structure constant from Dias et al. (2024). Note that both η and $\Delta\alpha/\alpha_0$ almost perfectly scale with the initial value of η (η_∞), and therefore we fix $\eta_\infty = 0.1$.

The first of the potentials to be described is the massive rolling potential, which given by

$$V(\phi) = V_0 \exp\left[\frac{1}{2}M^2\phi^2\right] . \tag{2.58}$$

It represents an effectively massive potential, since $\ln V = \ln V_0 + \frac{1}{2}M^2\phi^2$. The field ϕ can be replaced by a dimensionless one $\eta = M\phi$. The equation of motion for this new field becomes

$$\frac{\eta'' + \gamma\eta'}{R^2 - (\eta')^2} + 3\eta' + \eta R^2 = 0 , \tag{2.59}$$

where $R = M/H$, and $\gamma = \mathrm{d}\ln H/\mathrm{d}\ln a$. It is evident that the equations only depend on R, η, and V_0, along with their derivatives with respect to the logarithm of the scale factor, denoted here by a prime. The evolution of η, and the variations of α can be seen in Fig. 2.1.

The condition $|\dot{\phi}| < 1$ imposes the constraint $|\eta'| < R$, which can also be derived from the equations of motion. The variation of the fine-structure constant is given by

$$\frac{\Delta\alpha}{\alpha_0} = \exp\left(\frac{\eta_0^2 - \eta^2}{2}\right) - 1 , \tag{2.60}$$

where $\eta_0 = \eta(z=0)$, and its logarithmic derivative is $\alpha'/\alpha = -\eta \cdot \eta'$.

Inverse Power-Law Potential

The inverse power-law potential is given by

$$V(\phi) = V_0(N\phi)^{-n} , \tag{2.61}$$

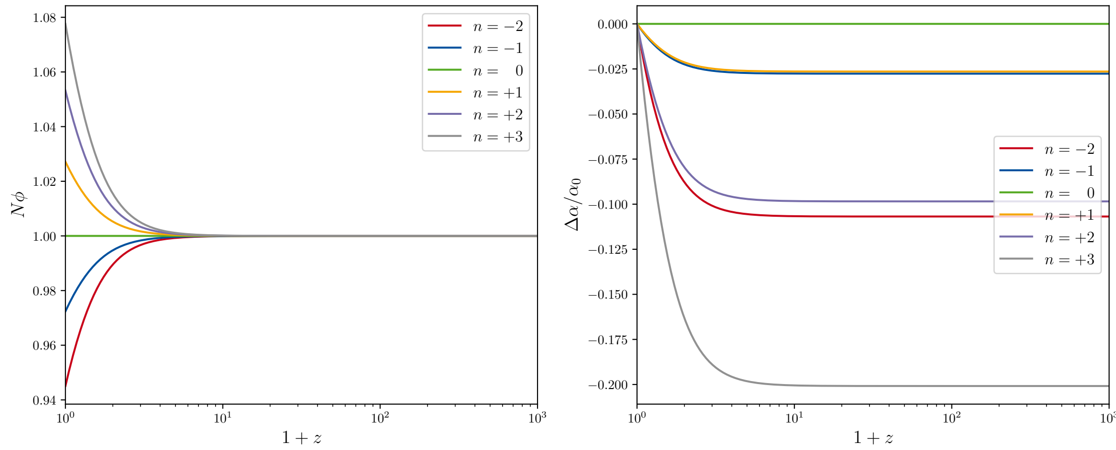

Figure 2.2: Same plots as in Fig. 2.1 but for the inverse power-law potential. We set $\phi_\infty = 10^4$Mpc $\approx 3.34h/H_0$, balancing it with $N = 10^{-3}$Mpc^{-1} for easier visualization. From Dias et al. (2024).

where N is an arbitrary constant, and $V_0 = V(\phi = 1/N)$. In this formulation, N cancels out from the equations of motion and the expressions for the fine-structure constant, making it physically irrelevant. The equation of motion for this potential is

$$\frac{\ddot{\phi}}{1-\dot{\phi}^2} + 3H\dot{\phi} - \frac{n}{\phi} = 0\,, \tag{2.62}$$

For this potential, the variation of the fine-structure constant is

$$\frac{\Delta\alpha}{\alpha_0} = \left(\frac{\phi}{\phi_0}\right)^n - 1\,, \tag{2.63}$$

with $\alpha'/\alpha = -n\phi'/\phi$. Prior studies by Garousi, Sami & Tsujikawa (2005) and Copeland et al. (2005) indicate that this potential supports accelerated expansion asymptotically only if $n < 2$. However, even for $n \geq 2$, transient acceleration can last long enough to be cosmologically significant. When $n = 0$, the model is fully equivalent to a cosmological constant, and no constraints are expected for ϕ_∞. Figure 2.2 shows example field evolutions for different values of n.

Anti-Massive Potential

The anti-massive potential is given by

$$V(\phi) = V_0 \exp\left[-\frac{M^2}{2}\phi^2\right]\,, \tag{2.64}$$

and is the direct equivalent of the massive potential. Using the same transformations with $\eta = M\phi$, we define $R = M/H$, and $\gamma = \mathrm{d}\ln H/\mathrm{d}\ln a$. The fine-structure constant

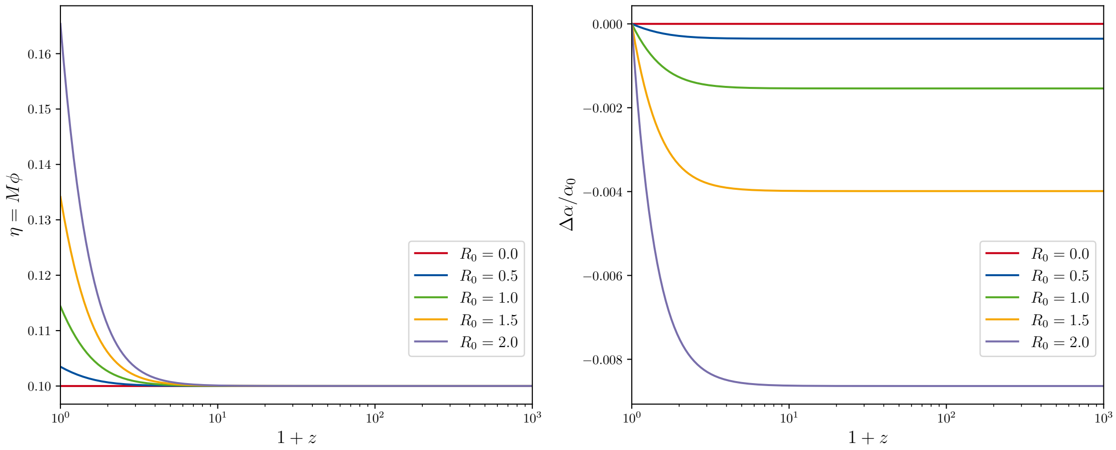

FIGURE 2.3: Same plots as in Fig. 2.1 but for the anti-massive potential. We set $\eta_\infty = 0.1$ and test various values of R_0. From Dias et al. (2024).

variation is

$$\frac{\Delta\alpha}{\alpha_0} = \exp\left(\eta^2 - \eta_0^2\right) - 1 \, , \tag{2.65}$$

with $\alpha'/\alpha = \eta \cdot \eta'$. Figure 2.3 illustrates examples of field evolutions for different values of R_0. In this scenario, the field moves away from the origin ($\eta = 0$) as soon as $R \sim 1$ during cosmic evolution. It is generally expected that this behavior is strongly constrained by local data.

2.6 The Swampland and Cosmological Implications

String theory, as our best candidate for a unified framework of quantum field theory and gravity, proposes a "landscape" of consistent low-energy effective field theories. Surrounding this landscape is the so-called Swampland, a set of quantum field theories that are inconsistent with quantum gravity.[2] To differentiate between viable theories and those in the Swampland, a set of criteria—known as the Swampland conjectures—have been proposed. These conjectures are particularly relevant for cosmology, and place stringent constraints on effective field theories describing the Universe. Here, we discuss the two most relevant criteria, their implications for cosmological models, and their role in testing the viability of quintessence as a dynamical alternative to a cosmological constant (Agrawal et al., 2018).

Distance conjecture:
This conjecture states that the traversable range of scalar fields in field space is bounded by

$$\frac{\Delta\phi}{M_{Pl}} \lesssim \mathcal{O}(1) \, , \tag{2.66}$$

[2] A complete review can be found in Palti (2019) and Beest et al. (2022).

where M_{Pl} is the reduced Planck mass. The conjecture suggests that beyond a finite range in field space, the validity of the effective field theory breaks down, limiting the field excursion $\Delta\phi$. This restriction has profound implications for scalar-field-driven cosmology, as it constrains the dynamics of fields responsible for phenomena such as inflation or dark energy.

The de Sitter conjecture:
The de Sitter Conjecture places a bound on the slope of the scalar potential $V(\phi)$, requiring either

$$\lambda(\phi) = M_{Pl}\frac{|V'(\phi)|}{V(\phi)} \gtrsim \mathcal{O}(1) \qquad \text{or} \qquad g(\phi) = -M_{Pl}^2\frac{V''(\phi)}{V(\phi)} \gtrsim \mathcal{O}(1)\,, \tag{2.67}$$

where primes denote derivatives with respect to ϕ. We will denote these two constraints as the first and second Swampland criterion, respectively. For the de Sitter criteria to hold, either $\lambda(z)$ or $g(z)$ must be positive and, at least, of order unity.

Testing the Swampland with Cosmological Data

To test these criteria, we analyze cosmological datasets within the framework of quintessence. In this model, dark energy is treated as a dynamical degree of freedom described by a scalar field minimally coupled to gravity. The action for quintessence is given by

$$S = \int d^4x\sqrt{-g}\left[\frac{M_{Pl}^2}{2}R - \frac{1}{2}g^{\mu\nu}G_{ij}\partial_\mu\phi^i\partial_\nu\phi^j - V(\phi) + ...\right]\,, \tag{2.68}$$

where G_{ij} is a metric over field space, reducing to 1 in the single-field case and $g_{\mu\nu}$ is the usual metric. For a single scalar field, the Klein-Gordon equation governing its evolution is

$$\ddot{\phi} + 3H\dot{\phi} + V'(\phi) = 0\,, \tag{2.69}$$

with the field density and pressure given by

$$\rho_\phi = \frac{1}{2}\dot{\phi}^2 + V \qquad \text{and} \qquad P_\phi = \frac{1}{2}\dot{\phi}^2 - V\,. \tag{2.70}$$

For this model, the expression for $\Delta\alpha/\alpha$ has to be postulated. However, one should expect to encounter a varying fine-structure constant for the UV-complete theory within the framework of string theory, unless there is some symmetry preventing this. The Lagrangian for the electromagnetic sector becomes

$$\mathcal{L}_{EM} = -\frac{1}{4}B_F(\phi)\,F_{\mu\nu}F^{\mu\nu}. \tag{2.71}$$

Since we don't expect α to significantly change at cosmological scales, we can Taylor expand the coupling function at first order as $B_F(\phi) \simeq 1 + \zeta \cdot (\phi - \phi_0)$ leading to

$$\frac{\Delta\alpha}{\alpha} \simeq -\zeta\,\Delta\phi. \tag{2.72}$$

Furthermore, as earlier, by taking the derivative of $\Delta\alpha/\alpha$ with respect to $\ln a$, one finds the time variation of the fine-structure constant:

$$\frac{1}{\alpha_0}\frac{d\alpha}{d\ln a} = -\zeta\frac{d\phi}{d\ln a}. \tag{2.73}$$

In Schöneberg et al. (2023), a vast number of potentials are explored. However, perhaps the most interesting one is the simple exponential model with

$$V(\phi) = A\exp(\lambda\phi/M_{Pl})\ , \tag{2.74}$$

where λ is a constant. For this case, the first Swampland criterion is taken to be constant, since $\lambda(z) \equiv M_{Pl}|V'/V| = \lambda$. By taking the second derivative of the potential with respect to the field we find $V''/V = \lambda^2$ implying $g(z) = -\lambda^2 < 0$, meaning that the second Swampland criterion is always violated. In Raveri, Hu & Sethi (2019), an expression relating the distance with the de Sitter conjecture is derived and is given by

$$|\Delta\phi/M_{Pl}| \approx \frac{\lambda}{3}\left[\frac{1}{\sqrt{1-\Omega_m}}\ln\left(\frac{1+\sqrt{1-\Omega_m}}{1-\sqrt{1-\Omega_m}}\right) - 2\right] \approx 0.29\lambda\ , \tag{2.75}$$

where $\Omega \approx 0.31$ has been used. This relation is represented in Fig. 2.4, and it allows

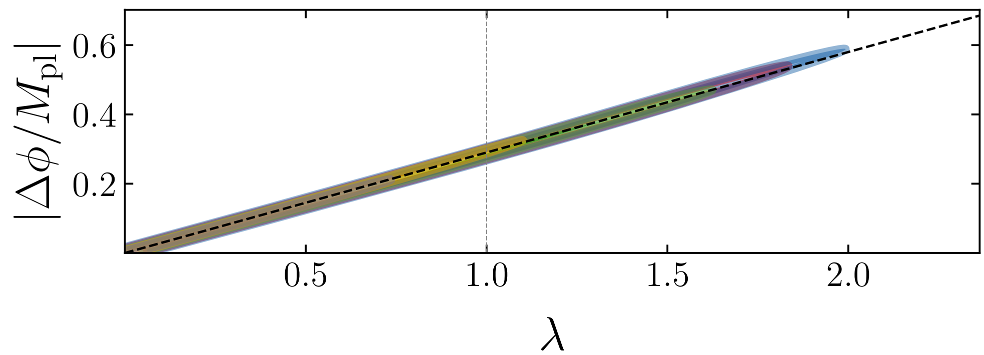

FIGURE 2.4: Correlation between the two Swampland criteria in the exponential case, from Schöneberg et al. (2023).

to conclude that the focus should be investigating the first Swampland criterion. This is because the second criterion is, by definition, always violated and the distance conjecture is more easily satisfied.

Recent studies have highlighted tensions between refined versions of the Swampland criteria and cosmological observations, as detailed in Agrawal et al. (2018), Gashti & Sadeghi (2022), and Fukuda et al. (2019). Provided the conjectures are accepted, they serve as valuable tools for testing cosmological models, in particular, models with dynamical dark energy.[3] In the next section, the datasets and methodology used to constrain this models will be described.

[3] More details on the implications of the Swampland conjectures to dark energy can be found in Heisenberg et al. (2018), Heisenberg et al. (2019), Wang (2020), and Raveri, Hu & Sethi (2019).

3

Datasets and methodology

To constrain the parameters of the models described in Chapter 2, we need a powerful code that can compute the dynamics of all the cosmological components throughout the evolution of the Universe, in addition to the dynamics of the fields previously described. The so-called Boltzmann solvers allow the computation of cosmological parameters as an output of these dynamics, while they can be modified to take into account variations of the fundamental constants. They can also compute perturbations, but it goes beyond the scope of this thesis as we do not inquire about spatial variations of α. The Cosmic Linear Anisotropy Solving System (Lesgourgues, 2011), or `CLASS`, was chosen as it is a code that fulfills all of the above mentioned requirements, and was already being used by certain collaborators.[1] In order to derive constraints for both the cosmological parameters and the model specific ones, the `MontePython v3.5` code for Bayesian MCMC inference was used (Brinckmann and Lesgourgues, 2019).[2] Together with `GetDist` (Lewis, 2019), for the visualizing data and producing contour plots, we reach an effective methodology to constrain the proposed models by exploring the synergies between these codes.[3] It is relevant to note that in later works (Dias et al., 2024), `Liquidcosmo` was used as a replacement for `GetDist`.[4] `Liquidcosmo` was developed by Nils Schöneberg (ICC, Barcelona University), and his code allowed for a facilitated production of contour plots, removing some problems encountered with `GetDist`.

To use `CLASS` to constrain the models described in the previous Chapter it is necessary to modify the Boltzmann solver to incorporate the dynamics of the fields. This is not an easy task due to the complexity of the code. For the extended Bekenstein and runaway dilaton model, these alterations were performed by Léo Vacher (SISSA, Trieste) and Nils

[1] Available at `https://github.com/lesgourg/class_public`.
[2] Available at `https://github.com/brinckmann/montepython_public`.
[3] Available at `https://github.com/cmbant/getdist`.
[4] Available at `https://github.com/schoeneberg/liquidcosmo`.

Schöneberg, and I was able to accompany the process, getting familiarized with the code. The modifications to the `CLASS` software for the rolling tachyon were implemented by me with the invaluable help, advice and guidance of Léo Vacher and Nils Schöneberg.

It is relevant to mention that, for the rolling tachyon project, the computational work that was conducted by me (and several runs for the Swampland project), with the support of INCD funded by FCT and FEDER under the project FCT/CPCA/2022/01, with reference 2022.72694.CPCA.A0, and under the Advanced Computing Project "Variation of fundamental constants - Constraining models beyond the Standard Model of Cosmology" with reference 2023.10382.CPCA.A1.[5]

For the four models explored in this thesis, a similar combination of datasets was used. A succinct description of the data used in common throughout the four papers will follow, along with certain exceptions.

Common datasets

Throughout this thesis the following likelihoods, for cosmological data, include:

– Planck: CMB data from the *Planck* 2018 data release, using the *Planck* legacy likelihood Aghanim et al. (2020a), and the lensing (Aghanim et al., 2020b).[6]

– BAO: we use the DR12 data from the SDSS-III BOSS survey (Alam et al., 2017) as well as the SDSS main galaxy sample (Ross et al., 2015) and the 6dFGS sample (Beutler et al., 2011).[7]

– Supernovae: The Pantheon+ supernova sample from Scolnic et al. (2022), comprising 1701 uncalibrated supernovae light curves with redshifts up to $z = 2.26$.

– Cosmic chronometers (CC): $H(z)$ measurements from Moresco et al. (2022).

Regarding fine-structure data the likelihoods are:

– Atomic clocks (AC): Local data to place bounds on the drift rate of the fine-structure constant from Filzinger et al. (2023).

– Oklo: The analysis of the abundances from the natural nuclear reactor at Oklo allows us to obtain a bound for $\Delta\alpha/\alpha$, from Petrov et al. (2006).

– Quasars: A set of more than 300 measurements from VLT-UVES, Keck-HIRES, HARPS and Subaru instruments in Webb et al. (2011) and Murphy & Cooksey

[5] The project can be found in `https://doi.org/10.54499/2023.10382.CPCA.A1`.
[6] Available at `https://pla.esac.esa.int/`.
[7] We haven't used updated datasets like DR16, in Alam et al. (2021), and DESI BAO, in Adame et al. (2024a) and Adame et al. (2024b), as they don't majorly affect the parameter constraints in the models. This way, we did minimized the convergence time of all the runs.

(2017), and described in Martins (2017).[8] Finally, we also use the recent ESPRESSO spectrograph measurement, in Murphy et al. (2022).

Finally, we use data from MICROSCOPE to put constraints on the Eötvös parameter, from Touboul et al. (2022). Its important to note that we did not use the likelihoods from MICROSCOPE to constrain the rolling tachyon model, but more on this in Chapter 4.

Exceptions

There are certain exceptions to the list above appearing in the extended Bekenstein and runaway dilaton models. These exceptions are Supernovae data, where we used the Pantheon dataset (Riess et al., 2018). Regarding fine-structure data, the likelihoods are the Atomic clocks (AC), for which we used Lange et al. (2021).

Note that for the extended Bekenstein model we have used $H(z)$ measurements from Moresco et al. (2016) instead. It is also relevant to note that, in the paper regarding the Swampland paper (Schöneberg et al., 2023), we have used the updated BAO from SDSS DR16 (Alam et al., 2021) and the ground-based ACT and SPT data from Aiola et al. (2020) and Balkenhol et al. (2023), which provide the most precise non-Planck CMB anisotropy data to date.

[8] The original measurement papers can be found in Agafonova et al. (2011), Molaro et al. (2013), Evans et al. (2014), Songaila & Cowie (2014), Murphy, Malec & Prochaska (2016), and Kotuš, Murphy & Carswell (2017), for the interested reader.

4

Results and Discussion

In this Chapter, the results from the extended Bekenstein model (Vacher et al., 2022), the runaway dilaton model (Vacher et al., 2023), the dilaton model (Dias et al., 2024), and from quintessence in the context of the Swampland (Schöneberg et al., 2023) will be discussed. For the purpose of conciseness, a selection of interesting cases are presented for each model. A complete description of these works can be found in the aforementioned papers. My primary contribution to this work involved testing the `CLASS` version for this model, running MCMC simulations and generating the plots using `GetDist`.

All the chains used in the papers presented in this thesis have a Gelman-Rubin convergence criterion of $|R–1| < 0.05$.

4.1 Extended Bekenstein

In this section, constraints for the extended Bekenstein model will be presented. As mentioned in Chapter 2, two different scenarios were explored in the context of this model. For both scenarios, the initial values of the field and field speed are set to zero ($z \to \infty$), since these values do not affect the evolution of the field due to an attractor behavior.

Universal matter coupling

In this scenario, a smaller parameter space was investigated, before constraining the full version, assuming that the field couples the identically to baryons and dark matter as $\zeta_m \equiv \zeta_b = \zeta_\chi$. There is no apparent reason for this to happen, but it allows for a direct comparison with previous constraints of this model, in Alves et al. (2018). An initial set of chains was run using the likelihoods described in Chapter 3 (referred to as "Current") and a second set where the MICROSCOPE prior was removed, and the atomic-clock likelihood was replaced with the one used in Alves et al. (2018), originally obtained in Rosenband et al. (2008) (dubbed "Alves"). Finally, a third scenario was considered, substituting the MICROSCOPE likelihood with an earlier measurement of the Eötvös parameter η, obtained from torsion balance experiments by the Eöt-Wash group (Wagner et al., 2012) (referred to as "Eöt-Wash"). This final case enabled us to evaluate the impact of WEP tests on the parameter space and quantify the advancements provided by the recent MICROSCOPE results. As mentioned before, the product $\eta_i \equiv \zeta_F \zeta_i$ is constrained (which should not be confused with the Eötvös parameter η), instead of the ζ_i parameters. Moreover, the products $\zeta_F\, \phi_0$ and $\zeta_F\, \phi_0'$ are derived quantities.

The contour plot for the extended Bekenstein model under the universal matter coupling are presented in Fig. 4.1. The contour plot for the comparison of the three scenarios

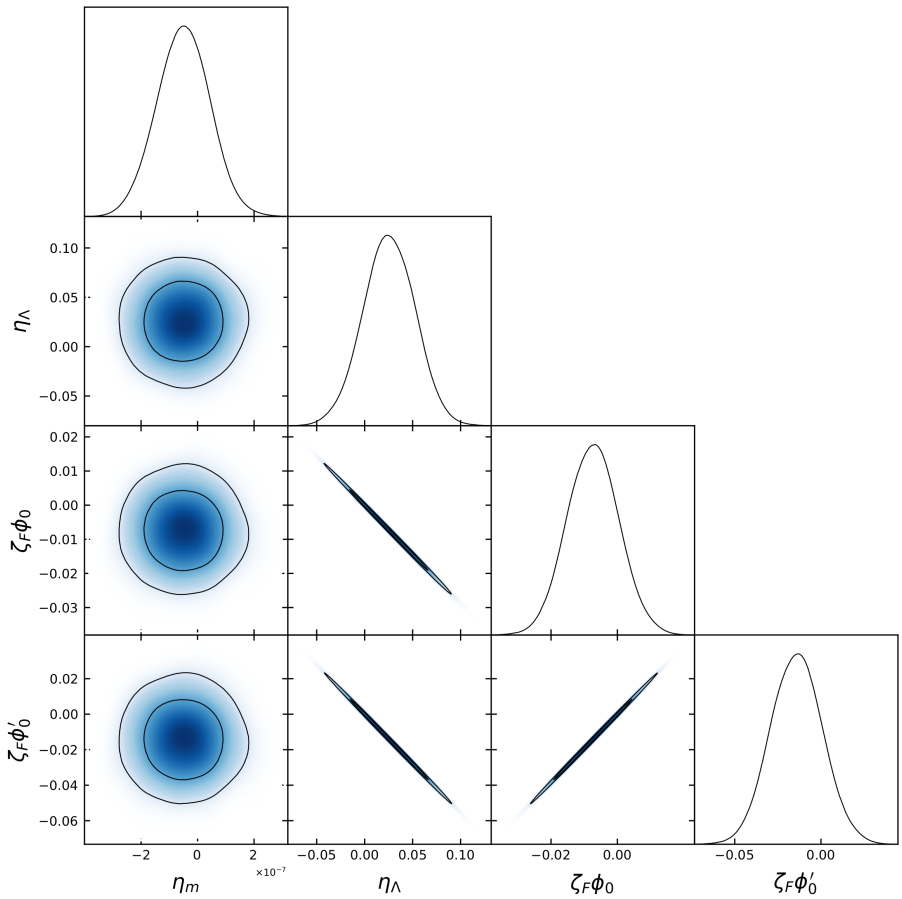

Figure 4.1: Contour plot for the extended Bekenstein model under the universal matter coupling assumption for the "Current" likelihood set. For both plots all parameters are expressed in ppm. From Vacher et al. (2022).

("Current", "Eöt-Wash" and "Alves") are presented in Fig. 4.2 and the corresponding best-fits are displayed in Table 4.1. From this table, it is possible to conclude that, for the "Alves" case the results are comparable with the ones obtained in Alves et al. (2018), constraining the two parameters at the ppm level. Additionally, one can notice straightaway

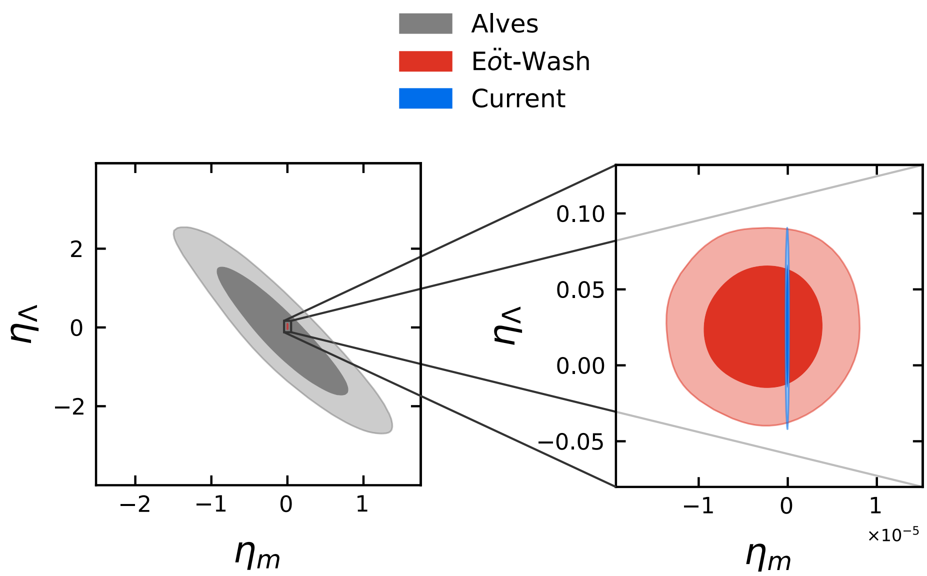

FIGURE 4.2: Contour plots for the extended Bekenstein model under the universal matter coupling assumption with three different likelihood sets: 'Alves' (Gray), 'Eöt-Wash' (Red) and 'Current' (Blue). All parameters are expressed in ppm. From Vacher et al. (2022)

Parameter	Current	Eöt-Wash	Alves
η_m	$\left(-0.54^{+0.86}_{-0.90}\right)\cdot 10^{-7}$	$\left(-0.25^{+0.45}_{-0.44}\right)\cdot 10^{-5}$	$0.05^{+0.60}_{-0.67}$
η_Λ	0.025 ± 0.027	$0.024^{+0.03}_{-0.027}$	-0.4 ± 1.1
$\zeta_F\phi_0$	$-0.0073^{+0.0081}_{-0.0076}$	$-0.007^{+0.0077}_{-0.0086}$	$-0.7^{+9.6}_{-8.5}$
$\zeta_F\phi_0'$	$-0.0014^{+0.0016}_{-0.0015}$	$-0.015^{+0.015}_{-0.017}$	0.17 ± 0.27

TABLE 4.1: Best-fit values of the parameters for the extended Bekenstein model universally coupled to matter with associated 68% confidence levels (C.L.) in ppm, from the combination of currently available data. For comparison, the analogous constraints for two earlier sets "Alves" and "Eöt-Wash" are also shown. This table is from Vacher et al. (2022).

a degeneracy between the η_m and the η_Λ parameters. The addition of priors coming from EEP violation experiments allows to break the degeneracy between this two parameters as it allows to directly constrain the coupling to matter, as can can be seen from Fig. 4.2. Indeed, the addition of either the MICROSCOPE or the Eöt-Wash likelihoods provides with tighter constraints on the matter coupling, with MICROSCOPE being one resulting in the sharpest constraints. However, for these two cases we do not see any further improvement on the constrains for the η_Λ parameter. In comparison with "Alves", the "Current" scenario leads to an improvement of the constraints by a factor of $\sim 10^8$ for η_m and ~ 100 for η_Λ. Couplings of order ppm are now excluded for this model.

Full extended Bekenstein model

We can now turn our attention to the full parameter space, where we do not assume an identical coupling to baryon and dark matter, leading to an extra parameter to constrain. This was the first time the full parameter set was constrained, highlighting the relevance of this work.

The contour plots for the full extended Bekenstein model can be found in Fig. 4.3, with the corresponding best-fits in Table 4.2. There is a lot of similarity to the previous scenario

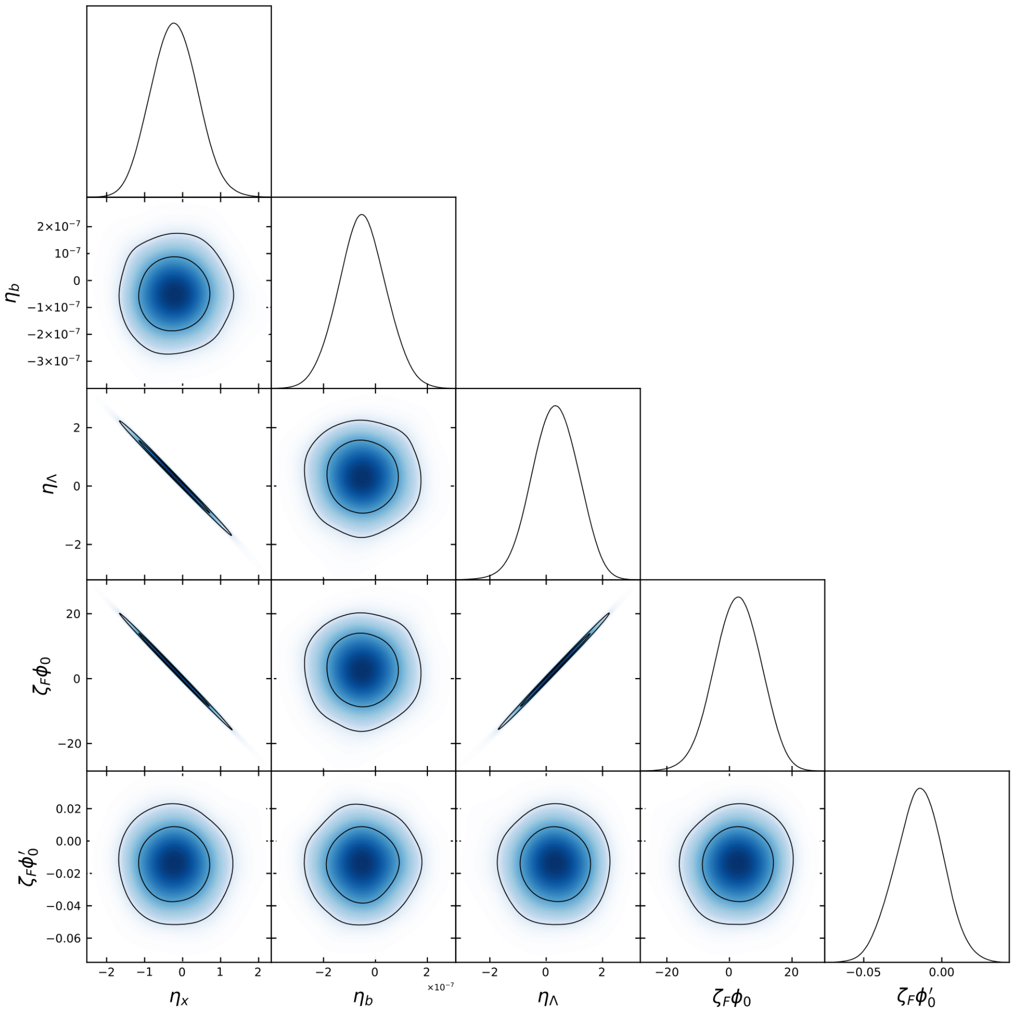

Figure 4.3: Contour plot of the Bekenstein parameters in the full extended Bekenstein model in ppm, from Vacher et al. (2022).

with MICROSCOPE breaking degeneracies, this time between η_b and η_Λ, leaving a strong degeneracy between the coupling to the cosmological constant and the dark matter particle. By constraining the field speed to be small, the atomic-clocks break the degeneracies between $\zeta_F\,\phi'$ and $(\eta_\chi\,, \eta_\Lambda)$. Similarly to what we find in the previous scenario, parameters of order ppm are excluded by our combination of datasets.

Parameter	68% C.L.
η_χ	$-0.24^{+0.63}_{-0.66}$
η_b	$\left(-0.54^{+0.93}_{-0.94}\right)\cdot 10^{-7}$
η_Λ	$0.34^{+0.88}_{-0.85}$
$\zeta_F\phi_0$	$2.87^{+8.0}_{-7.7}$
$\zeta_F\phi_0'$	$-0.015^{+0.016}_{-0.015}$

TABLE 4.2: Best-fit values of the parameters for the full extended Bekenstein model with associated 68% confidence levels (C.L.) in ppm. Table taken from Vacher et al. (2022).

As shown in Table 1 of Olive & Pospelov (2002), in this extended Bekenstein framework are contained several models beyond the standard model of cosmology and particle physics such as Brans-Dicke, Supersymmetry, or String Theory inspired. By excluding couplings greater than fractions of ppm, our constraints exclude their naturally expected values for most of these models. Bekenstein models provide a robust and general framework for investigating variations in the fine-structure constant on cosmic scales. While these models are anticipated to describe the low-energy limits of several extensions beyond the standard models of cosmology and particle physics, they are stringently constrained by current data, requiring them to closely approximate standard model behavior. In particular, our analysis demonstrates that couplings at the level of parts per million are ruled out across all the generalizations considered. The combined precision of local, astrophysical, and cosmological measurements exerts increasingly stringent constraints on viable models that incorporate variations in fundamental constants.

The convergence information and the contour plots for the cosmological parameters (for all scenarios) can be found in Appendix A of Vacher et al. (2022).

4.2 Runaway dilaton

The next model to consider is the string theory inspired, runaway dilaton where we derived constraints for a number of interesting scenarios. Throughout this work, the field was assumed to be spatially homogeneous. Moreover, the field equations present an attractor behavior, as can be seen in Fig. 4.4. For this reason, the values of ϕ_0 and ϕ_0' are treated as derived parameters and not sampled over. While not specified on the figures, their values are always expressed in units of $M_{Pl}/\sqrt{4\pi}$. My contribution to this work the production of the contour plots with `GetDist`.

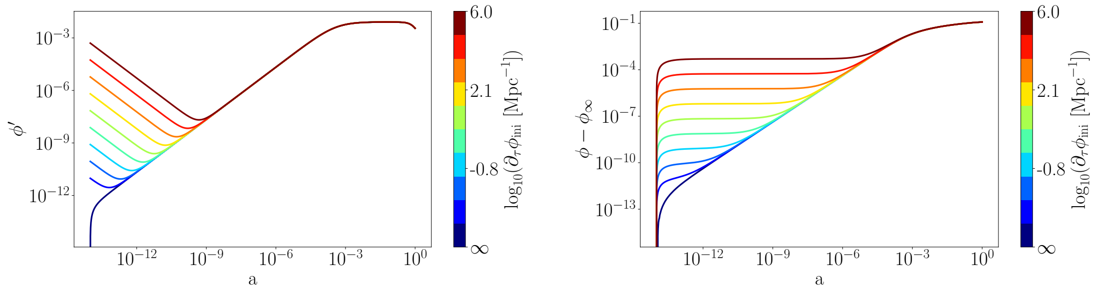

FIGURE 4.4: Evolution of the dilaton field and its speed with respect to the scale factor for different values of its initial speed with $V(\phi) = 0$, $\alpha_{m,0} = -1\times10^{-2}$, and $\alpha_{h,0} = -1\times10^{-5}$. Figure from Vacher et al. (2023).

Runaway dilaton and a constant coupling to dark energy

In previous studies (Martins and Vacher, 2019), the authors consider a scenario in which the field can be driven by a cosmological constant with a constant coupling (α_Λ). A prior on today's field speed, $|\phi'_0| = 0.0\pm0.1$, was assumed from separate constraints in Thomas, Kopp & Skordis (2016) and Tutusaus et al. (2016). This prior allows to simplify the the constraints coming from cosmological background expansion probes, consisting in the only constraint on today's field speed ϕ'_0. This work aims to explore and constrain this model by removing this assumption, using the likelihoods described in Chapter 3. For this particular case of a dilaton with a constant coupling to dark energy, a comparison between "Prior" and "No Prior" will be presented.

The contour plot, and corresponding best-fits, for these two cases is presented in Fig. 4.5 and Table 4.3 respectively, with "Prior" in blue and "No Prior" in red. These results provide, for the first time, a study of the full model, including $\alpha_{m,0}$. There is an improvement

Parameter	Prior on ϕ'_0	No prior on ϕ'_0
$\alpha_{h,0}$	$(-1.63\,^{+4.33}_{-4.71})\cdot10^{-6}$	$(0.21\,^{+2.97}_{-2.80})\cdot10^{-6}$
$\alpha_{m,0}$	$(-1.70\,^{+2.08}_{-5.71})\cdot10^{-2}$	$(-1.39\,^{+2.65}_{-6.03})\cdot10^{-2}$
α_Λ	$(0.50\,^{+8.94}_{-9.39})\cdot10^{-2}$	$(-0.16\,^{+2.34}_{-3.65})\cdot10^{-1}$
ϕ_0	$(16.7^{+3.68}_{-2.43})\cdot10^{-1}$	$(17.5^{+4.25}_{-3.23})\cdot10^{-1}$
ϕ'_0	$(0.20\,^{+9.97}_{-9.98})\cdot10^{-2}$	$(3.7\,^{+38.4}_{-31.0})\cdot10^{-2}$

TABLE 4.3: Best-fit values of the runaway dilaton parameters with associated 68% confidence levels (CL) in the case $V = 0$ and $\alpha_\Lambda \neq 0$, from Vacher et al. (2023).

on the constraints for $\alpha_{h,0}$ by an order of magnitude, in comparison to Martins & Vacher (2019) due to the latest MICROSCOPE constraints (Touboul et al., 2022). For the coupling to dark energy, using the prior on ϕ'_0 yields identical results to this previous study, due to the strong degeneracies between these two parameters (ϕ'_0 and α_Λ).

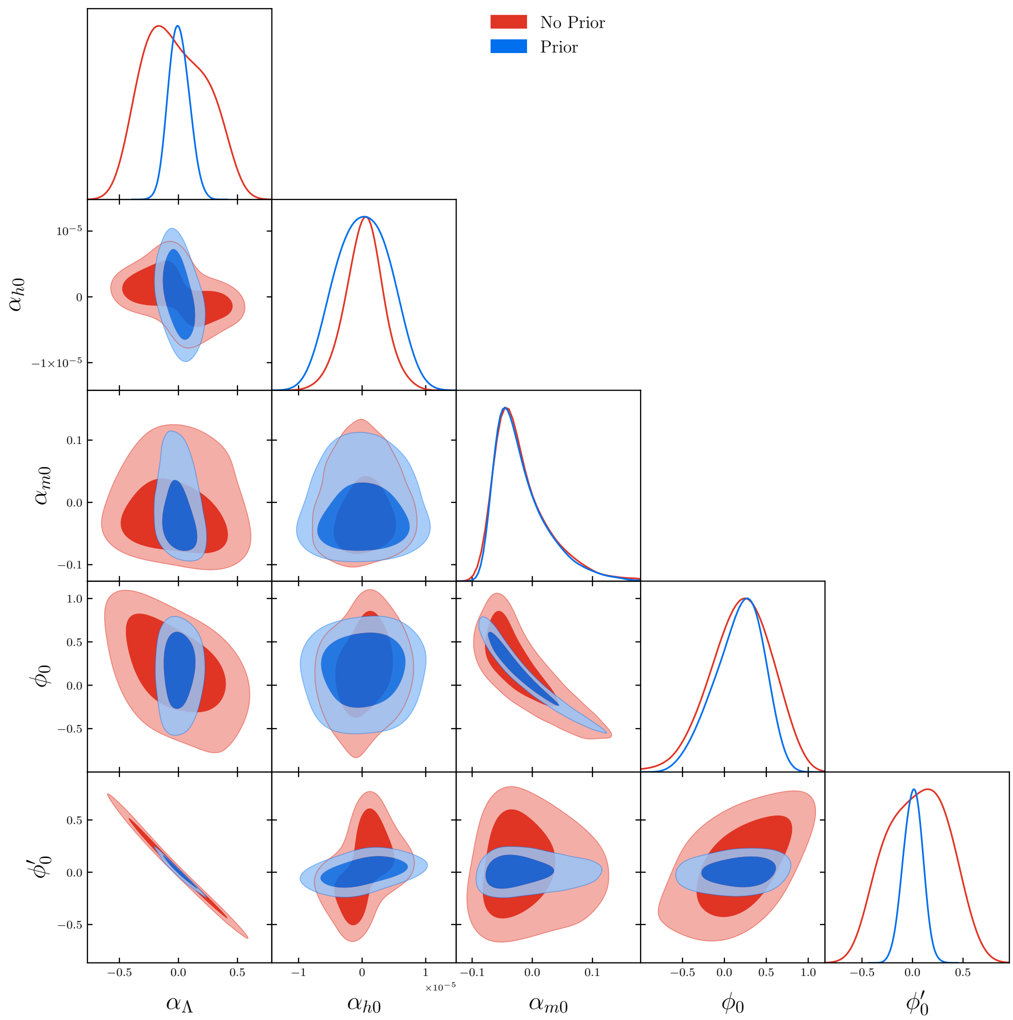

FIGURE 4.5: Posteriors of the dilaton parameters with a constant coupling to dark energy α_Λ with an extra prior on ϕ'_0 (blue) and without it (red), from Vacher et al. (2023).

One finds a strong degeneracy between the dark energy coupling and the field speed, as the impact of α_Λ is very strong around dark energy domination era. For the "No Prior" case, the posterior distributions are non-Gaussian, broadening for the α_Λ parameter, hence also for the field speed. The opposite can be verified for the coupling $\alpha_{h,0}$, where we find that, without providing any prior on ϕ'_0, the constraints are ~ 2 times tighter. By allowing the field speed to have a wider range of possible values we gain a greater amount of viable models with $\alpha_{h,0} \sim 0$, since the atomic clocks likelihood is constraining their product.

The contour plots illustrating the relationship between the dilaton parameters and H_0 are shown in Fig. 4.6. These plots reveal that the current value of the Hubble parameter, H_0, is significantly influenced by high values of ϕ'_0. Relaxing the prior on ϕ'_0 naturally permits higher H_0 values, with $H_0 = 68.2^{+0.51}_{-0.65}$ km/s/Mpc compared to $H_0 = 67.8 \pm 0.43$ km/s/Mpc when the prior is imposed. These findings may have implications for the ~ 4–5σ observational tension in the measured value of H_0 and the theoretical challenges associated with Λ as the canonical source of dark energy.

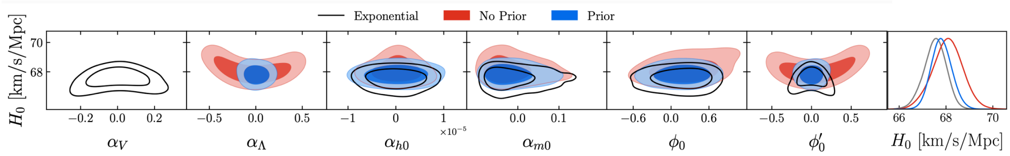

Figure 4.6: Contour plots of H_0 and the dilaton parameters in the cases of an exponential potential (black) and a constant coupling to dark energy α_Λ with an extra prior on ϕ'_0 (blue) and without it (red), from Vacher et al. (2023).

Exponential potential

It was also explored the case of a runaway dilaton with an exponential potential ($V(\phi) \propto e^{c\,\phi}$) where, in this case, dark energy is fully sourced by the runaway dilaton. A new parameter $\alpha_V = \frac{1}{4}\frac{\partial \ln V}{\partial \phi}$ is introduced. The contours are shown in Fig. 4.7, and the corresponding constraints are displayed in Table 4.4. We do not find any additional impact on the constraints of $\alpha_{h,0}$ and $\alpha_{m,0}$ coming from this additional degree of freedom.

Parameter	68 % CL
$\alpha_{h,0}$	$(0.01\,^{+4.22}_{-4.17}) \cdot 10^{-6}$
$\alpha_{m,0}$	$(-1.68\,^{+2.24}_{-5.78}) \cdot 10^{-2}$
α_V	$(0.04\,^{+1.12}_{-1.27}) \cdot 10^{-1}$
ϕ_0	$(1.64^{+3.82}_{-2.53}) \cdot 10^{-1}$
ϕ'_0	$(0.02\,^{+1.36}_{-1.26}) \cdot 10^{-1}$

Table 4.4: Best-fit values of the runaway dilaton parameters with associated 68% confidence levels (CL) for the exponential potential case. This table is taken from Vacher et al. (2023).

In this study, the first constraints on the complete parameter space of this model were derived, accounting for its full cosmological evolution with minimal assumptions regarding its couplings, thereby refining and extending previous analyses and demonstrating that order unity couplings—natural in the context of string theory—are excluded in all cases. Notably, the final data release of the MICROSCOPE experiment (Touboul et al., 2022) provided a significant contribution.

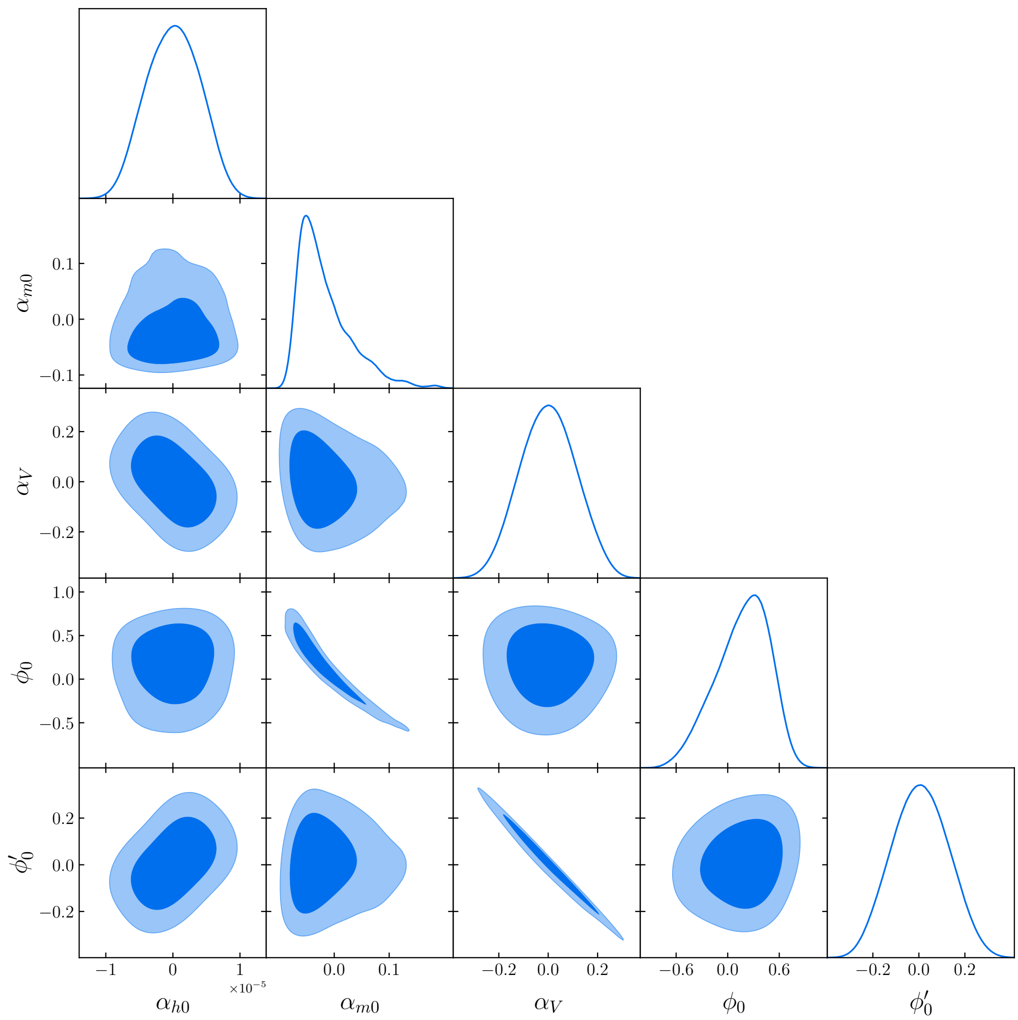

Figure 4.7: Contour plot for the dilaton parameters in the exponential potential scenario from Vacher et al. (2023).

4.3 Rolling tachyon

The third model studied, also inspired by string theory, is the rolling tachyon. This work builds upon previously conducted studies (Martins and Moucherek, 2016; Tavares and Martins, 2021), improving constraints and providing with a more systematic study of different potentials. In this study, two different datasets are used: the "All" dataset which encompasses all the likelihoods described in Chapter 3, and the "Cosmo" dataset that only includes the cosmological likelihoods. My contribution to this work, as first author, encompassed implementing and testing the modifications to the `CLASS` code, running the MCMC chains, generating plots with `Liquidcosmo`, and ultimately drafting the manuscript.

Massive rolling scalar potential

The constraints on the parameter space of the massive rolling scalar potential can be found in Fig. 4.8. In this figure two regimes of the parameters R_0 are explored: $R_0 \lesssim 1$ (left plot)

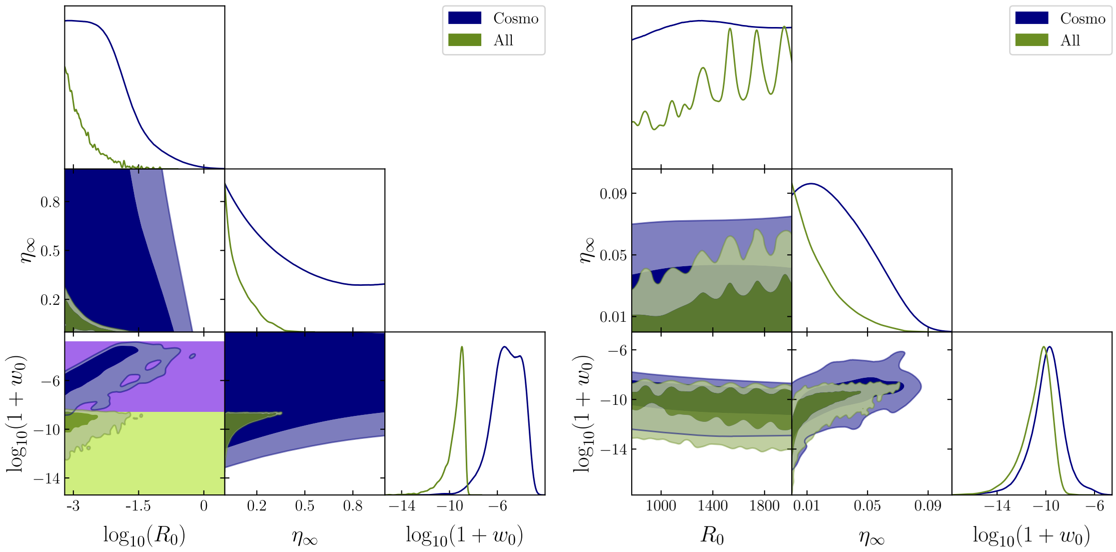

FIGURE 4.8: Constraints on the massive rolling scalar potential from cosmological and fine-structure data. We show the 68% and 95% marginalized constraints as dark and bright shaded regions. The blue color corresponds to cosmological data only, while the green color adds constraints from fine-structure constant data. The purple region in the bottom left panel shows where manual studies suggest that the contour would extend for larger priors on η_∞ (see footnote 1). Contour plot from Dias et al. (2024).

and $R_0 \gg 1$ (right plot). The variation of the fine-structure constant is small in both cases. In the former, since the field is barely evolving, the potential remains mostly constant, leading to small variations of α. For the later case, the models displays an oscillating field (as can be seen from Fig. 2.1), which are damped by the Hubble drag leaving the at the bottom of the potential well.

It is possible to see that, for the $R_0 \lesssim 1$ case, there is an upper limit on η_∞ due to higher values of η_∞ resulting in larger field excursions and thus larger $\Delta\alpha/\alpha$. Hence, it becomes clear that the local-fine structure constraints will impose very tight bounds on the parameters, including an upper bound on η_∞ to prevent these large field excursions. We also constrain the value of $1 + w_0$, using the relation between the field speed and w from Eq. (2.45). For the "Cosmo" case this constraint is at the level of around 10^{-3} compared to roughly 10^{-9} for the "All" data, a result that we observe for all potentials that cause late-time movement.[1]

[1] There is a slight problem with very large η_∞ that are difficult to numerically sample due to the squared exponential. For this reason, a purple region was added in the lower left hand panel of Fig. 4.8 that highlights the w_0 values we would expect to be in principle accessible if higher η_∞ values could be sampled.

For the case of $R_0 \gg 1$ we can deduce upper limits on η_∞ that are mostly independent on R_0, which is smaller when we add fine-structure constant data. Without this data, the upper limit on η_∞ is given by the corresponding $\Delta\alpha/\alpha$ at CMB times. With α data the upper bound is oscillatory allowing for the fine-structure bounds to be avoided.

Inverse power-law potential

For this potential, as can be seen in Fig. 4.9, there is no major difference between the two datasets for the parameter n. The main difference comes from the lower bound on ϕ_∞. There exists a strong correlation between the value of ϕ_∞ and the present-day field

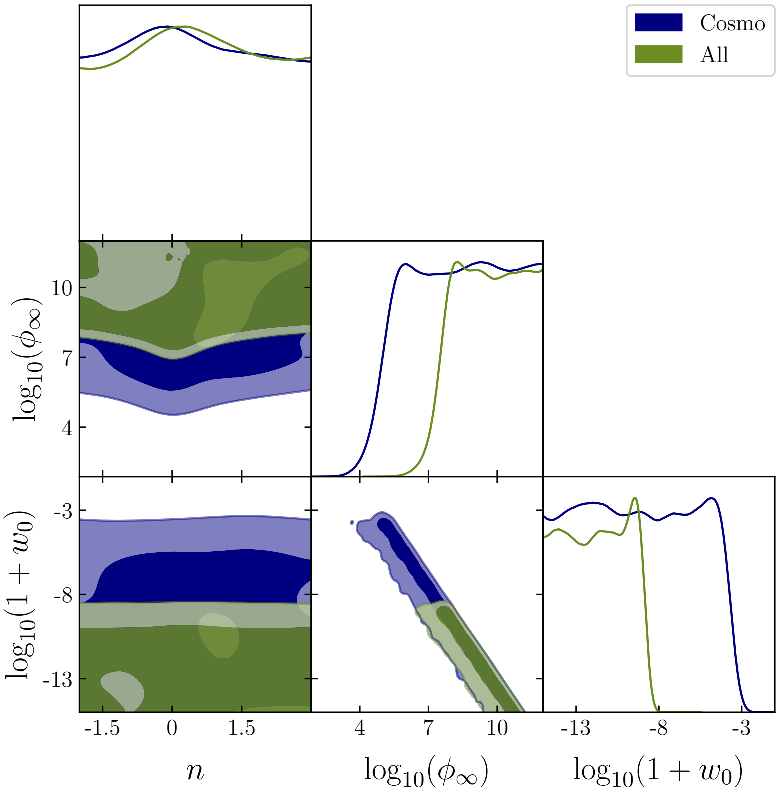

FIGURE 4.9: Constraints on the inverse power-law potential from cosmological and fine-structure data. We show the 68% and 95% marginalized constraints as dark and bright shaded regions. The blue color corresponds to cosmological data only, while the green color adds constraints from fine-structure constant data,from Dias et al. (2024).

velocity, which can be expressed as $\log_{10}[1 + w_0] = 2\log_{10}[\dot\phi|_{z=0}]$. This relationship imposes stringent constraints on $1 + w_0$, effectively ruling out significant deviations from a cosmological constant-like behavior. Consistent with what was described above, we obtain constraints at the level of approximately 10^{-3} for the "Cosmo" case, compared to about 10^{-9} for the "All" case.

Anti-massive potential

The results for this potential are displayed in Fig. 4.10. It is important to highlight that the

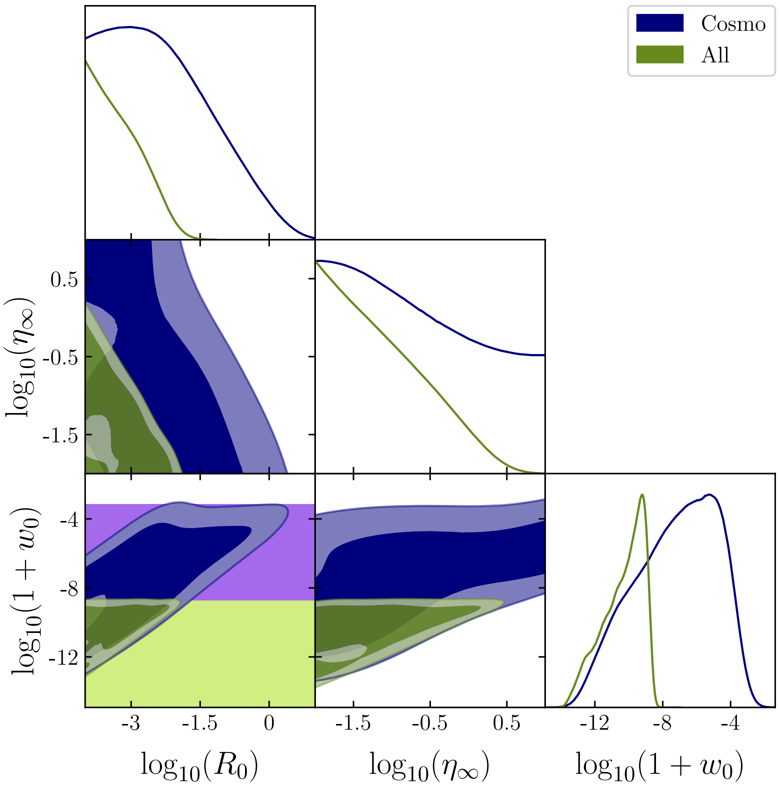

Figure 4.10: 68% and 95% CL contours for the anti-massive potential case. In the 2D contours on the bottom row the purple/light-green regions show where manual studies suggest that the contour would extend for broader priors, from Dias et al. (2024).

contours in this figure appear "incomplete" due to the finite width of the priors. To illustrate the expected behavior with broader priors, the green and purple regions have been manually extended, as detailed in footnote 1. In this context, we also find that cosmologically significant deviations from a cosmological constant, expressed in terms of $1 + w_0$, are ruled out. This exclusion arises from both cosmological data (through its effects on the CMB) and fine-structure data, yielding constraints on $1 + w_0$ that are consistent with those discussed earlier.

There are several general conclusions to be drawn from this work, despite the wide variety of potentials investigated. As highlighted above, and summarized in Table 4.5 and Fig. 4.11, the equation of state parameter today ($w_0 = w_\phi(z = 0)$) is generically constrained in these potentials, which is discussed in **??**. We find that $1 + w_0$, $\mathrm{d}\ln\alpha/\mathrm{d}\ln a$, and $\Delta\alpha/\alpha_0$ are all expected to be of the same order of magnitude, for any potential as long as it does not have a minimum or plateau at $V(\phi) > 0$. This leads to the natural expectation that CMB data will constrain $1 + w_0$ to approximately 10^{-3}, while fine-structure

		"Cosmo"		"All"	
Potentials	Constraint type	Constraint	$\log_{10}(1+w_0)$	Constraint	$\log_{10}(1+w_0)$
Massive (left)	$\log_{10}(R_0)+\log_{10}(\eta_\infty)$	< -0.84	< -2.8	< -3.7	< -8.5
Massive (right)	η_∞	$< +0.087$	< -6.6	$< +0.058$	< -8.6
Inverse power-law	$\log_{10}(\lvert n\rvert)-\log_{10}(\phi_\infty)$	< -4.5	< -2.9	< -7.2	< -8.3
Anti-massive	$\log_{10}(R_0)+\log_{10}(\eta_\infty)$	< -0.77	< -2.7	< -3.6	< -8.4

TABLE 4.5: Upper bounds on $1+w_0$ and for the parameters of the potential for each investigated potential. In the first column we state the potential, in the second column which kind of constraint we report on in the third and fifth column. These correspond to the physical constraints imposed by the data for combinations of the underlying parameters. Instead of giving the usual 95% CL upper bound, we instead quote where the posterior has dropped to below 5% of its maximum value. This way of quoting the upper limit is more resistant to the arbitrary choice of priors on the underlying parameters. This table is taken from Dias et al. (2024).

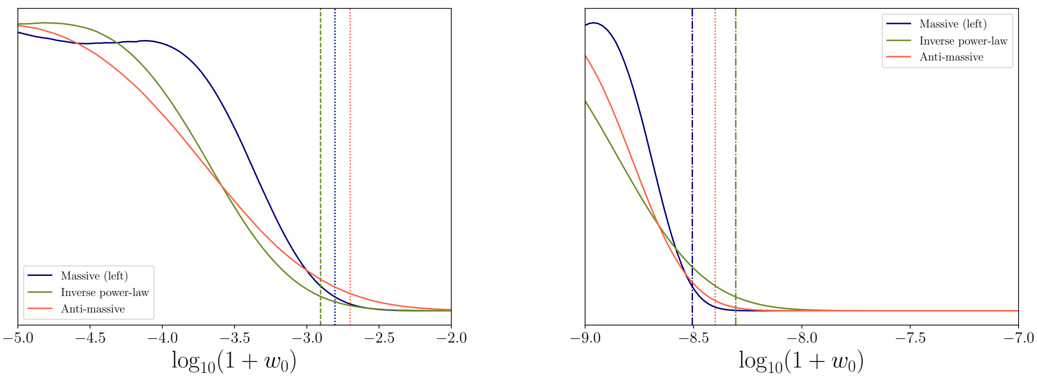

FIGURE 4.11: Posterior distribution for all the potentials in study (named according to Table 4.5). The left plot represents the "Cosmo" dataset and the right one the "All" dataset. The dashed lines represent the upper limits on $\log_{10}(1+w_0)$ for each potential as reported in Table 4.5. Figure adapted from Dias et al. (2024).

data will impose a tighter constraint at the level of $1+w_0 \sim 10^{-9}$, effectively limiting the Tachyon field from deviating significantly from behavior resembling a cosmological constant. As further discussed in **??**, incorporating free-fall data, such as the latest results from the MICROSCOPE mission (Touboul et al., 2022), could potentially tighten the bounds on deviations from a cosmological constant to $1+w_0 \sim 10^{-11}$. However, explicitly including these constraints, beyond an order-of-magnitude estimate, proves to be highly non-trivial. Doing so would require a generalization of the derivation of the Eötvös parameter from canonical massive fields to tachyon fields with arbitrary potentials. Although the field is constrained to exhibit canonical evolution (as $\dot{\phi} \ll 1$), this extension remains a topic for future investigation. Nonetheless, the rolling tachyon model is now so tightly constrained by fine-structure data to closely resemble ΛCDM that further refinements to the results would not alter our conclusions.

4.4 Swampland

Finally, the last investigation is that of the Swampland conjectures. The main idea is to confront the Swampland criteria (detailed in Chapter 2) with the most recent cosmological data, in the context of a quintessence field that is responsible for the late time accelerated expansion of the Universe and the variation of the fine-structure constant. My personal contribution to this work was, running preliminary chains to test the modified `CLASS` version, and running the final chains.

This model was subjected to a variety of datasets to investigate which cosmological probes are more relevant in constraining the parameters, and how do the most recent data fare in comparison with older probes. In Fig. 4.12 we show a comparison of the constraints for different cosmological probes, with the most interesting constraints summarized in Table 4.6. The probes with most constraining power are BAO and Pantheon supernovae.

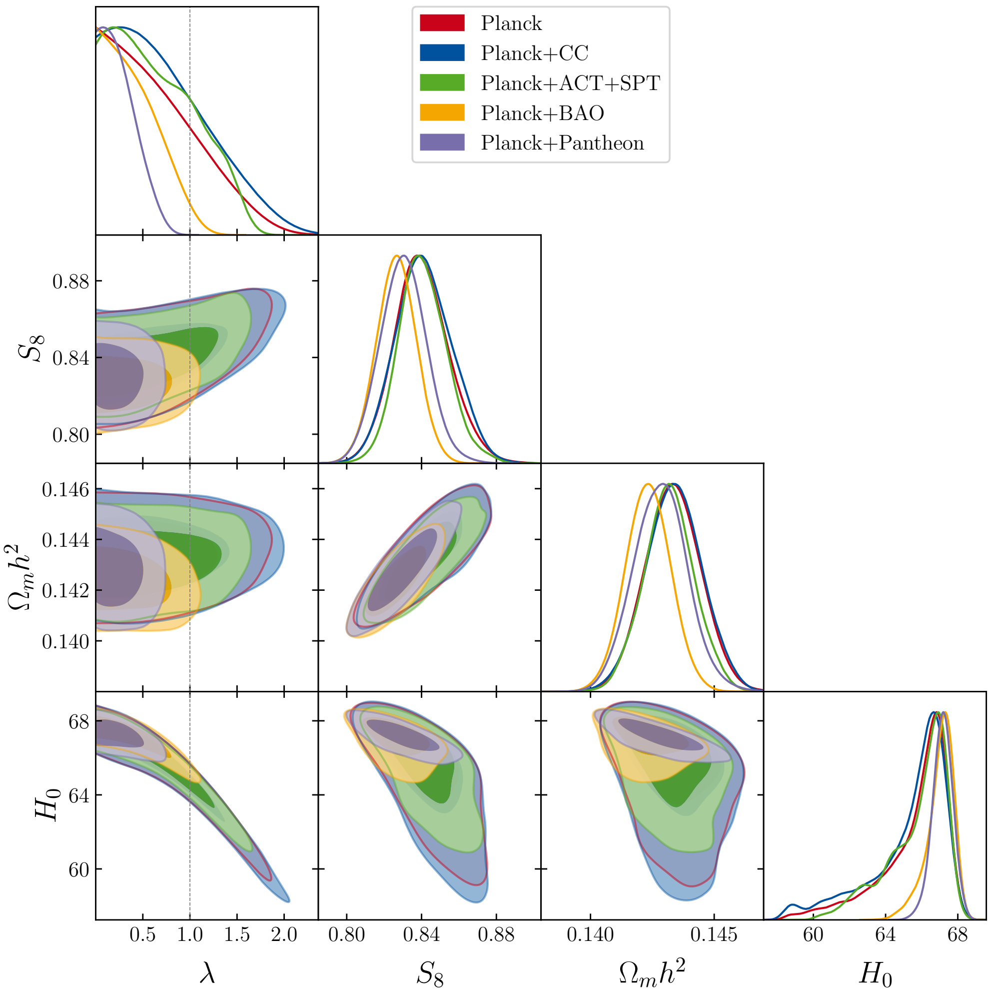

Figure 4.12: Comparison of the constraints on the exponential model for a variety of data sets, from Schöneberg et al. (2023).

Data combination	H_0 [km/s/Mpc]	λ (95% CL)	$P(\lambda > 1)$ in %
Planck	$65.6^{+1.6}_{-1.9}$	< 1.6	24
Planck + CC	$65.3^{+1.8}_{-2.2}$	< 1.7	28
Planck + ACT+SPT	$65.8^{+1.5}_{-1.7}$	< 1.4	24
Planck + BAO	67.02 ± 0.72	< 0.94	2.9
Planck + Pantheon	67.15 ± 0.56	< 0.62	< 0.001

TABLE 4.6: Constraints on H_0 and λ in the exponential coupled quintessence field model. We also cite the probability to exceed $\lambda > 1$, from Schöneberg et al. (2023).

BAO data probe the late evolution and Ω_m such that the probability of having $\lambda > 1$ is below 5%, and Pantheon allow for a constraint of $\lambda < 0.62$ (95% CL) when combined with Planck.

To evaluate the impact of using updated BAO and SN data, we present in Fig. 4.13 a comparison between the older and newer datasets. Interestingly, the newer data yield less stringent bounds on the λ parameter. This counterintuitive result can be explained by the fact that the updated Pantheon+ dataset, in particular, favors slightly higher values of Ω_m compared to the older data. This implies a lower abundance of the dark energy component, which consequently decreases the constraints on λ. These constraints are also summarized in Table 4.7.

Data combination	H_0 [km/s/Mpc]	λ (95% CL)	$P(\lambda > 1)$ in %
Planck + BAO	67.02 ± 0.72	< 0.94	2.9
Planck + BAO DR16	65.7 ± 1.2	< 1.3	23
Planck + Pantheon	67.15 ± 0.56	< 0.62	< 0.001
Planck + Pantheon+	66.59 ± 0.62	< 0.80	0.24

TABLE 4.7: Same as Table 4.6 for old and new BAO and Pantheon data. Contour plot from Schöneberg et al. (2023).

Finally, when applying the full dataset, dubbed $\mathcal{A}$ (involving Planck, BAO, Pantheon, CC, ACT, and SPT data), we observe that the results are quite similar, as shown in Fig. 4.14, indicating that the constraining power is primarily driven by BAO and supernovae data. Here too the old data is more restrictive and has tighter constraints. It is also shown that the constraints on λ tighten when incorporating a prior on H_0 from Riess et al. (2022). These results are summarized in Table 4.8.

Overall, we find that current data are only in a relatively mild tension with the Swampland criteria.

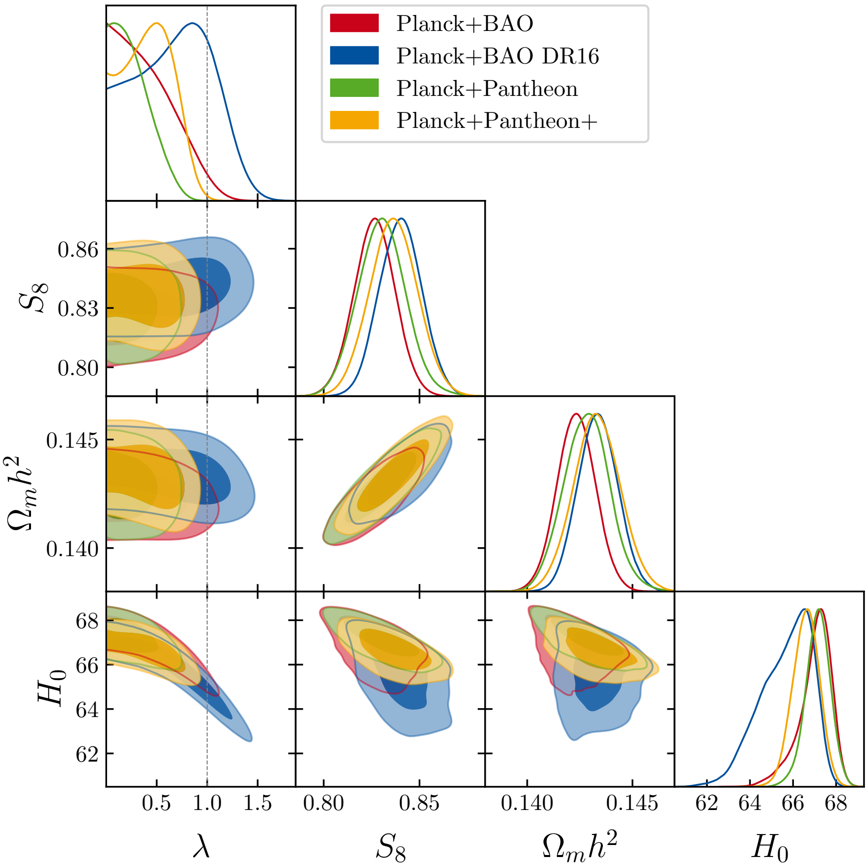

FIGURE 4.13: Comparison of the constraints on the exponential model compared between older and newer late-time cosmological data (BAO and SN), from Schöneberg et al. (2023)

Data combination	H_0 [km/s/Mpc]	λ (95% CL)	$P(\lambda > 1)$ in %
$\mathcal{A}$	$66.36^{+0.56}_{-0.54}$	< 0.85	0.33
$\mathcal{A} + H_0$	67.70 ± 0.50	< 0.60	< 0.001
$\mathcal{A}_{\rm old}$	67.38 ± 0.40	< 0.60	< 0.001
$\mathcal{A}_{\rm old} + H_0$	67.84 ± 0.39	< 0.46	< 0.001

TABLE 4.8: Same as Table 4.6 for combinations involving the $\mathcal{A}$=Planck, BAO, Pantheon, CC, ACT, and SPT data combination, and also for added H_0 priors from Riess et al. (2022). Table taken from Schöneberg et al. (2023).

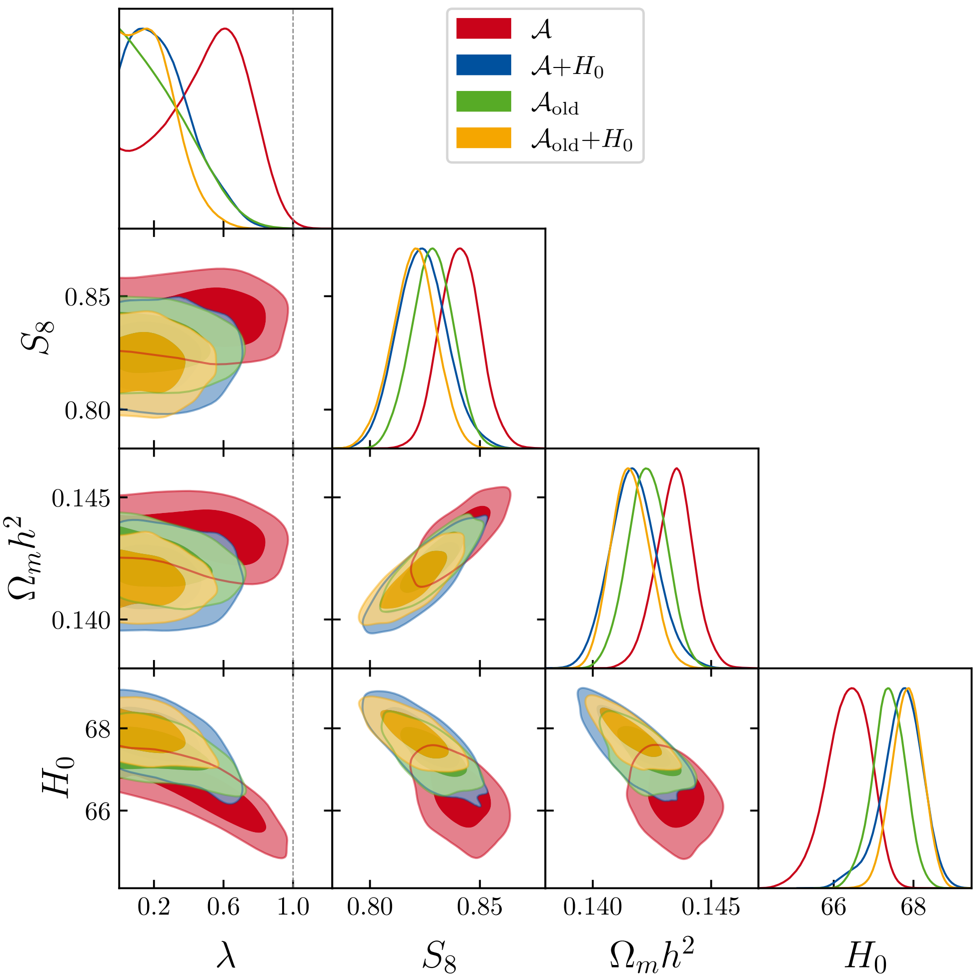

FIGURE 4.14: Comparison of the constraints on the exponential model for a variety of all data, from Schöneberg et al. (2023).

5

Conclusions

The study of the fine-structure constant and its potential variations provides a powerful framework to test important fundamental cosmology paradigms such as dark energy and the Einstein Equivalence Principle. Throughout this thesis, models like the extended Bekenstein, runaway dilaton, rolling tachyon, and even Swampland-inspired frameworks were explored, proving to be a consistent methodology to study this phenomena. Taking advantage of the synergy between local, astrophysical and cosmological high-precision measurements we were able to constrain the parameters of these models, allowing to explore modifications to ΛCDM, thus opening a window to possible extensions of fundamental physics.

The extended Bekenstein's phenomenological framework stands out as a general and consistent approach for modeling variations of α over cosmic scales. For the universal matter coupling scenario, we achieved significant improvements from previous constraints (Alves et al., 2018), driven by the inclusion of precise local data such as MICROSCOPE's universality of free fall measurements. We report an improvement of a factor of ~ 100 for η_Λ and $\sim 10^8$ for η_m. The full parameter space was also explored, resulting in the first set of constraints for the case. Our investigation revealed that couplings of the order of parts per million are excluded.

The runaway dilaton framework, appearing as a string theory inspired model, provides a mechanism for exploring the stability of fundamental constants and their cosmological consequences. Our study presented the first comprehensive constraints on the full parameter space of this model. Dilaton models are particularly relevant in the context of dark energy and the accelerated expansion of the universe. It is believed that a redshift-dependent α, as predicted in these models, could influence recombination processes, providing potential solutions to the Hubble tension. Our analysis demonstrated that runaway dilaton fields could act as dynamical dark energy under a specific choice of potential, and that order unity coupling are excluded in all cases.

Rolling tachyon fields, originating from the dynamics of D-branes in string theory, represent a class of non-canonical scalar fields that naturally induce variations in α. Our investigation encompassed a variety of proposed tachyon potentials, yielding tight constraints on their dynamics. We conclude that the constraints for a deviation from a cosmological constant are of the order of $1 + w_0 \sim 10^{-3}$, using cosmological datasets only, and of the order $1 + w_0 \sim 10^{-9}$, using fine-structure data. This is valid for any potential that does not have a minimum or plateau at $V(\phi) > 0$. These models are mostly equivalent to canonical scalar fields, as $\dot{\phi} \ll 1$, and thus cannot produce a cosmologically relevant variation of α at the epoch of recombination. In conclusion, the tachyon is not expected to be detected through cosmological data and, with the addition of fine-structure constant data, becomes even more indistinguishable from ΛCDM.

The Swampland conjectures, which seek to delineate the boundary between consistent and inconsistent effective field theories within string theory, have profound implications for late-time cosmology. These conjectures impose constraints on the slopes of scalar field potentials. Our analysis confirmed that mild tensions exist between the de Sitter conjectures and cosmological observations, particularly for quintessence models of dark energy. For exponential potentials, we derived constraints on the slope parameter λ, finding $\lambda < 0.85$ (95% CL) when using all available data, and tighter bounds ($\lambda < 0.60$) when incorporating a high-H_0 prior. Interestingly, we observed that the inclusion of updated BAO and supernova data slightly alleviated this tension, owing to their preference for a lower dark energy density. The current constraints still allow significant flexibility for string-theoretic model building, but forecasted improvements in precision from surveys like DESI (Aghamousa et al., 2016) are expected to further challenge the Swampland criteria. This may eventually render the conjectures incompatible with cosmological data, posing a significant challenge to string-inspired models of dark energy.

Next generation experiments will certainly lead to an increase of the precision at which we measure α, through the use of novel techniques in nuclear clock systems (Beeks et al., 2024) and high-precision spectrometers like ESPRESSO (Pepe et al., 2021) or ANDES (Martins et al., 2024). Consequently, it will enhance our ability to test the stability of fundamental constants, deepening our understanding of alternative approaches to ΛCDM. These efforts will not only refine our constraints on the models studied here but also open new pathways for exploring the nature of dark energy, the validity of the Swampland conjectures, and the role of string theory in cosmology. By continuing to probe the fine-structure constant and related phenomena, we edge closer to answering some of the most profound questions about the universe and its underlying principles.

Bibliography

[1] J.D.F. Dias, Nils Schöneberg, Léo Vacher, C.J.A.P. Martins, and Samy Vinzl. "A speed limit on tachyon fields from cosmological and fine-structure data". In: *J. Cosmology Astropart. Phys.* 2024.11 (Nov. 2024), p. 030. DOI: 10.1088/1475-7516/2024/11/030.

[2] Nils Schöneberg, Léo Vacher, J.D.F. Dias, Martim M.C.D. Carvalho, and C.J.A.P. Martins. "News from the Swampland — constraining string theory with astrophysics and cosmology". In: *J. Cosmology Astropart. Phys.* 2023.10 (Oct. 2023), p. 039. DOI: 10.1088/1475-7516/2023/10/039.

[3] Léo Vacher, Nils Schöneberg, J. D. F. Dias, C. J. A. P. Martins, and Francisco Pimenta. "Runaway dilaton models: Improved constraints from the full cosmological evolution". In: *Phys. Rev. D* 107 (10 May 2023), p. 104002. DOI: 10.1103/PhysRevD.107.104002.

[4] Léo Vacher, J. D. F. Dias, Nils Schöneberg, C. J. A. P. Martins, Samy Vinzl, Savvas Nesseris, Guadalupe Cañas-Herrera, and Matteo Martinelli. "Constraints on extended Bekenstein models from cosmological, astrophysical, and local data". In: *Phys. Rev. D* 106 (8 Oct. 2022), p. 083522. DOI: 10.1103/PhysRevD.106.083522.

[5] E. P. Hubble. "A relation between distance and radial velocity among extra-galactic nebulae". In: *Proc. Natl. Acad. Sci. U. S. A.* 15.3 (Mar. 1929), pp. 168–173.

[6] A Friedman. "Über die Krümmung des Raumes". In: *Eur. Phys. J. A* 10.1 (Dec. 1922), pp. 377–386.

[7] G. Lemaitre. "A Homogeneous Universe of Constant Mass and Growing Radius Accounting for the Radial Velocity of Extragalactic Nebulae". In: *Annales Soc. Sci. Bruxelles A* 47 (1927), pp. 49–59. DOI: 10.1007/s10714-013-1548-3.

[8] V. M. Slipher. "Nebulae". In: *Proceedings of the American Philosophical Society* 56 (Jan. 1917), pp. 403–409.

[9] E. P. Hubble. “Extragalactic nebulae.” In: *The Astrophysical Journal* 64 (Dec. 1926), pp. 321–369. DOI: 10.1086/143018.

[10] D. J. Fixsen. “The temperature of the cosmic microwave background”. In: *The Astrophysical Journal* 707.2 (Nov. 2009), p. 916. DOI: 10.1088/0004-637X/707/2/916.

[11] G. Gamow. “Expanding Universe and the Origin of Elements”. In: *Phys. Rev.* 70 (7-8 Oct. 1946), pp. 572–573. DOI: 10.1103/PhysRev.70.572.2.

[12] S. Chandrasekhar and Louis R. Henrich. “An Attempt to Interpret the Relative Abundances of the Elements and Their Isotopes.” In: *The Astrophysical Journal* 95 (Mar. 1942), p. 288. DOI: 10.1086/144395.

[13] G. Gamow. “The evolution of the universe”. en. In: *Nature* 162.4122 (Oct. 1948), pp. 680–682.

[14] R. A. Alpher, H. Bethe, and G. Gamow. “The origin of chemical elements”. In: *Phys. Rev.* 73.7 (Apr. 1948), pp. 803–804.

[15] A. A. Penzias and R. W. Wilson. “A Measurement of Excess Antenna Temperature at 4080 Mc/s.” In: *The Astrophysical Journal* 142 (July 1965), pp. 419–421. DOI: 10.1086/148307.

[16] R. H. Dicke, P. J. E. Peebles, P. G. Roll, and D. T. Wilkinson. “Cosmic Black-Body Radiation.” In: *The Astrophysical Journal* 142 (July 1965), pp. 414–419. DOI: 10.1086/148306.

[17] S. Weinberg. *Cosmology*. OUP Oxford, 2008. ISBN: 9780191523601.

[18] D. Branch and D. L. Miller. “Type IA Supernovae as Standard Candles”. In: *ApJ Letters* 405 (Mar. 1993), p. L5. DOI: 10.1086/186752.

[19] Adam G. Riess et al. “Observational Evidence from Supernovae for an Accelerating Universe and a Cosmological Constant”. In: *The Astronomical Journal* 116.3 (Sept. 1998), pp. 1009–1038. DOI: 10.1086/300499. arXiv: astro-ph/9805201 [astro-ph].

[20] S. Perlmutter et al. “Measurements of Ω and Λ from 42 High-Redshift Supernovae”. In: *The Astrophysical Journal* 517.2 (June 1999), pp. 565–586. DOI: 10.1086/307221. arXiv: astro-ph/9812133 [astro-ph].

[21] R. Jimenez and A. Loeb. “Constraining Cosmological Parameters Based on Relative Galaxy Ages”. In: *The Astrophysical Journal* 573.1 (July 2002), pp. 37–42. DOI: 10.1086/340549. arXiv: astro-ph/0106145 [astro-ph].

[22] Daniel J. Eisenstein et al. "Detection of the Baryon Acoustic Peak in the Large-Scale Correlation Function of SDSS Luminous Red Galaxies". In: *The Astrophysical Journal* 633.2 (Nov. 2005), pp. 560–574. DOI: 10.1086/466512. arXiv: astro-ph/0501171 [astro-ph].

[23] M. Betoule et al. "Improved cosmological constraints from a joint analysis of the SDSS-II and SNLS supernova samples". In: *Astronomy and Astrophysics* 568, A22 (Aug. 2014), A22. DOI: 10.1051/0004-6361/201423413. arXiv: 1401.4064 [astro-ph.CO].

[24] Balakrishna S. Haridasu, Vladimir V. Luković, Rocco D'Agostino, and Nicola Vittorio. "Strong evidence for an accelerating Universe". In: *Astronomy and Astrophysics* 600, L1 (Apr. 2017), p. L1. DOI: 10.1051/0004-6361/201730469. arXiv: 1702.08244 [astro-ph.CO].

[25] Planck Collaboration et al. "Planck 2018 results. VI. Cosmological parameters". In: *Astronomy and Astrophysics* 641, A6 (Sept. 2020), A6. DOI: 10.1051/0004-6361/201833910. arXiv: 1807.06209 [astro-ph.CO].

[26] D. Huterer and M. S. Turner. "Prospects for probing the dark energy via supernova distance measurements". In: *Physical Review D* 60.8 (Aug. 1999). ISSN: 1089-4918. DOI: 10.1103/physrevd.60.081301.

[27] F Zwicky. "The redshift of extragalactic nebulae". In: *Helvetica Physica Acta* 6.II (1933), p. 110.

[28] Y. Sofue, Y. Tutui, M. Honma, A. Tomita, T. Takamiya, J. Koda, and Y. Takeda. "Central Rotation Curves of Spiral Galaxies". In: *The Astrophysical Journal* 523.1 (Sept. 1999), p. 136. DOI: 10.1086/307731. URL: https://dx.doi.org/10.1086/307731.

[29] Y. Sofue and V. Rubin. "Rotation Curves of Spiral Galaxies". In: *Annual Review of Astronomy and Astrophysics* 39.1 (Sept. 2001), pp. 137–174. ISSN: 1545-4282. DOI: 10.1146/annurev.astro.39.1.137. URL: http://dx.doi.org/10.1146/annurev.astro.39.1.137.

[30] Horace W. Babcock. "The rotation of the Andromeda Nebula". In: *Lick Observatory Bulletin* 498 (Jan. 1939), pp. 41–51. DOI: 10.5479/ADS/bib/1939LicOB.19.41B.

[31] Vera C. Rubin and W. Kent Ford Jr. "Rotation of the Andromeda Nebula from a Spectroscopic Survey of Emission Regions". In: *The Astrophysical Journal* 159 (Feb. 1970), p. 379. DOI: 10.1086/150317.

[32] D. Clowe, M. Bradač, Anthony H. Gonzalez, M. Markevitch, S. W. Randall, C. Jones, and D. Zaritsky. “A Direct Empirical Proof of the Existence of Dark Matter”. In: *The Astrophysical Journal* 648.2 (Aug. 2006), pp. L109–L113. ISSN: 1538-4357. DOI: 10.1086/508162. URL: http://dx.doi.org/10.1086/508162.

[33] W. Hu and S. Dodelson. “Cosmic Microwave Background Anisotropies”. In: *Annual Review of Astronomy and Astrophysics* 40 (2002), pp. 171–216. ISSN: 1545-4282. DOI: https://doi.org/10.1146/annurev.astro.40.060401.093926.

[34] B. P. Abbott, R. Abbott, T. D. Abbott, M. R. Abernathy, F. Acernese, K. Ackley, C. Adams, and T. Adams. “Observation of Gravitational Waves from a Binary Black Hole Merger”. In: *Phys. Rev. Lett.* 116 (6 Feb. 2016), p. 061102. DOI: 10.1103/PhysRevLett.116.061102.

[35] Albert Einstein. “Zur allgemeinen Relativitätstheorie”. In: *Sitzungsberichte der Königlich Preußischen Akademie der Wissenschaften* (Nov. 1915), pp. 778–786.

[36] Albert Einstein. “Zur allgemeinen Relativitätstheorie (Nachtrag)”. In: *Sitzungsberichte der Königlich Preußischen Akademie der Wissenschaften* (Nov. 1915), pp. 799–801.

[37] Albert Einstein. “Erklärung der Perihelbewegung des Merkur aus der allgemeinen Relativitätstheorie”. In: *Sitzungsberichte der Königlich Preußischen Akademie der Wissenschaften* (Nov. 1915), pp. 831–839.

[38] Albert Einstein. “Die Feldgleichungen der Gravitation”. In: *Sitzungsberichte der Königlich Preußischen Akademie der Wissenschaften* (Nov. 1915), pp. 844–847.

[39] Clifford M. Will. “The Confrontation between General Relativity and Experiment”. In: *Living Rev. Rel.* 17 (2014), p. 4. DOI: 10.12942/lrr-2014-4. arXiv: 1403.7377 [gr-qc].

[40] Albert Einstein. “Kosmologische Betrachtungen zur allgemeinen Relativitätstheorie”. In: *Sitzungsberichte der Königlich Preußischen Akademie der Wissenschaften* (Jan. 1917), pp. 142–152.

[41] Steven Weinberg. “The cosmological constant problem”. In: *Rev. Mod. Phys.* 61 (1 Jan. 1989), pp. 1–23. DOI: 10.1103/RevModPhys.61.1.

[42] L. Abbott. “The mystery of the cosmological constant”. In: *Scientific American* 258 (May 1988), pp. 106–113. DOI: 10.1038/scientificamerican0588-106.

[43] N Straumann. “The mystery of the cosmic vacuum energy density and the accelerated expansion of the Universe”. In: *European Journal of Physics* 20.6 (Nov. 1999), pp. 419–427. ISSN: 1361-6404. DOI: 10.1088/0143-0807/20/6/307.

[44] L. Amendola and S. Tsujikawa. *Dark Energy: Theory and Observations*. Cambridge University Press, 2010. ISBN: 9781139488570.

[45] Ya. B. Zel'dovich, Andrzej Krasinski, and Ya. B. Zeldovich. "The Cosmological constant and the theory of elementary particles". In: *Sov. Phys. Usp.* 11 (1968), pp. 381–393. DOI: 10.1007/s10714-008-0624-6.

[46] G. Lemaitre. "Evolution of the Expanding Universe". In: *Proceedings of the National Academy of Science* 20.1 (Jan. 1934), pp. 12–17. DOI: 10.1073/pnas.20.1.12.

[47] Planck Collaboration et al. "Planck 2018 results - I. Overview and the cosmological legacy of Planck". In: *Astronomy & Astrophysics* 641 (2020), A1. DOI: 10.1051/0004-6361/201833880.

[48] Adam G. Riess et al. "A Comprehensive Measurement of the Local Value of the Hubble Constant with 1 km/s/Mpc Uncertainty from the Hubble Space Telescope and the SH0ES Team". In: *The Astrophysical Journal Letters* 934.1 (July 2022), p. L7. ISSN: 2041-8213. DOI: 10.3847/2041-8213/ac5c5b.

[49] José Luis Bernal, Licia Verde, and Adam G. Riess. "The trouble with H_0". In: *J. Cosmology Astropart. Phys.* 2016.10 (Oct. 2016), p. 019. DOI: 10.1088/1475-7516/2016/10/019.

[50] Marc Kamionkowski and Adam G. Riess. *The Hubble Tension and Early Dark Energy*. 2022. arXiv: 2211.04492 [astro-ph.CO]. URL: https://arxiv.org/abs/2211.04492.

[51] Licia Verde, Nils Schöneberg, and Héctor Gil-Marín. *A tale of many H_0*. 2023. arXiv: 2311.13305 [astro-ph.CO]. URL: https://arxiv.org/abs/2311.13305.

[52] Eleonora Di Valentino et al. "In the realm of the Hubble tension—a review of solutions". In: *Classical and Quantum Gravity* 38.15 (July 2021), p. 153001. ISSN: 1361-6382. DOI: 10.1088/1361-6382/ac086d.

[53] Marian Douspis, Laura Salvati, and Nabila Aghanim. *On the tension between Large Scale Structures and Cosmic Microwave Background*. 2019. arXiv: 1901.05289 [astro-ph.CO]. URL: https://arxiv.org/abs/1901.05289.

[54] V. Ghirardini et al. "The SRG/eROSITA all-sky survey: Cosmology constraints from cluster abundances in the western Galactic hemisphere". In: *Astronomy & Astrophysics* 689 (Sept. 2024), A298. ISSN: 1432-0746. DOI: 10.1051/0004-6361/202348852.

[55] Brian D. Fields. "The Primordial Lithium Problem". In: *Annual Review of Nuclear and Particle Science* 61.Volume 61, 2011 (2011), pp. 47–68. ISSN: 1545-4134. DOI: https://doi.org/10.1146/annurev-nucl-102010-130445.

[56] Stefano Profumo, Leonardo Giani, and Oliver F. Piattella. *An Introduction to Particle Dark Matter*. 2019. arXiv: 1910.05610 [hep-ph]. URL: https://arxiv.org/abs/1910.05610.

[57] A. Arbey and F. Mahmoudi. "Dark matter and the early Universe: A review". In: *Progress in Particle and Nuclear Physics* 119 (July 2021), p. 103865. ISSN: 0146-6410. DOI: 10.1016/j.ppnp.2021.103865.

[58] Dragan Huterer and Daniel L Shafer. "Dark energy two decades after: Observables, probes, consistency tests". In: *Rept. Prog. Phys.* 81.1 (2018), p. 016901. DOI: 10.1088/1361-6633/aa997e. arXiv: 1709.01091 [astro-ph.CO].

[59] Raul Jimenez, Peter Thejll, Uffe G. JØrgensen, James MacDonald, and Bernard Pagel. "Ages of globular clusters: a new approach". In: *Monthly Notices of the Royal Astronomical Society* 282.3 (Nov. 1996), pp. 926–942. ISSN: 1365-2966. DOI: 10.1093/mnras/282.3.926. URL: http://dx.doi.org/10.1093/mnras/282.3.926.

[60] Howard E. Bond, Edmund P. Nelan, Don A. VandenBerg, Gail H. Schaefer, and Dianne Harmer. "HD 140283: A Star in the Solar Neighborhood that Formed Shortly After the Big Bang". In: *The Astrophysical Journal* 765.1 (Feb. 2013), p. L12. ISSN: 2041-8213. DOI: 10.1088/2041-8205/765/1/l12.

[61] T. M. C. Abbott et al. "First Cosmology Results using Type Ia Supernovae from the Dark Energy Survey: Constraints on Cosmological Parameters". In: *The Astrophysical Journal Letters* 872.2 (Feb. 2019), p. L30. ISSN: 2041-8213. DOI: 10.3847/2041-8213/ab04fa.

[62] Dillon Brout et al. "The Pantheon+ Analysis: Cosmological Constraints". In: *Astrophys. J.* 938.2 (2022), p. 110. DOI: 10.3847/1538-4357/ac8e04. arXiv: 2202.04077 [astro-ph.CO].

[63] M. Chevallier and D. Polarski. "Acceleration Universes with Scaling Dark Matter". In: *International Journal of Modern Physics D* 10.02 (Apr. 2001), pp. 213–223. ISSN: 1793-6594. DOI: 10.1142/s0218271801000822.

[64] Eric V. Linder. "Exploring the Expansion History of the Universe". In: *Physical Review Letters* 90.9 (Mar. 2003). ISSN: 1079-7114. DOI: 10.1103/physrevlett.90.091301. URL: http://dx.doi.org/10.1103/PhysRevLett.90.091301.

[65] Bruce A. Bassett and Renee Hlozek. "Baryon Acoustic Oscillations". In: (Oct. 2009). arXiv: 0910.5224 [astro-ph.CO].

[66] A. G. Adame et al. "DESI 2024 VI: Cosmological Constraints from the Measurements of Baryon Acoustic Oscillations". In: (Apr. 2024). arXiv: 2404.03002 [astro-ph.CO].

[67] A. G. Adame et al. "DESI 2024 VII: Cosmological Constraints from the Full-Shape Modeling of Clustering Measurements". In: (Nov. 2024). arXiv: 2411.12022 [astro-ph.CO].

[68] Verónica Motta, Miguel A. García-Aspeitia, Alberto Hernández-Almada, Juan Magaña, and Tomás Verdugo. "Taxonomy of Dark Energy Models". In: *Universe* 7.6 (2021), p. 163. DOI: 10.3390/universe7060163. arXiv: 2104.04642 [astro-ph.CO].

[69] Shinji Tsujikawa. "Quintessence: A Review". In: *Class. Quant. Grav.* 30 (2013), p. 214003. DOI: 10.1088/0264-9381/30/21/214003. arXiv: 1304.1961 [gr-qc].

[70] Shinji Tsujikawa. "Modified gravity models of dark energy". In: *Lect. Notes Phys.* 800 (2010), pp. 99–145. DOI: 10.1007/978-3-642-10598-2_3. arXiv: 1101.0191 [gr-qc].

[71] Jean-Philippe Uzan. "Fundamental constants: from measurement to the universe, a window on gravitation and cosmology". In: (Oct. 2024). arXiv: 2410.07281 [astro-ph.CO].

[72] P. A. M. Dirac. "The Cosmological Constants". In: *Nature* 139.3512 (Feb. 1937), pp. 323–323. ISSN: 1476-4687. DOI: 10.1038/139323a0.

[73] P. A. M. Dirac. "A new basis for cosmology". In: *Proceedings of the Royal Society of London. Series A. Mathematical and Physical Sciences* 165.921 (1938), pp. 199–208. DOI: 10.1098/rspa.1938.0053. eprint: https://royalsocietypublishing.org/doi/pdf/10.1098/rspa.1938.0053.

[74] P. Jordan. "Die physikalischen Weltkonstanten". In: *Naturwissenschaften* 25.32 (Aug. 1937), pp. 513–517. ISSN: 1432-1904. DOI: 10.1007/BF01498368.

[75] Jean-Philippe Uzan. "Varying Constants, Gravitation and Cosmology". In: *Living Reviews in Relativity* 14.1, 2 (Mar. 2011), p. 2. DOI: 10.12942/lrr-2011-2. arXiv: 1009.5514 [astro-ph.CO].

[76] C. J. A. P. Martins. "The status of varying constants: a review of the physics, searches and implications". In: *Reports on Progress in Physics* 80.12, 126902 (Dec. 2017), p. 126902. DOI: 10.1088/1361-6633/aa860e. arXiv: 1709.02923 [astro-ph.CO].

[77] Peter J. Mohr, Eite Tiesinga, David B. Newell, and Barry N. Taylor. *Codata Internationally Recommended 2022 Values of the Fundamental Physical Constants*. en. May 2024. URL: https://tsapps.nist.gov/publication/get_pdf.cfm?pub_id=958002.

[78] A. Sommerfeld. “Zur Quantentheorie der Spektrallinien. Ann Phys 51:1-94, 125-167”. In: *Annalen der Physik* 356 (Mar. 1916), pp. 1–94. DOI: 10.1002/andp.19163561702.

[79] John K. Webb, Victor V. Flambaum, Christopher W. Churchill, Michael J. Drinkwater, and John D. Barrow. “Evidence for time variation of the fine structure constant”. In: *Phys. Rev. Lett.* 82 (1999), pp. 884–887. DOI: 10.1103/PhysRevLett.82.884. arXiv: astro-ph/9803165.

[80] J. K. Webb, J. A. King, M. T. Murphy, V. V. Flambaum, R. F. Carswell, and M. B. Bainbridge. “Indications of a spatial variation of the fine structure constant”. In: *Phys. Rev. Lett.* 107 (2011), p. 191101. DOI: 10.1103/PhysRevLett.107.191101. arXiv: 1008.3907 [astro-ph.CO].

[81] R. Lange et al. “Improved limits for violations of local position invariance from atomic clock comparisons”. In: *Phys. Rev. Lett.* 126.1 (2021), p. 011102. DOI: 10.1103/PhysRevLett.126.011102. arXiv: 2010.06620 [physics.atom-ph].

[82] M. Filzinger et al. “Improved Limits on the Coupling of Ultralight Bosonic Dark Matter to Photons from Optical Atomic Clock Comparisons”. In: *Phys. Rev. Lett.* 130.25 (2023), p. 253001. DOI: 10.1103/PhysRevLett.130.253001. arXiv: 2301.03433 [physics.atom-ph].

[83] Pavel Fadeev, Julian C. Berengut, and Victor V. Flambaum. “Sensitivity of ^{229}Th nuclear clock transition to variation of the fine-structure constant”. In: *Phys. Rev. A* 102 (5 Nov. 2020), p. 052833. DOI: 10.1103/PhysRevA.102.052833.

[84] Thibault Damour and Freeman Dyson. “The Oklo bound on the time variation of the fine structure constant revisited”. In: *Nucl. Phys. B* 480 (1996), pp. 37–54. DOI: 10.1016/S0550-3213(96)00467-1. arXiv: hep-ph/9606486.

[85] C. R. Gould, E. I. Sharapov, and S. K. Lamoreaux. “Time variability of α from realistic models of Oklo reactors”. In: *Phys. Rev. C* 74 (2 Aug. 2006), p. 024607. DOI: 10.1103/PhysRevC.74.024607.

[86] M. S. Onegin. “Investigation of the fundamental constants stability based on the reactor Oklo burn-up analysis”. In: *Mod. Phys. Lett. A* 27 (2012), p. 1250232. DOI: 10.1142/S021773231250232X. arXiv: 1010.6299 [nucl-th].

[87] Jonathan B. Whitmore and Michael T. Murphy. “Impact of instrumental systematic errors on fine-structure constant measurements with quasar spectra”. In: *Mon. Not. Roy. Astron. Soc.* 447.1 (2015), pp. 446–462. DOI: 10.1093/mnras/stu2420. arXiv: 1409.4467 [astro-ph.IM].

[88] Michael T. Murphy and Kathy L. Cooksey. “Subaru Telescope limits on cosmological variations in the fine-structure constant”. In: *Mon. Not. Roy. Astron. Soc.* 471.4 (2017), pp. 4930–4945. DOI: 10.1093/mnras/stx1949. arXiv: 1708.00014 [astro-ph.CO].

[89] Dinko Milaković, Chung-Chi Lee, Robert F. Carswell, John K. Webb, Paolo Molaro, and Luca Pasquini. “A new era of fine structure constant measurements at high redshift”. In: *Mon. Not. Roy. Astron. Soc.* 500.1 (2020), pp. 1–21. DOI: 10.1093/mnras/staa3217. arXiv: 2008.10619 [astro-ph.CO].

[90] Michael T. Murphy et al. “Fundamental physics with ESPRESSO: Precise limit on variations in the fine-structure constant towards the bright quasar HE 0515−4414”. In: *Astron. Astrophys.* 658 (2022), A123. DOI: 10.1051/0004-6361/202142257. arXiv: 2112.05819 [astro-ph.CO].

[91] Silvia Galli, C. J. A. P. Martins, Alessandro Melchiorri, and Eloisa Menegoni. “Testing the Variation of Fundamental Constants with the CMB”. In: *Astrophys. Space Sci. Proc.* (2011). Ed. by Carlos Martins and Paolo Molaro, pp. 59–67. DOI: 10.1007/978-3-642-19397-2_7.

[92] Luke Hart and Jens Chluba. “New constraints on time-dependent variations of fundamental constants using Planck data”. In: *Mon. Not. Roy. Astron. Soc.* 474.2 (2018), pp. 1850–1861. DOI: 10.1093/mnras/stx2783. arXiv: 1705.03925 [astro-ph.CO].

[93] Deal, M. and Martins, C. J. A. P. “Primordial nucleosynthesis with varying fundamental constants - Solutions to the lithium problem and the deuterium discrepancy”. In: *Astron. Astrophys.* 653 (2021), A48. DOI: 10.1051/0004-6361/202140725.

[94] Luke Hart and Jens Chluba. “Updated fundamental constant constraints from Planck 2018 data and possible relations to the Hubble tension”. In: *Monthly Notices of the Royal Astronomical Society* 493.3 (Feb. 2020), pp. 3255–3263. ISSN: 1365-2966. DOI: 10.1093/mnras/staa412. URL: http://dx.doi.org/10.1093/mnras/staa412.

[95] Jens Chluba and Luke Hart. *Varying fundamental constants meet Hubble*. 2023. arXiv: 2309.12083 [astro-ph.CO]. URL: https://arxiv.org/abs/2309.12083.

[96] Nanoom Lee, Yacine Ali-Haïmoud, Nils Schöneberg, and Vivian Poulin. “What It Takes to Solve the Hubble Tension through Modifications of Cosmological Recombination”. In: *Physical Review Letters* 130.16 (Apr. 2023). ISSN: 1079-7114. DOI: 10.1103/physrevlett.130.161003. URL: http://dx.doi.org/10.1103/PhysRevLett.130.161003.

[97] Toyokazu Sekiguchi and Tomo Takahashi. “Early recombination as a solution to the H_0 tension”. In: *Physical Review D* 103.8 (Apr. 2021). issn: 2470-0029. doi: 10.1103/physrevd.103.083507.

[98] Nils Schöneberg and Léo Vacher. “The mass effect – Variations of masses and their impact on cosmology”. In: (July 2024). arXiv: 2407.16845 [astro-ph.CO].

[99] Léo Vacher and Nils Schöneberg. “Incompatibility of fine-structure constant variations at recombination with local observations”. In: *Phys. Rev. D* 109.10 (2024), p. 103520. doi: 10.1103/PhysRevD.109.103520. arXiv: 2403.02256 [astro-ph.CO].

[100] Pierre Touboul et al. “$MICROSCOPE$ Mission: Final Results of the Test of the Equivalence Principle”. In: *Phys. Rev. Lett.* 129 (12 Sept. 2022), p. 121102. doi: 10.1103/PhysRevLett.129.121102.

[101] T. A. Wagner, S. Schlamminger, J. H. Gundlach, and E. G. Adelberger. “Torsion-balance tests of the weak equivalence principle”. In: *Classical and Quantum Gravity* 29.18, 184002 (Sept. 2012), p. 184002. doi: 10.1088/0264-9381/29/18/184002. arXiv: 1207.2442 [gr-qc].

[102] J. Müller, F. Hofmann, and L. Biskupek. “Testing various facets of the equivalence principle using lunar laser ranging”. In: *Class. Quant. Grav.* 29 (2012), p. 184006. doi: 10.1088/0264-9381/29/18/184006.

[103] James Halverson, Cody Long, and Benjamin Sung. “Algorithmic universality in F-theory compactifications”. In: *Phys. Rev. D* 96.12 (2017), p. 126006. doi: 10.1103/PhysRevD.96.126006. arXiv: 1706.02299 [hep-th].

[104] Cumrun Vafa. “The String landscape and the swampland”. In: (Sept. 2005). arXiv: hep-th/0509212.

[105] Eran Palti. “The Swampland: Introduction and Review”. In: *Fortsch. Phys.* 67.6 (2019), p. 1900037. doi: 10.1002/prop.201900037. arXiv: 1903.06239 [hep-th].

[106] Jacob D. Bekenstein. “Fine-structure constant: Is it really a constant?” In: *Phys. Rev. D* 25 (6 Mar. 1982), pp. 1527–1539. doi: 10.1103/PhysRevD.25.1527.

[107] Jacob D. Bekenstein. “Fine structure constant variability, equivalence principle and cosmology”. In: *Phys. Rev. D* 66 (2002), p. 123514. doi: 10.1103/PhysRevD.66.123514. arXiv: gr-qc/0208081.

[108] Havard Bunes Sandvik, John D. Barrow, and Joao Magueijo. “A simple cosmology with a varying fine structure constant”. In: *Phys. Rev. Lett.* 88 (2002), p. 031302. doi: 10.1103/PhysRevLett.88.031302. arXiv: astro-ph/0107512.

[109] Joao Magueijo, Havard B. Sandvik, and T. W. B. Kibble. “Nielsen-Olesen vortex in varying alpha theories”. In: *Phys. Rev. D* 64 (2001), p. 023521. doi: 10.1103/PhysRevD.64.023521. arXiv: hep-ph/0101155.

[110] John D. Barrow, Havard Bunes Sandvik, and Joao Magueijo. "The behavior of varying alpha cosmologies". In: *Phys. Rev. D* 65 (2002), p. 063504. DOI: 10.1103/PhysRevD.65.063504. arXiv: astro-ph/0109414.

[111] John D. Barrow, Joao Magueijo, and Havard Bunes Sandvik. "Variations of alpha in space and time". In: *Phys. Rev. D* 66 (2002), p. 043515. DOI: 10.1103/PhysRevD.66.043515. arXiv: astro-ph/0202129.

[112] Th. Kaluza. "Zum Unitätsproblem der Physik". In: *Sitzungsber. Preuss. Akad. Wiss. Berlin (Math. Phys.)* 1921 (1921), pp. 966–972. DOI: 10.1142/S0218271818700017. arXiv: 1803.08616 [physics.hist-ph].

[113] Steven Weinberg. "A Model of Leptons". In: *Phys. Rev. Lett.* 19 (21 Nov. 1967), pp. 1264–1266. DOI: 10.1103/PhysRevLett.19.1264.

[114] C. DeWitt and B. DeWitt, eds. *Relativité, Groupes et Topologie: Proceedings, Ecole d'été de Physique Théorique, Session XIII, Les Houches, France, Jul 1 - Aug 24, 1963*. New York: Gordon and Breach, 1964.

[115] T. Damour and A.M. Polyakov. "The string dilation and a least coupling principle". In: *Nuclear Physics B* 423.2 (1994), pp. 532–558. ISSN: 0550-3213. DOI: https://doi.org/10.1016/0550-3213(94)90143-0.

[116] Thibault Damour. "Theoretical Aspects of the Equivalence Principle". In: *Class. Quant. Grav.* 29 (2012), p. 184001. DOI: 10.1088/0264-9381/29/18/184001. arXiv: 1202.6311 [gr-qc].

[117] Jean-Philippe Uzan. "The fundamental constants and their variation: observational and theoretical status". In: *Rev. Mod. Phys.* 75 (2 Apr. 2003), pp. 403–455. DOI: 10.1103/RevModPhys.75.403.

[118] Keith A. Olive and Maxim Pospelov. "Evolution of the fine structure constant driven by dark matter and the cosmological constant". In: *Phys. Rev. D* 65 (2002), p. 085044. DOI: 10.1103/PhysRevD.65.085044. arXiv: hep-ph/0110377.

[119] B. Bertotti, L. Iess, and P. Tortora. "A test of general relativity using radio links with the Cassini spacecraft". In: *Nature* 425 (Sept. 2003), pp. 374–376. DOI: https://doi.org/10.1038/nature01997.

[120] T. Damour, F. Piazza, and G. Veneziano. "Violations of the equivalence principle in a dilaton-runaway scenario". In: *Phys. Rev. D* 66 (4 Aug. 2002), p. 046007. DOI: 10.1103/PhysRevD.66.046007.

[121] Ashoke Sen. "Rolling Tachyon". In: *Journal of High Energy Physics* 2002.04 (Apr. 2002), pp. 048–048. DOI: 10.1088/1126-6708/2002/04/048. URL: https://doi.org/10.1088/1126-6708/2002/04/048.

[122] R.G. Leigh. "Dirac-Born-Infeld action from Dirichlet σ-model". In: *Modern Physics Letters A* 04.28 (1989), pp. 2767–2772. DOI: 10.1142/S0217732389003099. eprint: https://doi.org/10.1142/S0217732389003099.

[123] G W Gibbons. "Cosmological evolution of the rolling tachyon". In: *Phys. Lett. B* 537 (2002), pp. 1–4. DOI: 10.1016/S0370-2693(02)01881-6. arXiv: hep-th/0204008.

[124] P. A. M. Dirac. "An Extensible Model of the Electron". In: *Proceedings of the Royal Society of London. Series A, Mathematical and Physical Sciences* 268.1332 (1962), pp. 57–67. ISSN: 00804630. URL: http://www.jstor.org/stable/2414316 (visited on 06/26/2024).

[125] M. Born and L. Infeld. "Foundations of the New Field Theory". In: *Proceedings of the Royal Society of London. Series A, Containing Papers of a Mathematical and Physical Character* 144.852 (1934), pp. 425–451. ISSN: 09501207. URL: http://www.jstor.org/stable/2935568 (visited on 06/26/2024).

[126] Ashoke Sen. "Tachyon Matter". In: *Journal of High Energy Physics* 2002.7, 065 (July 2002), p. 065. DOI: 10.1088/1126-6708/2002/07/065. arXiv: hep-th/0203265 [hep-th].

[127] Mohammad R. Garousi, M. Sami, and Shinji Tsujikawa. "Constraints on Dirac-Born-Infeld type dark energy models from varying alpha". In: *Phys. Rev. D* 71.8, 083005 (8 Apr. 2005), p. 083005. DOI: 10.1103/PhysRevD.71.083005. arXiv: hep-th/0412002 [hep-th].

[128] Edmund J. Copeland, Mohammad R. Garousi, M. Sami, and Shinji Tsujikawa. "What is needed of a tachyon if it is to be the dark energy?" In: *Phys. Rev. D.* 71.4, 043003 (Feb. 2005), p. 043003. DOI: 10.1103/PhysRevD.71.043003. arXiv: hep-th/0411192 [hep-th].

[129] C. J. A. P. Martins and F. M. O. Moucherek. "Cosmological and astrophysical constraints on tachyon dark energy models". In: *Phys. Rev. D* 93.12, 123524 (12 June 2016), p. 123524. DOI: 10.1103/PhysRevD.93.123524. arXiv: 1606.08380 [astro-ph.CO].

[130] Marieke van Beest, José Calderón-Infante, Delaram Mirfendereski, and Irene Valenzuela. "Lectures on the Swampland Program in String Compactifications". In: *Phys. Rept.* 989 (2022), pp. 1–50. DOI: 10.1016/j.physrep.2022.09.002. arXiv: 2102.01111 [hep-th].

[131] Prateek Agrawal, Georges Obied, Paul J. Steinhardt, and Cumrun Vafa. "On the Cosmological Implications of the String Swampland". In: *Phys. Lett. B* 784 (2018), pp. 271–276. DOI: 10.1016/j.physletb.2018.07.040. arXiv: 1806.09718 [hep-th].

[132] Marco Raveri, Wayne Hu, and Savdeep Sethi. "Swampland Conjectures and Late-Time Cosmology". In: *Phys. Rev. D* 99.8 (2019), p. 083518. DOI: 10.1103/PhysRevD.99.083518. arXiv: 1812.10448 [hep-th].

[133] S. Noori Gashti and J. Sadeghi. "Inflation, swampland and landscape". In: *Int. J. Mod. Phys. A* 37.04 (2022), p. 2250006. DOI: 10.1142/S0217751X22500063. arXiv: 2112.04196 [gr-qc].

[134] Hajime Fukuda, Ryo Saito, Satoshi Shirai, and Masahito Yamazaki. "Phenomenological Consequences of the Refined Swampland Conjecture". In: *Phys. Rev. D* 99.8 (2019), p. 083520. DOI: 10.1103/PhysRevD.99.083520. arXiv: 1810.06532 [hep-th].

[135] Lavinia Heisenberg, Matthias Bartelmann, Robert Brandenberger, and Alexandre Refregier. "Dark Energy in the Swampland". In: *Phys. Rev. D* 98.12 (2018), p. 123502. DOI: 10.1103/PhysRevD.98.123502. arXiv: 1808.02877 [astro-ph.CO].

[136] Lavinia Heisenberg, Matthias Bartelmann, Robert Brandenberger, and Alexandre Refregier. "Dark Energy in the Swampland II". In: *Sci. China Phys. Mech. Astron.* 62.9 (2019), p. 990421. DOI: 10.1007/s11433-019-9392-7. arXiv: 1809.00154 [astro-ph.CO].

[137] Deng Wang. "The multi-feature universe: Large parameter space cosmology and the swampland". In: *Phys. Dark Univ.* 28 (2020), p. 100545. DOI: 10.1016/j.dark.2020.100545. arXiv: 1809.04854 [astro-ph.CO].

[138] Julien Lesgourgues. "The Cosmic Linear Anisotropy Solving System (CLASS) I: Overview". In: *arXiv e-prints* (Apr. 2011). DOI: 10.48550/arXiv.1104.2932. arXiv: 1104.2932 [astro-ph.IM].

[139] Thejs Brinckmann and Julien Lesgourgues. "MontePython 3: boosted MCMC sampler and other features". In: *Phys. Dark Univ.* 24 (2019), p. 100260. DOI: 10.1016/j.dark.2018.100260. arXiv: 1804.07261 [astro-ph.CO].

[140] Antony Lewis. "GetDist: a Python package for analysing Monte Carlo samples". In: (Oct. 2019). arXiv: 1910.13970 [astro-ph.IM].

[141] N. Aghanim et al. "Planck 2018 results. V. CMB power spectra and likelihoods". In: *Astron. Astrophys.* 641 (2020), A5. DOI: 10.1051/0004-6361/201936386. arXiv: 1907.12875 [astro-ph.CO].

[142] N. Aghanim et al. "Planck 2018 results. VIII. Gravitational lensing". In: *Astron. Astrophys.* 641 (2020), A8. DOI: 10.1051/0004-6361/201833886. arXiv: 1807.06210 [astro-ph.CO].

[143] Shadab Alam et al. "The clustering of galaxies in the completed SDSS-III Baryon Oscillation Spectroscopic Survey: cosmological analysis of the DR12 galaxy sample". In: *Mon. Not. Roy. Astron. Soc.* 470.3 (2017), pp. 2617–2652. DOI: 10.1093/mnras/stx721. arXiv: 1607.03155 [astro-ph.CO].

[144] Ashley J. Ross, Lado Samushia, Cullan Howlett, Will J. Percival, Angela Burden, and Marc Manera. "The clustering of the SDSS DR7 main Galaxy sample – I. A 4 per cent distance measure at $z = 0.15$". In: *Mon. Not. Roy. Astron. Soc.* 449.1 (2015), pp. 835–847. DOI: 10.1093/mnras/stv154. arXiv: 1409.3242 [astro-ph.CO].

[145] Florian Beutler et al. "The 6dF Galaxy Survey: baryon acoustic oscillations and the local Hubble constant: 6dFGS: BAOs and the local Hubble constant". In: *Monthly Notices of the Royal Astronomical Society* 416.4 (July 2011), pp. 3017–3032. ISSN: 0035-8711. DOI: 10.1111/j.1365-2966.2011.19250.x.

[146] Shadab Alam et al. "Completed SDSS-IV extended Baryon Oscillation Spectroscopic Survey: Cosmological implications from two decades of spectroscopic surveys at the Apache Point Observatory". In: *Phys. Rev. D* 103.8 (2021), p. 083533. DOI: 10.1103/PhysRevD.103.083533. arXiv: 2007.08991 [astro-ph.CO].

[147] Dan Scolnic et al. "The Pantheon+ Analysis: The Full Data Set and Light-curve Release". In: *Astrophys. J.* 938.2 (2022), p. 113. DOI: 10.3847/1538-4357/ac8b7a. arXiv: 2112.03863 [astro-ph.CO].

[148] Michele Moresco et al. "Unveiling the Universe with emerging cosmological probes". In: *Living Rev. Rel.* 25.1 (2022), p. 6. DOI: 10.1007/s41114-022-00040-z. arXiv: 2201.07241 [astro-ph.CO].

[149] Yu. V. Petrov, A. I. Nazarov, M. S. Onegin, V. Yu. Petrov, and E. G. Sakhnovsky. "Natural nuclear reactor Oklo and variation of fundamental constants. Part 1. Computation of neutronic of fresh core". In: *Phys. Rev. C* 74 (2006), p. 064610. DOI: 10.1103/PhysRevC.74.064610. arXiv: hep-ph/0506186.

[150] I. I. Agafonova, P. Molaro, S. A. Levshakov, and J. L. Hou. "First measurement of Mg isotope abundances at high redshifts and accurate estimate of $\Delta\alpha/\alpha$". In: *Astronomy & Astrophysics* 529 (Mar. 2011), A28. ISSN: 1432-0746. DOI: 10.1051/0004-6361/201016194.

[151] P. Molaro et al. "The UVES Large Program for testing fundamental physics I. Bounds on a change in α towards quasar HE 2217-2818". In: *Astronomy & Astrophysics* 555 (July 2013), A68. DOI: 10.1051/0004-6361/201321351. URL: https://doi.org/10.1051/0004-6361/201321351.

[152] T. M. Evans et al. "The UVES Large Program for testing fundamental physics – III. Constraints on the fine-structure constant from three telescopes". In: *Mon. Not. Roy. Astron. Soc.* 445.1 (2014), pp. 128–150. DOI: 10.1093/mnras/stu1754. arXiv: 1409.1923 [astro-ph.CO].

[153] A. Songaila and L. L. Cowie. "Constraining the Variation of the Fine Structure Constant with Observations of Narrow Quasar Absorption Lines". In: *Astrophys. J.* 793 (2014), p. 103. DOI: 10.1088/0004-637X/793/2/103. arXiv: 1406.3628 [astro-ph.CO].

[154] Michael T. Murphy, Adrian L. Malec, and J. Xavier Prochaska. "Precise limits on cosmological variability of the fine-structure constant with zinc and chromium quasar absorption lines". In: *Mon. Not. Roy. Astron. Soc.* 461.3 (2016), pp. 2461–2479. DOI: 10.1093/mnras/stw1482. arXiv: 1606.06293 [astro-ph.CO].

[155] Srđan M. Kotuš, Michael T. Murphy, and Robert F. Carswell. "High-precision limit on variation in the fine-structure constant from a single quasar absorption system". In: *Mon. Not. Roy. Astron. Soc.* 464.3 (2017), pp. 3679–3703. DOI: 10.1093/mnras/stw2543. arXiv: 1609.03860 [astro-ph.CO].

[156] Adam G. Riess et al. "Type Ia Supernova Distances at Redshift > 1.5 from the Hubble Space Telescope Multi-cycle Treasury Programs: The Early Expansion Rate". In: *Astrophys. J.* 853.2 (2018), p. 126. DOI: 10.3847/1538-4357/aaa5a9. arXiv: 1710.00844 [astro-ph.CO].

[157] Michele Moresco et al. "A 6% measurement of the Hubble parameter at $z \sim 0.45$: direct evidence of the epoch of cosmic re-acceleration". In: *J. Cosmology Astropart. Phys.* 05 (2016), p. 014. DOI: 10.1088/1475-7516/2016/05/014. arXiv: 1601.01701 [astro-ph.CO].

[158] Simone Aiola et al. "The Atacama Cosmology Telescope: DR4 maps and cosmological parameters". In: *J. Cosmology Astropart. Phys.* 2020.12, 047 (Dec. 2020), p. 047. DOI: 10.1088/1475-7516/2020/12/047. arXiv: 2007.07288 [astro-ph.CO].

[159] L. Balkenhol et al. "Measurement of the CMB temperature power spectrum and constraints on cosmology from the SPT-3G 2018 T T , T E , and E E dataset". In: *Phys. Rev. D.* 108.2, 023510 (July 2023), p. 023510. DOI: 10.1103/PhysRevD.108.023510. arXiv: 2212.05642 [astro-ph.CO].

[160] C. S. Alves, A. C. O. Leite, C. J. A. P. Martins, T. A. Silva, S. A. Berge, and B. S. A. Silva. "Current and future constraints on extended Bekenstein-type models for a varying fine-structure constant". In: *Phys. Rev. D.* 97.2, 023522 (Jan. 2018), p. 023522. DOI: 10.1103/PhysRevD.97.023522. arXiv: 1801.08089 [astro-ph.CO].

[161] T. Rosenband et al. "Frequency Ratio of Al^+ and Hg^+ Single-Ion Optical Clocks; Metrology at the 17th Decimal Place". In: *Science* 319.5871 (2008), pp. 1808–1812. DOI: 10.1126/science.1154622. eprint: https://www.science.org/doi/pdf/10.1126/science.1154622.

[162] C. J. A. P. Martins and L. Vacher. "Astrophysical and local constraints on string theory: Runaway dilaton models". In: *Phys. Rev. D* 100 (12 Dec. 2019), p. 123514. DOI: 10.1103/PhysRevD.100.123514.

[163] Daniel B. Thomas, Michael Kopp, and Constantinos Skordis. "Constraining the Properties of Dark Matter with Observations of the Cosmic Microwave Background". In: *The Astrophysical Journal* 830.2, 155 (Oct. 2016), p. 155. DOI: 10.3847/0004-637X/830/2/155. arXiv: 1601.05097 [astro-ph.CO].

[164] Isaac Tutusaus, Brahim Lamine, Alain Blanchard, Arnaud Dupays, Yvan Rousset, and Yves Zolnierowski. "Dark sectors of the Universe: A Euclid survey approach". In: *Phys. Rev. D.* 94.12, 123515 (Dec. 2016), p. 123515. DOI: 10.1103/PhysRevD.94.123515. arXiv: 1607.08016 [astro-ph.CO].

[165] V. C. Tavares and C. J. A. P. Martins. "Varying alpha generalized Dirac-Born-Infeld models". In: *Phys. Rev. D* 103 (2 Jan. 2021), p. 023525. DOI: 10.1103/PhysRevD.103.023525. URL: https://link.aps.org/doi/10.1103/PhysRevD.103.023525.

[166] Amir Aghamousa et al. "The DESI Experiment Part I: Science,Targeting, and Survey Design". In: (Oct. 2016). arXiv: 1611.00036 [astro-ph.IM].

[167] Kjeld Beeks et al. "Fine-structure constant sensitivity of the Th-229 nuclear clock transition". In: *arXiv e-prints*, arXiv:2407.17300 (July 2024), arXiv:2407.17300. DOI: 10.48550/arXiv.2407.17300. arXiv: 2407.17300 [nucl-th].

[168] F. Pepe et al. "ESPRESSO at VLT - On-sky performance and first results". In: *Astron. Astrophys.* 645 (2021), A96. DOI: 10.1051/0004-6361/202038306. arXiv: 2010.00316 [astro-ph.IM].

[169] C. J. A. P. Martins et al. "Cosmology and fundamental physics with the ELT-ANDES spectrograph". In: *Experimental Astronomy* 57.1, 5 (Feb. 2024), p. 5. DOI: 10.1007/s10686-024-09928-w. arXiv: 2311.16274 [astro-ph.CO].